

**Golden Goal Regulates Target
Specificity in the *Drosophila* Lamina**

Dissertation

**der Fakultät für Biologie
der Ludwig-Maximilians-Universität München**

Angefertigt am Max Planck Institut für Neurobiologie

**Vorgelegt von
Irina Hein**

München, 10. Dezember 2012

Erstgutachter: Prof. Dr. Alexander Borst
Zweitgutachter: Prof. Dr. Barbara Conradt
Tag der mündlichen Prüfung: 12. 04. 2013

Ehrenwörtliche Versicherung

Hiermit, erkläre ich, dass ich die vorliegende Dissertation selbständig und ohne unerlaubte Hilfe angefertigt habe. Ich habe mich dabei keiner anderen als der von mir ausdrücklich bezeichneten Hilfen und Quellen bedient.

Erklärung

Ich erkläre hiermit, dass ich mich nicht anderweitig ohne Erfolg einer Doktorprüfung unterzogen habe. Die Dissertation wurde in ihrer jetzigen oder ähnlichen Form bei keiner anderen Hochschule eingereicht und hat noch keinen sonstigen Prüfungszwecken gedient.

München, Dezember 2012

Irina Hein

Die vorliegende Arbeit wurde zwischen März 2009 und November 2012 unter der Leitung von Dr. Takashi Suzuki und Dr. Ilona Kadow am Max-Planck-Institut für Neurobiologie in Martinsried durchgeführt

TABLE OF CONTENTS

Index of Figures	III
List of abbreviations	IV
ABSTRACT	1
DEUTSCHE ZUSAMMENFASSUNG	3
1 INTRODUCTION	5
1.1 Principles of Axon guidance	6
1.2 Molecular mechanisms of visual system formation	7
1.3 Anatomy and neuronal projections of the <i>Drosophila</i> visual system	12
1.4 Control of visual system development in <i>Drosophila</i>	15
1.5 This thesis	25
2 MATERIAL AND METHODS	26
2.1 Media and Standards	26
2.2 Instruments	26
2.3 Fly maintenance	28
2.4 <i>Drosophila</i> genetics	28
2.5 Dissections and Immunohistochemistry	37
2.6 Molecular methods	40
2.7 Statistical tests and software	42
2.8 Summary of experimental genotypes	43
3 RESULTS	46
3.1 Gogo is required for proper cartridge assembly	46
3.2 Gogo is required for spatial distribution of R cell fascicles along the lamina plexus	50
3.3 R1-R8 axons do not displaying bundling defects	54
3.4 R4 target cartridge selection is disrupted when Gogo is absent in R axons	56
3.5 Absence of Gogo in R cells disrupts lateral patterning of Lamina neurons	59
3.6 Gogo is not required cell-autonomously in R cells for lateral cartridge selection	61
3.7 Gogo is not required in neighboring axons for lateral cartridge selection	65
3.8 Gogo is required in R axons of neighboring ommatidia	67
3.9 Gogo function in R8 is sufficient to form a smooth topographic map along lamina plexus	71
3.10 Gogo is crucial for centripetal elongation of R1-R6 axons	73
3.11 Gogo is insufficient in single R axons to cause bundling during cartridge elongation	76

3.12	R axon elongation within cartridges is directly regulated by Gogo function	77
3.13	Gogo function is concentration-dependent during R axon elongation in target cartridges	79
4	DISCUSSION	83
4.1	Initial R1-R6 patterning depends on pioneer-follower interactions	84
4.2	Axon-target vs. axon-axon interactions	86
4.3	The role of Gogo during R1-R6 target cartridge selection	88
4.4	Redundancy compensates for the loss of Gogo in small fractions of R cells	91
4.5	Defining a new phenotype in the <i>Drosophila</i> lamina	93
4.6	Similarities and differences of Gogo function during medulla and lamina targeting	95
5	CONCLUSION	97
	REFERENCES	99
	ACKNOWLEDGEMENTS	106
	CURRICULUM VITAE	107

Index of Figures

Figure 2-1 Axon guidance forces.....	7
Figure 2-2 Schematic of molecular mechanisms of visual system formation.....	9
Figure 2-3 The <i>Drosophila</i> compound eye: anatomy and synaptic organization.....	14
Figure 2-4 Column formation in the lamina.....	18
Figure 2-5 Cartridge selection in the lamina.....	20
Figure 2-6 Gogo function during medulla targeting.....	23
Figure 3-1 The Flp/FRT system.....	31
Figure 4-1 Retinotopic map formation is disrupted in the absence of Gogo.....	48
Figure 4-2 Initial R cell projections in Gogo mutants are normal.....	50
Figure 4-3 Retinotopic map formation is disrupted in the absence of Gogo.....	52
Figure 4-4 Gogo mutant axons do not bundle during extension to the lamina plexus.....	55
Figure 4-5 Target cartridge selection in the absence of Gogo.....	58
Figure 4-6 lamina column formation in <i>gogo</i> mosaic eyes.....	60
Figure 4-7 Strategy of cMARCM and presentation of analysis of single labeled R cells.....	62
Figure 4-8 Gogo is not required in single R cells for lamina cartridge selection.....	64
Figure 4-9 Gogo is not providing non-cellautonomous signals to R1-R6 axons.....	66
Figure 4-10 Gogo is required in R axons of neighboring ommatidia for target cartridge selection.....	70
Figure 4-11 Gogo function in R8 is sufficient to maintain retinotopic map formation.....	72
Figure 4-12 In Gogo mosaic eyes R axons bundle with R axons from neighboring cartridges.....	74
Figure 4-13 single mutant R1-R6 axons during cartridge elongation.....	76
Figure 4-14 R1-R6 axon termini do not bundle in the absence of Fmi.....	78
Figure 4-15 Overexpression Gogo in pupal and adult brains.....	81
Figure 5-1 Target cartridge selection in the absence of Gogo.....	90
Figure 5-2 Redundancy in the absence of Gogo.....	92

List of abbreviations

The following list includes frequently used abbreviations. All other abbreviations are explained in the main text.

APF	(hours) after puparium formation
CAM	cell adhesion molecule
cMARCM	complementary MARCM
EM	electron microscopy
eyFLP	<i>eyeless</i> Flipase
FL	full-length
FLP	Flipase
<i>fmi</i>	<i>flamingo</i>
FRT	Flipase recognition target
GFP	Green fluorescent protein
GMR	Glass multiple reporter
<i>gogo</i>	<i>golden goal</i>
Ig	Immunoglobulin
L1-L5	lamina monopolar neurons 1-5
LOF	loss-of-function
R	photoreceptor
R1-R8	Photoreceptor R1-R8
RGC	retinal ganglion cell
Rh	rhodopsin
TEM	transmission electron microscopy
Tm	transmedulla neuron
TmY	transmedulla Y neuron
Trk	tropomyosin receptor kinase
UAS	upstream activating sequence
wt	wild-type

ABSTRACT

In the visual system of *Drosophila*, photoreceptor (R) neurons elaborate a precise retinotopic map of visual space in the brain. The retina consists of 750 ommatidia, each containing eight photoreceptor subtypes (R1-R8). R1-6 axons terminate in the first optic ganglion, the lamina. R7 and R8 axons extend through the lamina to innervate the second optic ganglion, the medulla. To maintain retinotopy in the lamina, R1-R6 photoreceptor axons have to undergo a complex axonal sorting during development, a process called neural superposition. The mechanisms responsible for the establishment of the highly organized connection pattern needed for retinotopy remain incompletely understood. The transmembrane receptor Golden goal (Gogo) is a known regulator of the developing *Drosophila* visual system. During R8 pathfinding, Gogo acts in two distinct steps. In larvae Gogo mediates repulsive axon-axon interactions between R8 axons in the medulla to maintain proper spacing. During pupal development, Gogo is required in R8 axons for afferent-target interactions to promote layer recognition. The aim of this thesis is to study how Gogo regulates target selection of R1-R6 axons in the lamina to increase our knowledge on how target specificity is controlled *in vivo*.

The present work shows that Gogo is required for R1-R6 axon lamina targeting and target cartridge selection in distinct developmental steps. To analyze the consequences of loss of *gogo* function specifically in photoreceptor cells, I generated genetic mosaic eyes using targeted mitotic recombination. During larval and early pupal development loss of *gogo* function in large clones of R axons results in a disruption of R1-R6 fascicle pattern formation across the lamina plexus. Using single photoreceptor type rescue, I provide evidence that the first outgrowing axon R8 uses Gogo to identify its intermediate target in the lamina and to function as a pioneer axon for all follower R1-R6 axons for their correct patterning along the lamina plexus. Interestingly, small clones of *gogo* deficient R axons perfectly integrate into a proper retinotopic map suggesting that surrounding R axons of the same or neighboring fascicles provide complementary spatial guidance. Thus, Gogo acts in a partially redundant fashion with local guidance cues provided by neighboring axons. Additionally, during pupal stages at the onset of photoreceptor sorting, I further show that R1-R6 axons fail to choose correct target cartridges in the lamina when Gogo is absent in a large fraction of R cells. I show that *gogo* mutant R1-R6 axons target correctly to wild-type areas, whereas wild-type R1-R6 axons fail to project correctly to areas innervated by mutant R axons. Interestingly, rescue of Gogo in R8 axons was not only sufficient for fascicle patterning earlier in development but also for R1-R6 axons to select their proper target cartridges in the lamina

during neural superposition. Finally, in a third developmental step, Gogo is required for the elongation of R1-R6 axons along lamina cartridges within the neuropile. In the absence of Gogo axons fail to elongate in parallel fashion and intermingle with mutant axons of neighboring cartridges. This suggests that Gogo, similar to its role in medulla targeting, permits photoreceptor axons to stay separated from each other.

Based on the results of this thesis, I propose that Gogo contributes to retinotopic map formation in the *Drosophila* lamina during three steps: initial target recognition of R1-R6 fascicles, target cartridge selection and cartridge elongation.

DEUTSCHE ZUSAMMENFASSUNG

Im visuellen System von *Drosophila* stellen Photorezeptorneurone eine präzise retinotopische Karte des visuellen Raumes im Gehirn dar. Die Retina besteht aus 750 Ommatidia, die sich jeweils aus acht verschiedenen Photorezeptorneuronen (R1-R8) zusammensetzen. Die R1-R6 Axone projizieren ins erste optische Ganglion, die Lamina. Die R7 und R8 Axone erstrecken sich durch die Lamina hindurch und innervieren das zweite optische Ganglion, die Medulla. In der Lamina erfordert der Aufbau einer korrekten retinotopischen Karte eine komplexe Umsortierung der R1-R6 Photorezeptoraxone während der Entwicklung. Die genauen Mechanismen dieser präzisen axonalen Sortierung sind bislang nicht vollständig aufgeklärt. Das Transmembranprotein Golden goal (Gogo) ist notwendig für die Entwicklung des visuellen Systems in *Drosophila*. Bisher konnte eine genauere Funktion von Gogo in R8 Axonen in verschiedenen Entwicklungsschritten der Medulla gezeigt werden. Im späten Larvenstadium reguliert Gogo repulsive Axon-Axon Interaktionen zwischen R8 Axonen und sorgt damit für deren richtige Abstände zueinander. Im Verlauf der pupalen Entwicklung ist Gogo notwendig in R8 Axonen für die Erkennung der richtigen Schichten in der Medulla. Gogo vermittelt hier Interaktionen zwischen R8 Axonen und postsynaptischen Zellen. Das Ziel der vorliegenden Arbeit ist es, die Funktion von Gogo bei der Zielerkennung von R1-R6 Axonen während der Entwicklung der Lamina zu untersuchen.

Ich zeige, dass Gogo in verschiedenen Schritten der R1-R6 Zielfindung während der Laminaentwicklung notwendig ist. Um den Funktionsverlust von Gogo zu analysieren, habe ich durch gezielte mitotische Rekombination genetische Mosaikaugen generiert. Wenn eine große Gruppe benachbarter Photorezeptoren *gogo* mutant ist, werden R1-R6 Faszikel im frühen Puppenstadium nicht mehr regelmäßig in der Lamina verteilt. Durch eine gezielte Rettung des Phänotyps zeige ich, dass Gogo in R8 Axonen gebraucht wird, damit R1-R6 Faszikel ihre intermediären Positionen in der Lamina finden und R8 als Pionieraxon für nachfolgende R1-R6 Axone fungiert. Interessanterweise, zeigt der Funktionsverlust von Gogo in kleinen Zellgruppen benachbarter Photorezeptoren keine Phänotypen. Das deutet darauf hin, dass wild-typische R1-R8 Faszikel die Wegfindung benachbarter mutanter R1-R8 Faszikel räumlich komplementieren. Gogo ist daher teilweise redundant zu anderen lokalen Wegfindungsmechanismen. Zu einem späteren Zeitpunkt der pupalen Entwicklung, wenn R1-R6 Axone zu verschiedenen Zielzellen sortiert werden, hat der Funktionsverlust von Gogo in einer größeren Zellgruppe eine inkorrekte Zielzellfindung von R1-R6 Axonen zur Folge. Weiter zeige ich, dass *gogo* mutante R1-R6 Axone ihre Zielzellen korrekt finden, wenn die Photorezeptoren im Zielbereich wild-typisch sind. Umgekehrt innervieren wild-

typische Axone falsche Zielzellen, wenn die Photorezeptoren im Zielbereich *gogo* mutant sind. Interessanterweise war die spezifische Expression von Gogo in R8 Axonen nicht nur ausreichend um den frühen Entwicklungsphänotyp zu retten, sondern auch ausreichend für die korrekte Wegfindung einzelner R1-R6 Axone während der neuralen Superposition zu retten. Im letzten Schritt der Laminainnervierung hat Gogo eine andere Funktion. Hier wird Gogo gebraucht, um die richtigen Abstände von R1-R6 Axonen während der Elongation der Termini zu regulieren. Ein Funktionsverlust von Gogo führt dazu, dass R1-R6 Axone nicht mehr parallel projizieren und sich untereinander überkreuzen. Das deutet darauf hin, dass Gogo eine ähnliche Funktion hat wie während der Medullainnervierung um Axone voneinander zu separieren.

Aufgrund der vorliegenden Ergebnisse in dieser Arbeit, ziehe ich den Schluß, dass Gogo an drei Schritten der Laminaentwicklung beteiligt ist: 1. während der Innervierung der R1-R6 Faszikel, 2. während der Auswahl finaler Zielzellen von R1-R6 Axonen und 3. während der Verlängerung von R1-R6 Termini.

1 INTRODUCTION

The fundamental basis of an animal's ability to perceive and respond to its environment depends on the processing of sensory information given by correct formation of neuronal circuits in the brain. A century ago [Ramon y Cajal](#) demonstrated that the nervous system is built up of individual neurons which are connected to each other through synapses. How neurons achieve synaptic specificity is still a central question in developmental neuroscience. How do neurons find their correct postsynaptic partners and how is this achieved on a molecular basis? One approach for understanding how circuits are constructed is the analysis of loss of function animals where developmental defects allow conclusions of a molecule's mechanism. Here I used the *Drosophila melanogaster* visual system to analyze how synapse specificity is achieved during development. *Drosophila* is an excellent model to study visual circuit formation. This is not only due to general advantages of fly genetics – such as short generation time, available genetic tools and easy manipulation. Several years' genetic studies of *Drosophila* revealed insights in the molecular and cellular mechanism specifying columnar and layered connections. In genetic screens a number of proteins have been identified that are required for the determination of axon outgrowth, axon targeting and topographic positioning of R cells. However, although many novel guidance molecules have been uncovered, the underlying molecular mechanisms remain insufficiently explored. I investigate how the transmembrane receptor Golden Goal (Gogo) functions to maintain proper retinotopy, a principle in visual systems that allow the continuous presentation of visual fields in the brain. Gogo has been previously described to mediate synaptic layer targeting in R8 axons ([Tomasi et al., 2008](#)). In particular, Gogo mediates repulsive interactions between R8 axons during medulla targeting and axon-target interactions to maintain retinotopy. In the lamina, the absence of Gogo disrupts the pattern formation elaborated by R1-R6 axons ([Hakeda-Suzuki et al., 2011](#)). However, while several studies focused on Gogo function during R8 medulla targeting ([Tomasi et al., 2008](#), [Hakeda-Suzuki et al., 2011](#), [Ohler et al., 2011](#), [Mann et al., 2012](#)), the underlying mechanisms in the lamina are not yet explored. Gogo is therefore a good candidate gene to analyze the mechanisms which are required to elaborate precise, stereotyped connections between photoreceptors and postsynaptic partners.

1.1 Principles of Axon guidance

During development, neurons extend their axons from their place of birth to their target neurons. The distance axons have to cover ranges from mm (e.g. interneurons) to more than one meter (e.g. human sciatic nerve). On their journey axons have to make various decisions: they turn, halt or extend, fasciculate or defasciculate (Tessier-Lavigne and Goodman, 1996, Dickson, 2002). How can an axon find the correct route from its cell body to its final synaptic target cell? In order to find their tracts, axons have a highly motile and sensitive growing tip - the growth cone - that is competent to sense, integrate and respond to different types of extracellular cues. These guidance cues are provided by neurons, glia and the extracellular matrix, and are able to transduce extracellular signals into changes in the morphology of an axon and thus influence guidance, branching, target recognition, synaptogenesis, and degeneration and regeneration. Guidance molecules can either act in long range or short range; they can be membrane- or matrixbound or secreted (figure 1-1). Regulated activation of signaling pathways at the growth cone promote either attraction or repulsion, resulting in growth cone collapse or axon extension. This is achieved through modulation of cytoskeletal dynamics within the growth cone (Tessier-Lavigne and Goodman, 1996, Dickson, 2002). Among the known guidance molecules, the canonical families of Netrins, Slits, Semaphorins and Ephrins are probably the best understood (Tessier-Lavigne and Goodman, 1996, Dickson, 2002, Raper and Mason, 2010). Signaling molecules also include certain morphogens, growth factors and modulatory cues. The latter influence the sensitivity of growth cones to respond to other guidance cues. Permissive cues are provided by cell adhesion molecules (CAMs) or components of the extracellular matrix (ECM) and promote axon extension by acting indirectly on the growth cone via receptor signaling (Raper and Mason, 2010).

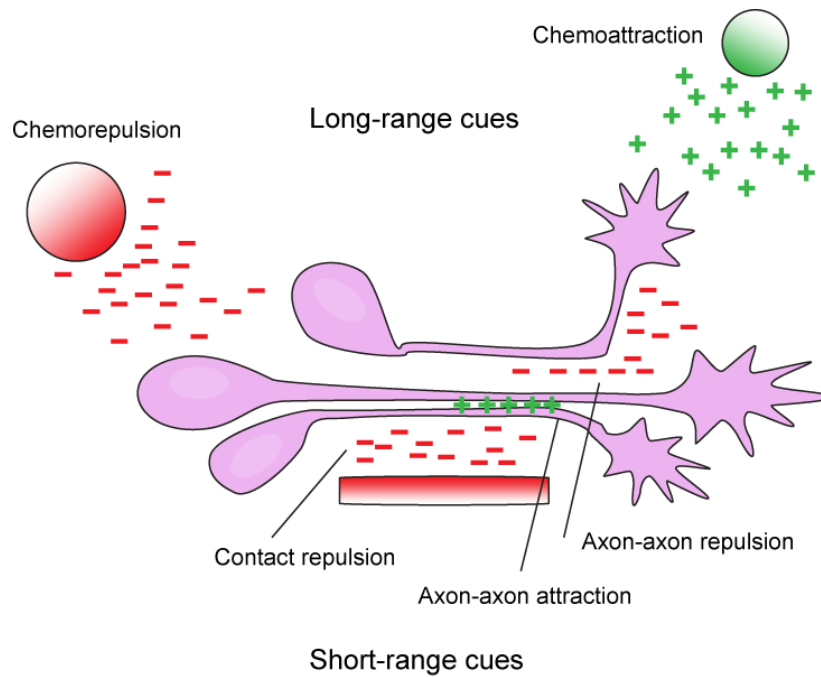


Figure 1-1 Axon guidance forces.

Long-range guidance cues can attract (chemoattraction) or repel (chemorepulsion) growth cones. Short-range guidance can be mediated by non-diffusible or local cues. In addition, attraction can be provided by axon-axon interactions resulting in selective fasciculation, whereas repulsion between neighboring axons can preserve a distance between them. Modified from (Tessier-Lavigne and Goodman, 1996).

1.2 Molecular mechanisms of visual system formation

A common feature of nervous systems is their organization in topographic maps. This means that neighboring neurons connect to neighboring target neurons resulting in parallel neuronal circuits displaying a columnar connection pattern. Columnar circuits are connected horizontally, forming different layered structured circuits. But how are precise connections specified through guidance cues during nervous system development? A classical model used to answer how topographic maps form during development is the visual system. This is due to the fact that the anatomy can be connected to the underlying function of the visual system. The retina creates a two-dimensional image of the environment. Photoreceptor neurons transduce the light to a two-dimensional field of post-synaptic neurons that reflect continuously the position of neighboring light points. The horizontal connections of this columns into different layers allow the processing of visual features like color detection, movement or brightness. Extensive studies of visual system development in a variety of

organisms have contributed to the identification of guidance cues and the molecular mechanisms underlying neuronal circuit development. In the following, I will summarize some of the important known molecular mechanisms for retinotopic mapping and layer-specific targeting.

Forming columnar connections by graded expression of axon guidance cues

About 50 years ago, [Roger Sperry](#) hypothesized that visual map formation depended on the graded expression of complementary molecules across the retina and the tectum ([Sperry, 1963](#)). Twenty-five years later the laboratory of [Friedrich Bonhoeffer](#) defined in an excellent *in vitro* assay the properties of guidance molecules in retinotopic map formation ([Walter et al., 1987](#)). In this assay, the membrane stripe assay, they found that retinal ganglion axons of chicks preferentially choose their appropriate topographic position between alternating stripes of anterior and posterior optic tectum membranes ([Walter et al., 1987](#)). In the vertebrate visual system, it has been demonstrated that gradients of the Eph/ephrin family of guidance cues are crucial for the overall layout of the retinotopic map ([figure 1-2 A](#)) ([Cheng et al., 1995](#), [Drescher et al., 1995](#)). Eph receptors and their ephrin ligands remain the dominant family controlling the organization of topographic connections in vertebrates. Initially ephrin-As were described to provide a repellent cue on retinal axons. Ephrin-As have been shown to determine the retinotectal anterior-posterior axis, while the ephrin-B subfamily acts as a mapping label along the dorso-ventral axis. Ephrins and their Eph receptors form countergradients along the axes. In chicken and mice, graded ephrin-A ligands are expressed in the tectum and the superior colliculus (SC), respectively, whereas the EphA receptors are expressed gradually in the retina along the temporal-nasal axes. In ephrin-A knockouts temporal retinal axons are misguided to a more posterior region of the tectum ([Frisen et al., 1998](#), [Feldheim et al., 2000](#)). Several assays demonstrated that ephrin-As and ephrin-Bs can act in a repulsive and an attractive manner ([Luo and Flanagan, 2007](#)). Interestingly, this bifunctionality is concentration dependent, as shown in an *in vitro* assay, in which ephrin concentration and axonal position were quantitatively compared ([Hansen et al., 2004](#)). This argues for a model, where ephrins mediate concentration-dependent attraction and repulsion during topographic mapping. Other molecules that could act redundantly with Ephrins during retinal mapping are 'repulsive guidance molecule' (RGM), which is expressed in a posterior-anterior gradient and Semaphorin (Sema3D), which is expressed in the ventral region of the zebrafish tectum ([Monnier et al., 2002](#), [Liu et al., 2004](#)). However, RGM knockout mice did not display a phenotype and therefore the role of RGM during map formation is still tentative ([Niederkofler et al., 2004](#)). Altered levels of Sema3D cause abnormal retinal targeting in the zebrafish tectum, but it is still not clear whether its

expression is discrete or gradual (Liu et al., 2004). Interestingly, in addition to topographic mapping, Ephrins also act as short-range signals during visual system development. Along the dorso-ventral axis the cell-cell signaling molecules of the Wnt family affect the topographic position of retinal ganglion cells. In the mouse, the receptor tyrosine kinase Ryk mediates repulsion when Wnt3 is expressed in high levels, whereas attraction is promoted by Frizzled when Wnt3 concentration is low (Schmitt et al., 2006).

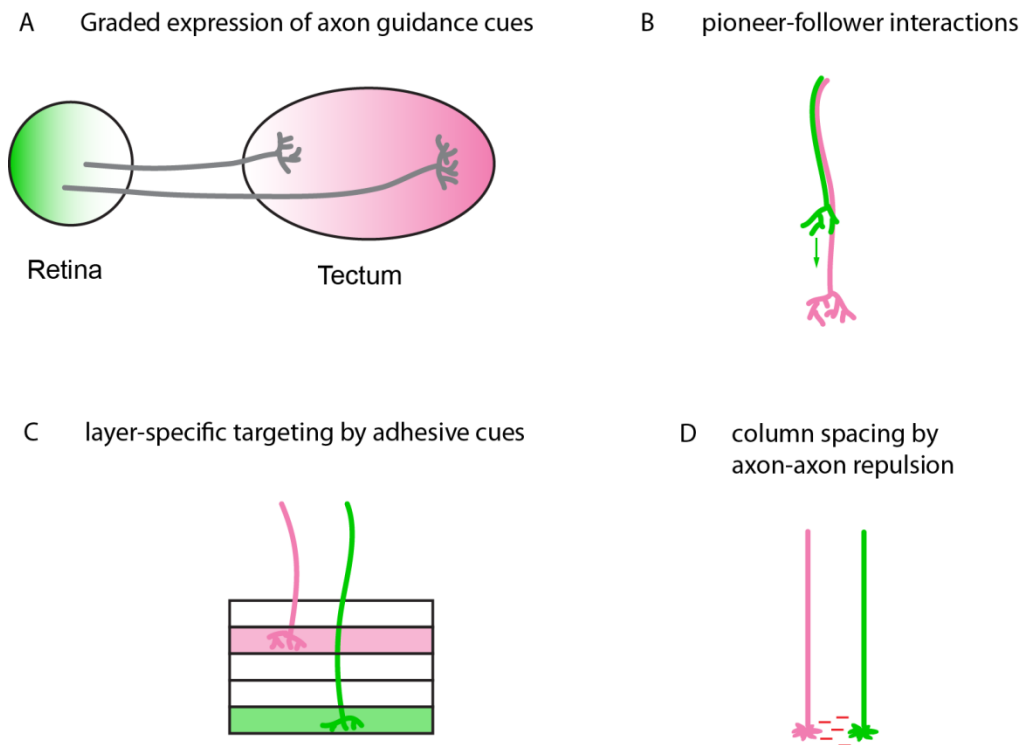


Figure 1-2 Schematic of molecular mechanisms of visual system formation.

(A) A common pathway to regulate topographic positioning is the graded expression of repulsive and attractive guidance cues. **(B)** Early outgrowing axons can determine tracts for later growing axons. **(C)** Layer specificity is often mediated by diffusible or membrane-bound short-range attractive cues. **(D)** Repulsive afferent-afferent interactions can regulate column restriction.

Assembly of the retinotopic map by pioneer-follower interactions

A remarkably feature of the visual system is that the relative position of retinal axons are already determined prior to axon-target interactions. A nice example comes from the Goldfish: ablation of half of the tectum results in a compression of the retinal axons into the remaining leftover of the tectum. Conversely, when parts of the retina are ablated, the remaining retinal axons spread over the entire tectal surface (Gaze and Sharma, 1968, Yoon, 1971, Yoon, 1976). This clearly reveals that visuotopic map development can not only be explained by the 'lock and key-principle', but also requires a 'self-organisation'. Recent studies indeed explained several mechanisms for self-organization based on axon-axon interactions rather than axon-target interactions. Experiments in the zebrafish demonstrated how pioneer axons can create a scaffold for follower axons during retinotopic map formation (figure 1-2, B) (Pittman et al., 2008). When Roundabout2 (*Robo2*) is absent, retinal axons mistarget (Hutson and Chien, 2002). Transplantation of *Robo2*⁻ pioneer axons in fish in which retinal axon outgrowth is blocked (*ath5* morphant fish) rescues the outgrowth of wild-type follower axons, but their projection pattern resemble the phenotype of *Robo2*⁻ axons (Pittman et al., 2008). When wild-type pioneer axons are transplanted in *Robo2* fishes in which outgrowth of retinal axons is blocked (*ath5* morphant fish), the projections of *Robo2* mutant axons closely resembles the wild-type, indicating an important role for pioneer-follower interactions in proper retinotopic map formation (Pittman et al., 2008). Axon guidance is in general (if not always) initiated by pioneer axons which are predicted to provide a scaffold for subsequent axons (Bate, 1976, Ho and Goodman, 1982, Raper et al., 1983, Raper and Mason, 2010). Despite those results, the molecular basis of this mechanism remains poorly understood.

Layer recognition by adhesion molecules. Molecular matching through adhesion molecules is thought to drive lamina-specific targeting, such that contact between pre- and postsynaptic neurons can only be stabilized between matching cells (figure 1-2 C). Molecules involved in lamina-specific targeting belong to the two major families of cell adhesion molecules (CAMs), the cadherin and immunoglobulin superfamilies (IgSF) (Shapiro et al., 2007, Takeichi, 2007). In the chick retina, pre- and postsynaptic neurons recognize each other by the homophilic IgSF molecules Sidekick1 (*Sdk1*), *Sdk2*, Down Syndrome Cell Adhesion Molecule (*DSCAM*) and *DSCAM*-like (Yoon, 1971, Yamagata et al., 2002, Yamagata and Sanes, 2008). All four genes are expressed in non-overlapping interneurons within appropriate layers of the Inner Plexiform Layer (IPL) in the retina and the Superior colliculus (SC). Contacts are mostly stabilized when pre- and post-synaptic cells express the same molecule. When the expression level of *Sdk1*, *Sdk2*, *Dscam* or *DscamL* is decreased by RNAi, RGC fail to innervate their appropriate layer and overshoot into other

layers. Conversely, misexpression of one of these four molecules redirects RGCs to the layer which expresses the corresponding molecule (Yamagata et al., 2002, Yamagata and Sanes, 2008). In the mouse, Dscam is required for self-avoidance and mosaic spacing, however, it is unclear if it is also required for layer-specificity (Fuerst et al., 2008, Fuerst et al., 2010). Other classes of molecules, such as Cadherins, have been implicated in cell-cell recognition, but their involvement in lamination is not yet clear (Inoue and Sanes, 1997, Poskanzer et al., 2003).

Homotypic repellent interactions. Retinal neurons are not only organized in layers but also in the horizontal plane of the retina. In vertebrates, the same cell-type is positioned in a regular way through one of the layers, an organization that is termed retinal mosaic. Spacing between dendrites can be achieved by repellent interactions (figure 1-2 D). Recently, it has been shown that the Down Syndrome Cell Adhesion molecule (DSCAM) mediates repulsive homotypic interactions between amacrine cells (Fuerst et al., 2008). A loss of DSCAM disrupts the spacing of the neurites. Conceptually this mechanism is similar to axon/dendrite tiling such that neurons of the same subtype completely cover a receptive field with minimal overlap of dendritic or axonal arbors. In *Drosophila* it has been shown that restriction of L1 lamina neurons into their columns is achieved through homophilic repulsive interactions mediated by Dscam2 (Millard et al., 2010).

During their journey, axons are confronted with many competitive guidance cues from different sources. It is the combination of different cues and mechanisms and the correct spatial and temporal expression of these cues that ensure the correct circuit formation (Raper and Mason, 2010). In addition to molecular guidance cues, growth cones can also integrate electric gradients and physical constraints. For instance, during the development of vertebrate visual systems, spontaneous neural activity in combination with molecules is crucial for path finding and target recognition (Raper and Mason, 2010). In *Drosophila*, it has been shown that the formation of neuronal circuits can be independent of neuronal activity. (Hiesinger et al., 2006). In the next chapter I will explain the anatomy of the adult *Drosophila* visual system, before I will focus on the underlying developmental cellular and molecular mechanisms.

1.3 Anatomy and neuronal projections of the *Drosophila* visual system

When [Santiago Ramon y Cajal](#) compared the complexity of retina from flies and vertebrates he was - despite the enormous differences in size - ...

“...amazed and confounded by the supreme constructive ingenuity revealed not only in the retina and dioptric apparatus of vertebrates but even in the meanest insect eye” page 576 ([Ramon y Cajal, 1923](#))

Since this time, biologists have noted remarkable similarities between the visual system of invertebrates and vertebrates – not only according to their anatomy, but also on a molecular basis. A detailed structural analysis of the *Drosophila melanogaster* visual system was conducted by [Meinertzhagen and O’Neil](#) in 1991 ([Meinertzhagen and O’Neil, 1991](#)). The *Drosophila* adult visual system comprises the compound eye and the optic lobe, which is subdivided in four optic ganglia, the medulla, lamina, lobula and lobula plate ([figure 1-3 A, B](#)) ([Meinertzhagen and O’Neil, 1991](#), [Meinertzhagen, 1993](#)); the latter two compose the lobula complex. The compound eye is a highly organized structure which comprises a precise, hexagonally defined structure. The retina is arranged in an array of about 750 units called ommatidia. Each retinal ommatidium contains eight different types of photoreceptor neurons or retinula (R) cells, along with supporting cells (i.e., cone cells). Their light-seeing rhabdomeres receive input from seven different optical axes beneath a single lens and innervate the two outermost ganglia, the lamina and the medulla. Based on their rhodopsin expression R cells are divided into three subtypes. The outer R cells, R1-R6, express Rhodopsin 1 (Rh1) ([O’Tousa et al., 1985](#), [Zuker et al., 1985](#)), responding to a broad spectrum of wavelengths ([Hardie, 1979](#)), and mediate spatial vision. The inner R7 and R8 cells provide chromatic information and express UV-sensitive Rh3 or Rh4 opsin or blue- and green light sensitive Rh5 or Rh6 opsin, respectively ([Fryxell and Meyerowitz, 1987](#), [Montell et al., 1987](#), [Zuker et al., 1987](#), [Chou et al., 1996](#), [Papatsenko et al., 1997](#)). R7 and R8 cells are specialized for color vision and the detection of polarized light. In the broader sense, R1-R6 can be compared with vertebrate rods and R7/R8 with vertebrate cones, but unlike their vertebrate glutamatergic counterparts, *Drosophila*’s photoreceptor neurons are histaminergic ([Hardie, 1987](#), [Sarthy, 1991](#)).

In contrast to vertebrates, *Drosophila* R axons do not form synapses in the retina, but project directly to the visual processing centers of the brain. According to their different functionality, R axons target to different optic ganglia ([Meinertzhagen and Hanson, 1993](#)): R1-R6 innervate the lamina, whereas R7 and R8 project through the lamina to terminate at different layers in the underlying medulla. In each ommatidium R1-R8 axons project in a way

to the brain such that photoreceptors receiving the same light input innervate the same lamina or medulla columns. As *Drosophila* has an open rhabdomere system, R1-R8 cells within the same ommatidium have different optical axes beneath the same lens. As a result of the eye's curvature, a set of R1-R6 cells that originate from different neighboring ommatidia share the same optical axis and receive input from the same point in visual space. In order to sustain retinotopy, R1-R6 cells form a complex pattern of connections with postsynaptic neurons within the lamina that reflect the spatial organization of their rhabdomeres. In other words, the input of the six R1-R6 axons that "see" the same point in space is pooled on the same set of lamina and widefield neurons (figure 1-3 C). The resulting synaptic units are called cartridges. This remarkable feature of axonal resorting is called neural superposition and increases the light detection sensitivity of the fly by enhancing the signal-to-noise ratio (Meinertzhagen and Hanson, 1993). Lamina neurons (L1-L3) of each cartridge, in turn, innervate different layers in a single medulla column via the optic chiasm. Additionally, medulla columns are innervated by two R7 and R8 neurons that "see" the same light point. In this way, the columnar organization of the retinotopic map is retained and as a consequence, each medulla column receives direct input from R7 and R8 and indirectly from R1-R6 (Fischbach and Dittrich, 1989).

The lamina, in contrast to the medulla contains more different types of neurons. Single medulla columns are subdivided into ten layers, M1-10. R7 and R8 target directly to M3 and M6, respectively, whereas L1-L3 terminate in one or a few of M1-M5 layers (figure 1-3 D). Postsynaptic neurons (e.g. medulla tangential neurons and medulla interneurons) also arborize in discrete medulla layers but can span over neighboring columns and thus increase the receptive field. While interneurons are restricted to the medulla, transmedulla neurons converge to the deeper lobula complex. TM neurons project to higher order neurons in the lobula and Transmedulla Y neurons to both the lobula and lobula plate, where multiple pathways transmit visual signals to central brain regions (Fischbach and Dittrich, 1989).

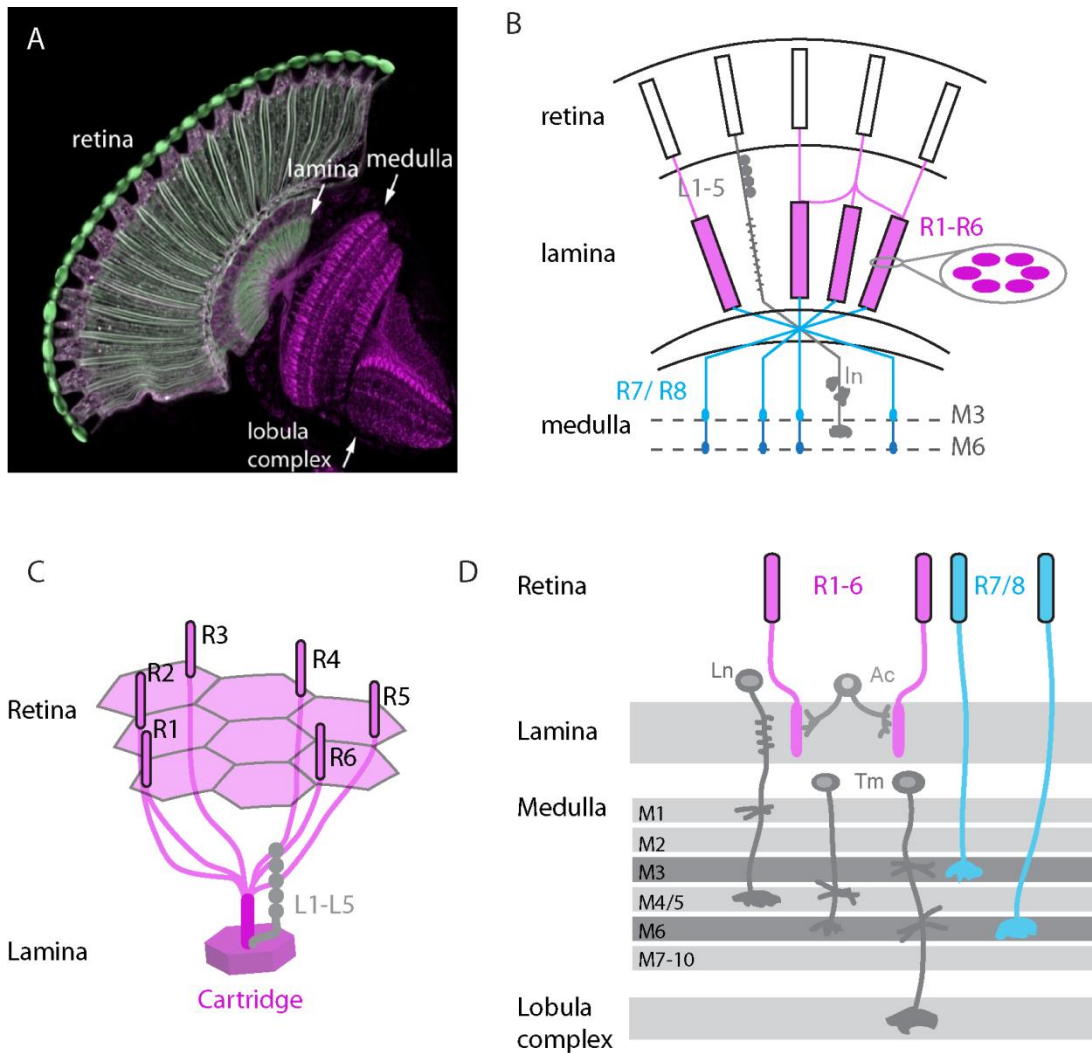


Figure 1-3 The *Drosophila* compound eye: anatomy and synaptic organization

(A) Cross section of the adult visual system. The retina is built up of about 750 ommatidia each covered by a single lens cells. The long rhabdomeres of the photoreceptor cells in the retina cover the major part of the eye. The lamina neuropile is located directly beneath the retina and is structured in columns. R7 and R8 form the optic chiasm and their axons cross to target the contralateral side of the brain. The medulla and the lobula complex are organized in layers and columns. **(B)** Schematic drawing of the compound eye in a horizontal view. R1-R6 innervate the lamina whereas R7 and R8 target to the M3 and M6 layers, respectively, in the underlying medulla (only M3 and M6 are shown). The cell bodies of lamina neurons are located between the retina and the lamina. **(C)** Six different R1-R6 axons from six neighboring ommatidia that receive the same light input converge to a set of lamina neurons to a single synaptic unit, the lamina cartridge. **(D)** R1-R6 are critical for motion vision and provide achromatic synaptic input to lamina neurons which in turn are connected to neurons in the medulla. R7 and R8 transfer chromatic synaptic input directly to transmedulla neurons in different layers of the medulla. Transmedulla neurons transfer visual information to higher-order neurons in the lobula complex (Modified from (Sanes and Zipursky, 2010, Hadjieconomou et al., 2011).

1.4 Control of visual system development in *Drosophila*

Early development of the visual system

Eye development in *Drosophila melanogaster* spans 10 days and occurs in a step-by-step fashion that takes place in three stages: 1) navigation of R axons to the right ganglion (medulla and lamina), 2) selection of the correct target region within the ganglion and 3) synapse formation with the proper target neurons. The compound eye of *Drosophila* (retina, lamina and medulla) emerges from two different primordia. The retina, as other adult holometabolous insect organs, arises from a hollow sac of embryonic tissue-specific progenitor cells, the eye imaginal disc. Lamina and medulla are derived from neuronal stem cells (neuroblasts) that are localized in the presumptive optic lobe. Both structures are connected to each other via the optic stalk. The eye-disc originates early during embryonic development and it grows by cell division until mid-instar larval stage, when each eye-disc contains about 10000 cells (Wolff and Ready, 1993). The transition from proliferation to differentiation starts with the appearance of a dorso-ventral wave of cells, the morphogenetic furrow. R cells assemble in two rows of ommatidial cluster until reaching the anterior margin of the eye disc after around 2 days. The proximate outgrowth of retinal axons occurs in a second temporal wave along the antero-posterior and dorso-ventral axes of the eye disc following the wave of R cell differentiation. During pupal development, which spans about 100 hours, immense reorganization of the visual system takes place. The eye disc is transformed into the pupal eye, the lamina is centered behind the retina and the medulla neuropile rotates 90° forming the optic chiasm. R1-R8 axons reach their final targets, and begin synaptogenesis within the second half of pupal development (Meinertzhagen and Hanson, 1993).

Within each ommatidium the R8 differentiates first and extend its growth cone through the optic stalk towards the brain. Its outgrowth is dependent on interactions with retinal glial cells (Hummel et al., 2002). R8 terminates in the medulla passing through the lamina. In sequential steps R8 is followed by R2 & R5, R3 & R4, and R1 & R6 (Meinertzhagen and Hanson, 1993). R1-R6 axons fasciculate and follow the trajectories of R8, but terminate at the lamina plexus between two rows of glia cells. R7 is the last one to differentiate and project through the lamina to terminate the medulla. During their journey towards the brain ommatidial fascicles strictly maintain their columnar organization and terminate in the lamina plexus in a topographic pattern, forming the initial topographic map (Meinertzhagen and Hanson, 1993). The discrete restriction to columns is crucial to maintain the relative position between single axons and between axonal fascicles with respect to ommatidial arrangement. A number of genes are required for R1-R6 axon spacing. Mutations in the adaptor protein

dreadlocks (dock), trio and p21-activated kinase (pak) lead to several phenotypes, including bundling of R axons that fail to order topographically (Garrity et al., 1996, Hing et al., 1999, Newsome et al., 2000b). In addition, the Netrin receptor Frazzled is necessary for R axons to project correctly, although Netrin itself does not appear to have a function in this system (Gong et al., 1999). In *Drosophila*, morphological studies revealed that R8 growth cones precede within each ommatidial fascicle (Meinertzhagen and O'Neil, 1991). As in vertebrates, retina development in *Drosophila* is mostly independent of the brain. When the fly's retina is ectopically transplanted (Chevais, 1937) or *eyeless* is ectopically expressed (Halder et al., 1995), retina development appears normal. In contrast, the development of the ganglia is dependent on inductive signals provided by R cells (Selleck and Steller, 1991, Huang and Kunes, 1996). Along the anterior-posterior axis, arriving R8 axons secrete the anterograde signal Hedgehog (Hh) which causes lamina precursor cells (LPCs) to undergo a final round of cell division and to differentiate (Huang and Kunes, 1996). Hh also promotes the expression of the transcription factor single-minded (Sim) which induces neurogenesis and differentiation in the lamina, ensuring that the number of lamina neuron columns matches the number of ommatidia (Huang and Kunes, 1996, 1998, Huang et al., 1998). Each ommatidial fascicle associates with a column of 5 LNs to form pre-cartridges. LNs and R1-R6 axons are correctly incorporated to pre-cartridges via the two nephrin/NEPH1 family cell-adhesion receptors Hibiris and Roughest which are expressed in LNs and R axons, respectively (Umetsu et al., 2006, Sugie et al., 2010). In addition, Hh indirectly promotes the expression of EGFR in LPCs, making them receptive to the R cell released epidermal growth factor (EGF)-like ligand Spitz (Spi), which is also crucial for the correct assembly of LNs and for their neurogenesis (Huang and Kunes, 1998, Huang et al., 1998, Chotard et al., 2005). Along the dorso-ventral axes non-canonical Wnt4 and Frizzled2 signaling has been shown to mediate retinotopic map formation (Sato et al., 2006). In the ventral part of the eye imaginal disc retinal axons express Frizzled2 which enables them to respond to target neuron-released Wnt4 signal. In the dorsal half, Frizzled2 expression is suppressed to prevent axons from projecting to the ventral region. R axons promote outgrowth of scaffold axons, which function as a substrate for glia migration (Dearborn and Kunes, 2004). Interestingly, as in vertebrates, the *Drosophila* Eph receptor has been shown to mediate ventral-dorsal retinal projections (Dearborn et al., 2002). Most recently a new autonomous regulator of Eph, Regulator of Eph expression (Reph), has been described to be necessary for graded Eph expression and the formation of the retinotopic map (Dearborn et al., 2012).

Lamina development

During larval stages R1-R6 axons gradually extend from the eye disc and terminate at the same layer at the lamina plexus between two rows of glia cells. Glia cells in the lamina have been shown to play a crucial role as intermediate targets for R1-R6 axons by providing a yet unidentified “stop” signal. Postsynaptic neurons are not required for R1-R6 axons to stop at the lamina plexus nor for the timing of R1-R8 axon outgrowth (Huang and Kunes, 1996). However, the termination is a result of afferent axon interactions and lamina glia (Huang et al., 1998, Suh et al., 2002, Chotard et al., 2005). Disruption of glia cells by genes that affect their determination, differentiation and migration, such as *glia cell missing (gcm) non-stop* or *JAB1*, results in most R1-R6 growth cones overshooting the lamina and extending to the medulla neuropile (Poeck et al., 2001, Suh et al., 2002). Additionally, several molecules enable R cells response to the glia derived “stop” signal. In particular, ganglion-specific targeting phenotypes have been observed in mutant flies affecting the receptor tyrosine kinase Off-track, Dock, the receptor tyrosine phosphatase PTP69D, the Leukogen-antigen-related-link (LAR), and the serine/threonine kinase Misshapen (Garrity et al., 1996, Garrity et al., 1999, Su et al., 2000, Clandinin et al., 2001b, Ruan et al., 2002, Cafferty et al., 2004). These molecules show less severe phenotypes than the glia affecting mutants – probably due to redundancy between their signaling mechanisms. Additionally, R cells require the nuclear protein Brakeless (Bks) to respond to the stop signal (Rao et al., 2000, Senti et al., 2000). Brakeless represses the expression of the TF Runt that is normally expressed in R7 and R8 (Kaminker et al., 2002). When Runt is mis-expressed in R2 and R5, R1-R6 axons do not stop at the lamina plexus but overshoot to the medulla without a change in cell identity (Kaminker et al., 2002). This also clearly indicates that between R1-R6 axons axon-axon interactions play a crucial role for correct targeting, as mis-expression of Runt solely in R2 and R5 triggers overshooting of all R1-R6 cells.

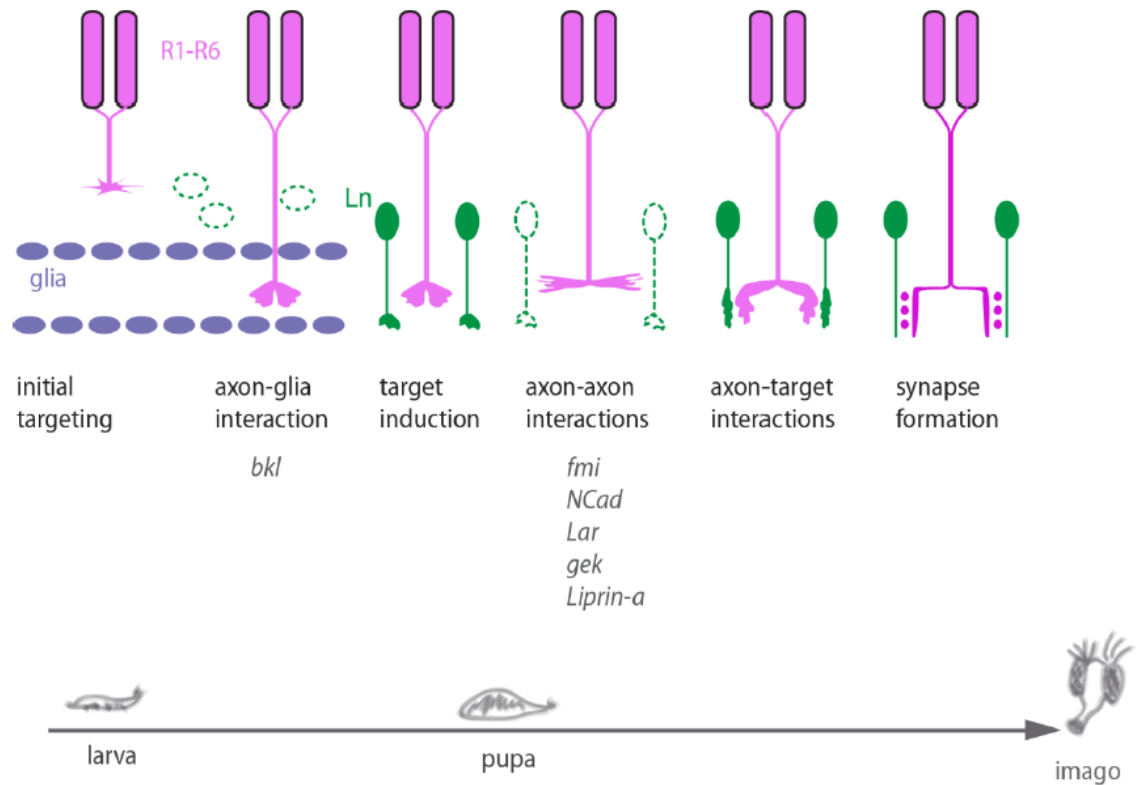


Figure 1-4 Column formation in the lamina

During 3rd instar larval stages, R1-R6 axons extend in a single fascicle towards the brain and terminate between two layers of glia cells which provide a stop signal to R cells. R cell signaling induces lamina neuron (LN) development and ensures that the number of lamina columns is equal to the number of ommatidial fascicles. Once R axons reached the lamina plexus they defasciculate during the first half of pupal development and extend laterally to innervate different LN columns. The direction of individual growth cones is determined by afferent-afferent interactions. After R axons select their target-cartridges they turn again and extend centripetally to synapse with parallel elongating LNs. Modified from (Sanes and Zipursky, 2010).

Once R1-R6 cells terminate their intermediate target they halt for about 36 hours to synchronize the timing of their further development (figure 1-4). Interestingly the pause of axon growth cones at the lamina plexus is regulated by nitric oxide (NO) provided from lamina neurons (Gibbs and Truman, 1998). While during larval development NO has no influence on axon guidance, removal of NO signaling during R1-R6 axon pause in early pupa causes them to overextend to the medulla. This indicates that intermediate targeting is crucial for correct R1-R6 targeting (Gibbs and Truman, 1998). Initially R1-R6 axons that originate from the same ommatidium innervate the brain in a single fascicle and associate with columns of 5 lamina neurons maintaining the spatial position of their cell-bodies in the

retina (Meinertzhagen, 1993). As described above, due to the curvature of the eye and the different optical axes of R1-R6 cells in the retina their axons have to be resorted during development to maintain retinotopic mapping (neural superposition). Within a narrow time window between 12.5% and 50% of pupal development R1-R6 growth cones leave their original fascicle and extend laterally to innervate different columns of lamina target neurons (figure 1-4). As a result, the six R1-R6 neurons (originating from different neighboring ommatidia) corresponding to the same point in visual space, converge onto the same set of LNs, forming a cartridge. Thus, each cartridge receives input from six termini, one of each R1-R6 from different ommatidia (i.e. one R1 axon from one ommatidium, one R2 axon of the neighboring ommatidia and so on). The pattern made by R1-R6 axons is highly reproducible and invariant, and is directly related to the orientation of bodies (figure 1-5). In pupae, R1-R8 cell bodies form a flower shaped structure and each R cell subtype can be identified based on its position and morphology. The lateral extensions made by R1-R6 axons are by 180° rotated with respect to their cell-bodies. Anatomical studies revealed that R1-R6 axons contact each other during the fasciculation process and that this interaction can be correlated to orientation changes made by each growth cone (Meinertzhagen and O'Neil, 1991). Clandinin and Zipursky subsequently used ablation studies to demonstrate that indeed afferent-afferent interactions play a major role in correct cartridge choice (Clandinin and Zipursky, 2000). In particular, they used mutants that transform subsets of R1-R6 cells into different cell types and analyzed the axonal behavior of the remaining R cells at the lamina plexus. They first demonstrated that defasciculation of R1-R6 is not changed in the mutant backgrounds of *phyllopod* (R1, R6 and R7 are transformed into cone cells), *lozenge^{sprite}* (R3 and R4 are transformed into R7) and *seven-up* (R3, R4, R1 and R6 are transformed into R7). When R1 and R6 axons are absent, R3 and R4 behave normally whereas R2 and R5 sometimes innervate aberrant targets. The absence of R3 and R4 alone leads to a high degree of mis-innervation of R1, R2, R5 and R6. R2 and R5 always fail to target correctly when all other R cells are absent (Clandinin and Zipursky, 2000). This strongly argues for axon interactions within the ommatidial bundle and further that the position of R3 and R4 determines directions of the other R axons. In contrast, axon-target interactions between R axons and lamina neurons seem to play only a secondary role in target specificity. When ommatidia cell-bodies in the *frizzled* mutant are by 180° rotated, the projection of the axon within the lamina is also by 180° rotated. However when ommatidia rotation is only 45° as it is the case in *nemo* mutants, the axonal projection is not re-orientated with respect to the cell-body (Clandinin and Zipursky, 2000).

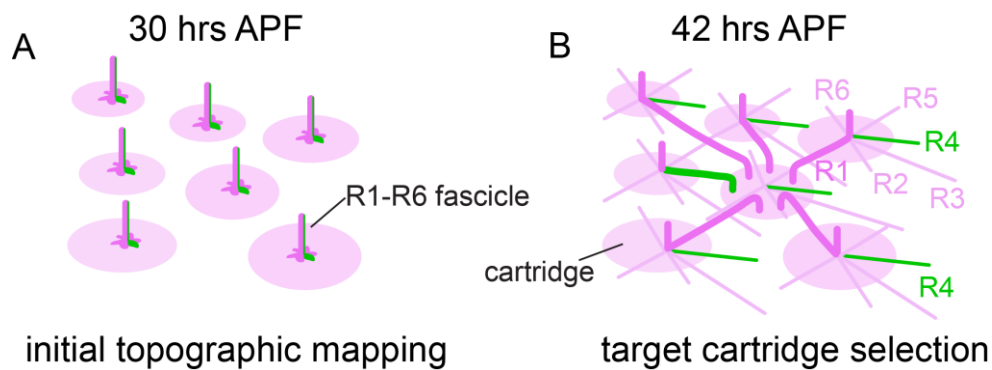


Figure 1-5 Cartridge selection in the lamina

(A-B) Schematics of cartridge assembly. **(A)** R1-6 axon fascicles reach the lamina plexus in a precise spatial pattern, forming the initial topographic map (30 hrs APF), whereas R8 projects through the lamina to innervate the medulla. **(B)** Subsequently, R1-6 growth cones defasciculate simultaneously and extend across the lamina surface to innervate neighboring target cartridges. The pattern made by each R1-R6 subtype is stereotypic and invariant with respect to the position of their ommatidial cell bodies. As a consequence of the neural superposition, each target cartridge is innervated by six R1-R6 axons that originate from six different ommatidia.

More insight into the molecular mechanisms of R1-R6 target cartridge selection came from an optomotor behavior screen in which several genes were discovered (Clandinin et al., 2001b, Lee et al., 2001). The cadherin related surface protein Flamingo (Fmi) was the first that was described for regulating R1-R6 lamina patterning and is expressed in all R cells during larval and pupal development (Lee et al., 2001). Fmi had been shown earlier to play a putative role in mediating dendritic field patterning (Gao et al., 2000) and planar cell polarity – also in ommatidial cell bodies (Chae et al., 1999, Lu et al., 1999). Loss of *flamingo* leads to a strong hypo- and hyperinnervation resulting in variable numbers of terminals per cartridge. Single cell analysis revealed that Flamingo is required non-cell autonomously in individual R cell axons (Chen and Clandinin, 2008). While mutant axons always choose the correct target cartridge, wild-type axons adjacent to mutant axons extend inappropriately. Altering Fmi levels in single R cell subtypes suggested that single growth cones are sensitive to expression levels in neighboring R cells. This indicates that Fmi is mediating the relative positions among afferents through homophilic repulsive interactions in a protein level-dependent manner (Chen and Clandinin, 2008). In the same screen for blind flies the homophilic adhesive receptor N-Cadherin, the receptor tyrosine kinase Leukocyte antigen-related (Lar) and the synaptic scaffolding molecule Liprin- α were discovered as regulators of

afferent-afferent interactions. In particular, the lack of either of these proteins prevented R1-R6 axon extension from the ommatidial bundle (Clandinin et al., 2001b, Lee et al., 2001, Prakash et al., 2005, Choe et al., 2006). Further work demonstrated that CadN, but not Lar and Liprin- α , are also required in target cartridges, likely to stabilize afferent-target interactions (Prakash et al., 2005). When CadN is absent in lamina neurons, wild-type R1-R6 axons preferentially choose CadN-positive target cartridges. Genetic and biochemical studies discovered that Lar, CadN and Liprin-a function in a complex to mediate these afferent-target interactions (Prakash et al., 2009). A similar role in the establishment of projections within the lamina has been shown for the Anaplastic lymphoma kinase (Alk) / low-density lipoprotein (LDL) receptor repeat-containing secreted factor Jelly belly (Jeb) signaling (Bazigou et al., 2007). Jeb mutant axons extend away from their home-cartridge and choose inappropriate targets (Bazigou et al., 2007). Most recently the serine-threonine kinase Genghis khan (Gek) has been described to mediate target selection in R1-R6 targeting (Gontang et al., 2011). Interestingly, Gek is the first gene discovered that is required for lamina but not for medulla targeting.

After selecting their target cartridges, R cells form pre-synapses with lamina monopolar neurons and travel centripetally along the lamina neuron axons. EM reconstructions provided a detailed description of synaptic connections in the lamina and the pre- and postsynaptic cells of more than 10 different types of neurons (Meinertzhagen and O'Neil, 1991). A single lamina cartridge contains five monopolar neuron cell types, L1-L5, amacrine and centrifugal interneurons (Meinertzhagen and Sorra, 2001). Several recent studies focused on the formation of tetrad synapses (Hiesinger et al., 2006, Rister et al., 2007, Katsov and Clandinin, 2008, Joesch et al., 2010). Each R1-R6 terminal forms about 50 multiple contact presynaptic sites. The main synapses are formed by one presynaptic terminal juxtaposed to four different postsynaptic elements, the tetrads. The postsynaptic elements include an invariable pair of L1 and L2 targets and variable elements out of L3, amacrine cells, and/or glia. L1-L5, in turn, project to M1-M5 layers within the medulla. The required part of L1 and L2 of every tetrad synapse is likely regulated by dendrites. At mid-pupal stages numerous L1 and L2 dendrites randomly cover R1-R6 termini, but regress in later stages leaving inappropriate targets. This synaptic specificity is mediated by Dscam1 and Dscam2 via homophilic repulsion (Millard et al., 2010). Interestingly, synapse number between R axons and LNs is not only independent of neuronal activity but also of the number of termini per cartridge, strongly suggesting a presynaptic determination of synapse formation (Hiesinger et al., 2006). However, the development of the complex connections within the lamina remains poorly understood.

Golden goal function during medulla targeting

R7, R8 and lamina neurons select different layers in the medulla in a two-step process (figure 2-6 A). The axons of R7, R8 and lamina neurons are restricted to their appropriate columns preserving the retinotopic map. R8 axons first extend sequentially to the developing medulla and transiently halt at the M1 layer at around 24hrs APF. R7 axons overtake R8 and transiently halt at the M3 layer. At the same time, lamina neurons extend to their specific medulla layers. From 50 hrs to 60 hrs APF R8 and R7 extend to their final M3 and M6 layers, respectively. A screen to identify genes involved in axon pathfinding in the visual system discovered the transmembrane protein Golden goal (Gogo) as a regulator for R8 medulla targeting. What is so far known about the function of Gogo during R8 target specificity? Gogo has been shown to be a multifunctional protein that mediates axon-axon and axon-target interactions in R8 axons (figure 1-6 B). Together with the adhesion molecule Capricious (Caps) and the atypical cadherin Flamingo (Fmi), Gogo is one of the three surface molecules described to mediate synaptic layer-specificity in R8 axons (Shishido et al., 1998, Shinza-Kameda et al., 2006, Berger et al., 2008, Tomasi et al., 2008). *gogo* encodes a 1272 aa single transmembrane protein (Tomasi et al., 2008). Its extracellular region contains a TSP1 and a CUB domain which are present in several proteins that direct cell growth and growth cone guidance. Additionally a conserved region of eight cysteins, the GOGO domain, has been described. Both, the GOGO and TSP1 domain are necessary for Gogo function during R8 targeting and homologs containing both domains were identified in other insects, nematodes and vertebrates. Although in third instar larval stages Gogo expression can only be detected in R8 growth cones and in medulla neurons, during early pupal development, later on it is present in R1-R6 growth cones. Gogo is also expressed in R7 axons but apparently not required there for medulla targeting. Gogo appears to have distinct function in different contexts: In larval stages it is required for axon-axon interactions between R8 axons. There it is hypothesized to function as a heterophilic receptor that repels R8 axons from each other and thus ensures column specificity (Tomasi et al., 2008). During layer-specific targeting of R8 axons Gogo promotes axon-target recognition at M1 temporary layer. Interestingly, a recent study shows that Gogo and Fmi co-operate in some aspects of layer-specific (Hakeda-Suzuki et al., 2011). Both genes are dynamically expressed in R8 at this developmental stage. Loss of *fmi* or *gogo* cause inappropriate stopping of R8 axons at the M1 intermediate layer (Lee et al., 2003, Senti et al., 2003, Tomasi et al., 2008). While Gogo alone promotes R8 axon adhesion at intermediate M1 layer, Gogo and Fmi collaborate during final M3 layer-targeting. Function analysis revealed that Gogo and Fmi interact with intracellular components through the Gogo cytoplasmic domain. Both genes are dynamically expressed in R8 at this developmental stage. Gogo overexpression leads to R8 stopping in M1, suggesting that Gogo promotes M1 target-recognition (Tomasi et al., 2008). Recent

work demonstrated that final M3 targeting depends on the interaction of Flamingo with Gogo and the actin-cytoskeleton regulator Hu-li tai shao (Hts) (Lee et al., 2003, Senti et al., 2003, Tomasi et al., 2008, Hakeda-Suzuki et al., 2011, Ohler et al., 2011).

Recently it has been demonstrated that the Gogo is also required for lamina targeting (Hakeda-Suzuki et al., 2011). The absence of Gogo causes defects in the adult lamina. While several studies elucidated already the underlying molecular mechanism during R8 medulla targeting, the role of Gogo during R1-R6 lamina pathfinding remains completely unclear. Although Gogo and Fmi display similar defects in the adult lamina, it seems likely that the guidance mechanism underlying R1-R6 target cartridge selection is distinct from R8 pathway finding: Unlike in R8 targeting, Fmi has a non-autonomous function in R1-R6 lamina target selection (Chen and Clandinin, 2008). Thus, it would be interesting to reveal the contribution of Gogo for cartridge formation.

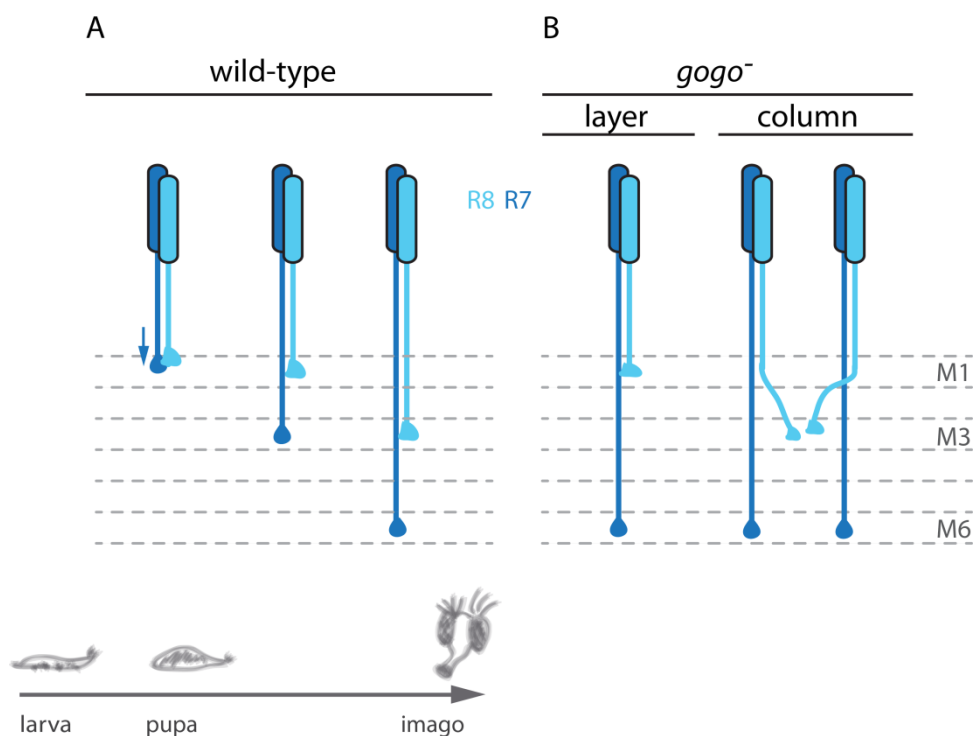


Figure 1-6 Gogo function during medulla targeting

(A) At the end of larval development growth cones of R8 and R7 temporarily halt and their growth cones come close together. During the first half of pupal development R8 proceeds to its intermediate layer M1, while R7 overtakes R8 and pauses at its temporary M3 layer. In a second step starting from around 55-60 hours APF R8 and R7 extend to their final layers M3 and M6, respectively, where they develop mature synapses with post-synaptic neurons.

During the target process, R7 and R8 maintain the position within the column. **(B)** Gogo mediates layer- and column-specific targeting. Loss of gogo leads to stalling of R8 axons at the intermediate layer M1. Moreover, Gogo permits axons to separate from each other. In the absence of Gogo R8 axons fail to maintain their columns and bundle with neighboring mutant axons.

1.5 This thesis

Given what is known about the construction, function and development of visual systems, this provides a unique model to study the mechanisms of retinotopic map formation. In particular, the visual system of *Drosophila* has two advantages: First, the *Drosophila* lamina as a model is highly reproducible and sufficiently precise in order to distinguish anatomical differences that occur between individuals and those reflecting irregularities within the species. Second, the genetic tools available in *Drosophila* combined with the detailed description of anatomy, development and function provide a good opportunity for studying retinotopic map formation *in vivo*.

Although several important axon guidance molecules and their underlying guidance mechanisms have already been identified, the mechanism for synapse specificity in the *Drosophila* visual system are still insufficiently explored. It has been previously shown that the absence of the transmembrane protein Gogo causes strong defects in the retinal connections of the medulla and lamina (Tomasi et al., 2008, Hakeda-Suzuki et al., 2011). However, unlike medulla targeting, the underlying guidance mechanisms in the lamina are unknown. The aim of this project is to perform function analysis to discover how Gogo function in R cells to establish neuronal connectivity in lamina cartridges. I will dissect possible roles of Gogo during the three independent steps of lamina development: the ganglion-specific targeting of R1-R6 fascicles, the selection of appropriate target cartridges, and the elongation of R1-R6 termini within target cartridges. Previous work on lamina development mainly focused on afferent-afferent interactions mediated by target cartridge selection, while initial topographic mapping and cartridge elongation have received less attention. Possible functions of Gogo can be explained by detailed analysis of different mosaic experiments. Available R cell type specific markers allow visualization of specific R cells and the analysis of single and multiple cell behavior in a mutant background during different stages of development. Subsequent rescue experiments can reveal any specific requirement of Gogo. Revealing how Gogo mediates cartridge formation can help to increase our current understanding of molecular mechanisms and general principles of retinotopic mapping.

2 MATERIAL AND METHODS

2.1 Media and Standards

Standard *Drosophila* medium

For a total volume of 50 l medium, 585 g agar was mixed in 30 l cold H₂O by heating to the boiling point. A homogenous broth of 5 kg corn flour, 925 g yeast, 500 g soy flour, 4 kg molasses and H₂O was fold in the dissolved agar. The mash was filled up with H₂O to total volume of 50 l and cooked at 96°C for 1.5 hrs. After the mixture was cooled down to 60°C, 315 ml propionic acid, 120 g methylparaben, 125 g niparsin/methylparaben, 1l of 20% ethanol and 500 ml of 10% phosphatidic acid were added. The hot mash was filled into plastic bottles (Ø25 and 50mm) with about 2.5 cm fly food covering the bottom part and stored at 4°C for maximum 4 weeks.

Blue Yeast paste

Instant dry yeast (Femipan Inc.) was mixed with Instant blue *Drosophila* medium (Fisher Scientific) and water. A large pinch of fresh blue yeast paste was added to fly crosses.

2.2 Instruments

Incubator Unichromat 1500	Uniequip.
Incubator Percival	Percival
Leica MZ16 Fluorescent Dissect scope	Leica Germany
Leica MS5 Stereomicroscope	Leica Germany
Leica MZ9.5 Stereomicroscope	Leica Germany
Leica Axioscope 2 plus Fluorescent Microscope	Leica Germany
Zeiss Axiovert S100	Zeiss Germany
Leica DFC 320 digital camera	Leica Germany

Olympus FV1000 confocal microscope	Olympus
blade microtome	Leica VT1000S

Table 1 List of chemicals

Chemical	Source
Acetic acid	Fluka
Agar-Agar	Roth
Agarose, high electrendosmosis	Biomol
Agarose NEEO Ultra - Qualtiaet	Roth
Ethanol abs.	Sigma Aldrich
EDTA	Sigma Aldrich
Fetal bovine serum	PromoCell GmbH
Formaldehyde (35%)	Roth
Formaldehyde (10%)	Roth
Glycerol	Merck
Heptane	Fluka
Hydrochloric acid	Merck
Isopropanol (2-propanol)	Sigma Aldrich
L-Glutamine 200mM	PAA Laborities
Methanol	Roth
Sodium chloride	Sigma Aldrich
Triton X-100	Roth
Tryptone	Sigma
Tween 20	Sigma

Yeast extract	Sigma Aldrich
Hydrochloric acid (HCl)	Merck
Sodium chloride	Sigma
Tris base	Sigma
EDTA	Sigma Aldrich

2.3 Fly maintenance

Drosophila flies were raised and amplified in plastic bottles (Ø25 and 50mm) on *Drosophila* standard medium at 18 or 25°C (generation time around 4 weeks and 10 days, respectively) and a constant humidity between 60 and 70%. To keep stocks, flies from F1 generations were transferred to fresh bottles. For experiments and for the generation of new genotypes virgins and males of different strains were crossed in a 3:1 ratio. Female and male flies can be distinguished based on their anatomy (figure). Females stay virgins for at least 4 hours post hatching and can additionally be recognized by specific features (figure). Virgins were collected in 3-4 hours intervals at 25°C, transferred to a new bottle and crossed to males. For separation or collection, flies were anesthetized for up to 5 minutes with CO₂ and sorted with help of a binocular.

2.4 *Drosophila* genetics

Balancer chromosomes

Homozygous lethal mutations are selected out in genomes after view generations. In *Drosophila* genetics balancer chromosomes are used in order to keep lethal mutations in the genome. A balancer chromosome displays several inverted repeats and translocations of chromosome sections. For this reason a recombination of homologues chromosomes is almost excluded. To recognize balancer chromosomes in embryos, pupae or adults they bear additional dominant or recessive non-lethal mutations that are easy to recognize.

Balancer chromosomes are homozygous lethal or cause sterility. This prevents that fly stocks lose the chromosome with homozygous lethal mutations.

Reporter gene expression

eyFLP2: Different *ey* (eyeless) enhancer fragments were used to induce mitotic recombination in the eye. The *eyFLP2* is a construct that carries a 258 bp long enhancer fragment of the *ey* gene upstream of the flipase (FLP) cDNA (Newsome et al., 2000a). The *ey* enhancer fragment used for the *eyFLP2* display a broad expression pattern of the *ey* gene. Expression can be detected in the eye and in a small fragment of brain cells. Mutant clone size induced with *eyFLP2* in the retina without cell lethal mutation ranges from 20-30%. Almost the entire retinal is mutant when using *eyFLP2* combined with a cell lethal mutation.

ey3.5FLP: *ey3.5FLP* is a specific 3.5kb enhancer fragment of the *ey* gene (Bazigou et al., 2007). The *ey3.5* enhancer fragment is specifically expressed in the eye. Unlike the *eyFLP2* enhancer fragment, expression is not detected in the brain.

Ey1xFLP.Exel: The *ey1xFLP*. Exel drives FLP expression with one copy of the *ey* enhancer (Exelixis, Inc.). Mutant mosaics are distinctly smaller than *eyFLP2*.

Rh1-lacZ: The *Rh1-lacZ* is an enhancer fragment of the Rhodopsin1 (*Rh1*) gene that is expressed in R1-R6 cells and directly fused to *lacZ* (Mismer and Rubin, 1987, Newsome et al., 2000a).

***gmr* (glass multiple reporter):** The *gmr* reporter contains five repeats of *Glass response element* from the *Rhodopsin1* (*Rh1*) gene and is expressed in all R cells behind the morphogenetic furrow (Hay et al., 1994, Freeman, 1996).

109-68-Gal4: 109-68-Gal4 is an enhancer trap insertion located on the second chromosome and is expressed specifically in R8 cells from 3rd instar larval stages on (Jarman and Ahmed, 1998, White and Jarman, 2000). The specificity of this line was re-examined by Takashi Suzuki.

mδ-Gal4: *mδ-Gal4* is an enhancer trap insertion on the second chromosome and drives expression in R3, R4 and R7 during larval stages and in R4 cells during the first half of pupal development (Prakash et al., 2009). I found that *mδ-Gal4* is expressed also in glia cells throughout pupal development and in adult flies.

FLP/FRT system

The FLP/FRT system is derived from yeast and is a site-directed recombination method which allows recombination in selective tissues *in vivo*. It is based on the flipase recombinase which recognizes short flipase recognition target (FRT) sites where it induces recombination (Golic and Lindquist, 1989). Targeted generation of genetic mosaic animals allows (1) the analysis of genes that cause lethality in homozygous mutants and (2) the specific temporal and spatial requirement of a gene. To generate mosaic animals, FRT sites has been introduced close to the centromeres of *Drosophila* chromosomes (Xu and Rubin, 1993). If homologue chromosome arms carry the same FRT sites, the flipase can induce recombination between two non-sister cells which exchanges chromosome arms (figure 3-1). This leads to two daughter cells that carry either two parental or two maternal chromatids, respectively. If the animal is heterozygous for a mutation this leads to one daughter cell that is homozygous mutant and one that carries both wild-type alleles. To induce recombination in a specific tissue, flipase expression is controlled by a specific enhancer fragment. For the generation of mosaic eyes, eye-specific enhancer fragments from the promotor of the *eyeless* gene (*ey*, *Drosophila* homologue of the *Pax6* gene) are well established and used in this work (Newsome et al., 2000a). They are described more detailed in the chapter 'reporter gene expression'. To distinguish homozygous mutant from wild-type clones, the wild-type chromosome carries a *w+* transgene that allows tracing of recombination efficiency in a *w-* background. Likewise, a gene encoding a fluorescent protein can be recombined on the wild-type or mutant chromosome arm. Mutant and wild-type clones can be distinguished by the fluorescent marker.

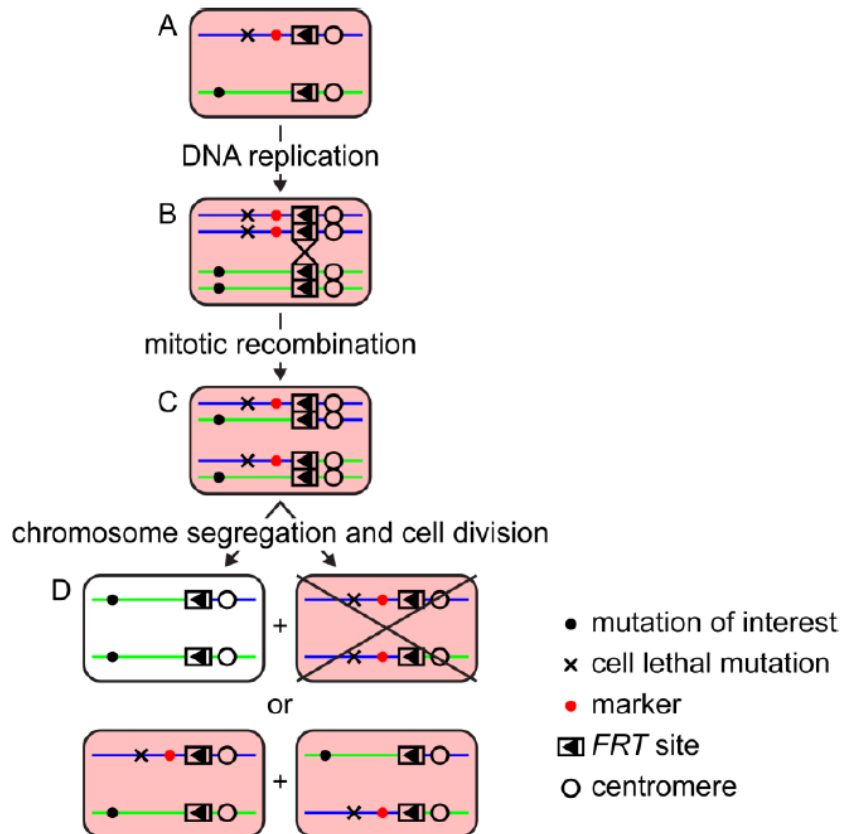


Figure 2-1 The Flp/FRT system

(A) The parental and the maternal chromatids contain FRT sides. One chromatid carries a mutation close to the centromere, while the heterologues chromatid is wild-type. **(B)** After DNA-replication the cell contains two pairs of homologues chromatids. **(C)** Targeted expression of the flipase recombinase can induce recombination between the FRT sites of heterologues chromatids. **(D)** After cell division, the two daughter cells can have different genotypes (genetic mosaic). One is homozygous for the mutation, while the other one is wild-type. (Adapted from Stephan Ohler, 2012).

Minute mutation

The minute mutation *M(3)i[55]* (*RpS17*) was used to increase the clone size in FLP/FRT induced mosaic eyes. The Minute mutation prevents proliferation and survival of homozygous cells and retards the proliferation of heterozygous cells (Morata and Ripoll, 1975). Minute was located in *trans* to the *Gogo* allele. After FLP/FRT induced recombination, cells were either homozygous for the *Minute* or *gogo*. When flipase is expressed under the control of *eyFLP2*, almost the entire retina is mutant (Newsome et al., 2000a).

Gal4/UAS system

The Gal4/UAS system is a method which allows the spatial and temporal expression of genes (Brand and Perrimon, 1993). Gal4 encodes for a transcription factor in yeast which binds to the *Upstream Activation Sequence (UAS)* and thereby activates gene transcription. The Gal4 is placed under the control of a native promoter. A variety of transgenic *Drosophila* Gal4 and reporter (UAS) lines are available that express Gal4 in specific tissues at specific time points and a UAS close to a gene of interest, respectively. By combining a Gal4 line with a UAS reporter line, the desired gene is expressed in the spatio-temporal expression pattern of the gene that controls the Gal4 expression. The advantage of the system is that different Gal4 lines can be combined with different reporter genes (e.g. GFP).

MARCM (Mosaic analysis with a repressible cell marker)

MARCM (Mosaic analysis with a repressible cell marker) is a broadly used genetic system in *Drosophila* that allows creation of single labeled mutant cells within an otherwise wild-type background (Lee and Luo, 1999, 2001). Heterozygous cells or wild-type cells remain unlabeled. The method is based on the combination of FLP/FRT and Gal4/UAS system. In addition, the gene of the Gal4 repressor Gal80 is located in *trans* to the mutation. Gal80 prevents activation of the UAS by Gal4. Targeted expression of a marker reporter gene (normally GFP) is repressed in heterozygous cells by the presence of Gal80. FRT-induced mitotic recombination by heat-shock flipase (hs-FLP) generates homozygous mutant cells that lack the Gal80 repressor. In these cells, the binding of Gal4 is no longer suppressed and GFP is expressed. Thus, homozygous mutant cells can be identified and analyzed by the expression of the marker.

Complementary (c) MARCM

In MARCM method wild-type cells are not labeled. In order to label wild-type but not mutant cells in the fly visual system the marker monomeric Kusabira Orange (mKOrange) under the control of the eye-specific promoter GMR was located in *cis* to the Gal80 repressor (Tomasi et al., 2008). After mitotic recombination the gene is lost in homozygous mutant cells and only expressed in wild-type cells.

Reverse (r) MARCM

The MARCM method allows analysis of single mutant cells and therefore the cell-autonomous requirement of a gene. To test the non-cell autonomous requirement of a gene in photoreceptor neurons, MARCM was modified. The reverse (r) MARCM method allows analysis of a wild-type neuron that is adjacent to mutant one. Here, the *G80* gene is located

in *trans* to the mutation. Therefore single wild-type cells, but not mutant cells express GFP. To identify the mutant cells, an additional fluorescent marker is located in *cis* to the mutation. After recombination, homozygous mutant cells lack the marker gene, whereas wild-type cells express the marker gene. Therefore, mutant cells are black within a labeled wild-type background and can thus be identified.

List of genetic elements

Table 2 Flybase IDs of genetic elements used in this thesis

<i>Genetic element</i>	<i>Flybase ID</i>	<i>use</i>
<i>FM3</i>	FBba0000002	X chromosome balancer
<i>FM7a</i>	FBba0000007	X chromosome balancer
<i>FM7c</i>	FBba0000009	X chromosome balancer
<i>CyO</i>	FBba0000025	2 nd chromosome balancer
<i>CyO, Kr-Gal4, UAS-GFP</i>	FBba0000315	2 nd chromosome balancer
<i>MKRS</i>	FBba0000066	3 rd chromosome balancer
<i>TM3, Sb1</i>	FBba0000187	3 rd chromosome balancer
<i>TM3, Sb1 Ser1, y+</i>	FBba0000149	3 rd chromosome balancer
<i>TM6B, y+</i>	FBba0000339	3 rd chromosome balancer marked by Antp ^{Hu} and y ⁺
<i>B1</i>	FBal0000817	dominant X chromosome marker mutation (eye shape)
<i>Pin*</i>	FBgn0003088	dominant 2 nd chromosome marker (shape of bristles)

<i>wg^{Sp-1}</i>	FBal0015984	dominant 2 nd chromosome marker (bristle number)
<i>Cy¹</i>	FBal0002196	dominant 2 nd chromosome marker (wing shape)
<i>Sb¹</i>	FBal0015145	dominant 3 rd chromosome marker (shape of bristles)
<i>Ser¹</i>	FBal0015427	dominant 3 rd chromosome marker (wing shape)
<i>Antp^{Hu}</i>	FBal0000583	dominant 3 rd chromosome marker (bristle number)
<i>w[*]</i>	FBgn0003996	rezessive X chromosome marker (eye color)
<i>w¹¹¹⁸</i>	FBal0018186	rezessive X chromosome marker (eye color)
<i>Rh1-lacz</i>	FBtp0007724	lacZ reporter
<i>FRT80B</i>	FBti0002073	<i>FRT</i> site for mitotic recombination left arm of 3rd chromosome
<i>FRT42B</i>	FBti0002072	<i>FRT</i> site for mitotic recombination right arm of 2nd chromosome
<i>gogoH1675</i>	FBal0242620	<i>gogo</i> mutation
<i>GMR-mCD8-KO</i>	FBtp0052779	KO marker marks all photoreceptor axons
<i>l(3)cl-L</i>	FBal0098713	recessive lethal mutation on right arm of 3 rd chromosome
<i>l(2)cl-R111</i>	FBal0104506	recessive lethal mutation on right arm of 2 nd chromosome
<i>mδ-Gal4</i>	FBti0148802	Gal4 line
<i>fmi[E59]</i>	FBal0101421	<i>flamingo</i> mutation
<i>hs-FLP</i>	FBti0002044	Flipase under the control of a heat-sensitive promoter
<i>eyFLP2</i>	FBti0015982	Flipase under the control of an eyeless enhancer fragment

<i>ey3.5</i>	FBtp0022600	Flipase under the control of an eyeless enhancer fragment
<i>Ey1xFLP.Ex</i>	FBti0040602	Flipase under the control of an eyeless enhancer fragment
<i>Gal4[109-68]</i>	FBrf0102537	Gal4 line

***Drosophila* transgenic lines**

Table 3 *Drosophila* stocks used in this thesis

genotype	Source
<i>w</i> ¹¹¹⁸	Bloomington Stock Center
<i>yw X; Pin/CyO</i> ⁺ II	Barry Dickson
<i>yw X; MKRS/TM6By</i> ⁺ III	Barry Dickson
<i>Yw X; Elp/CyO Kr-G U-GFP II; Ki/TM3 Kr-G U-GFP III</i>	Gaia Tavosanis
<i>w/Yy</i> ⁺ X; <i>nub b Sco lt stw/CyO</i> II; <i>MKRS/TM6By</i> ⁺	Bloomington Stock Center
<i>yw eyFLP2 C-lacZ X; M(3)i[55] FRT80B/TM6By</i> ⁺ III	Barry Dickson
<i>yw eyFLP2 C-lacZ X; gogo[D869]/TM6By</i> ⁺ III	Takashi Suzuki
<i>yw eyFLP2 C-lacZ X; gogo[H1675], FRT80/TM6By</i> ⁺ III	Takashi Suzuki
<i>yw eyFLP2 c-LacZ; Sp/CyO, y+</i> ; <i>MKRS/TM6B, y+</i>	Takashi Suzuki
<i>yw eyFLP2 c-LacZ; 3L cl FRT80B/TM6B, y+</i>	Takashi Suzuki
<i>yw; GMR-Gal4</i>	Barry Dickson
<i>GMR-Gal4 UAS-gogo/ CyO</i>	Tatiana Tomasi
<i>GMR-mCD8-KO (SS39)</i>	Satoko Suzuki
<i>eyFLP2 glass-LacZ Rh6-GFP</i>	Barry Dickson
<i>Gal4[109-68] / CyO</i>	Bloomington Stock Center

<i>Gal4[109-68] / CyO; 3Lcl, FRT80</i>	this thesis
<i>ey2FLP; Gal4[109-68] / CyO; 3Lcl, FRT80</i>	this thesis
<i>ey2FLP; Gal4[109-68] / CyO; gogo[H1675], FRT80</i>	this thesis
<i>mδ-Gal4, UAS-mCD8GFP/CyO Kr-GFP</i>	Thomas Clandinin
<i>Ey3.5; mδ-Gal4, UAS-mCD8GFP/CyO Kr-GFP; gogo[H1675], FRT80</i>	this thesis
<i>UAS-mCD8GFP</i>	Bloomington Stock Center
<i>elav-Gal4</i>	Bloomington Stock Center
<i>tub-Gal80, FRT80B</i>	Satoko Suzuki
<i>eyFLP2, FRT80B, gogo[H1675]/TM6B, y⁺</i>	Satoko Suzuki
<i>tub-Gal80, FRT80B, gogo[H1675]/TM6B, y⁺</i>	Satoko Suzuki
<i>Yw X; Pin/CyO II; UAS-mCD8GFP III</i>	Bloomington Stock Center
<i>UAS-gogo-FL-T2 II</i>	Stephan Ohler
<i>UAS-gogo-FL III</i>	Stephan Ohler
<i>UAS-gogo-FL II/CyO; UAS-gogo-FL III/TM6B</i>	this thesis
<i>eyFLP2; UAS-gogoFL / CyO; gogo[H1675], FRT80B/TM6By⁺</i>	this thesis
<i>GMR-KO tub-Gal80 FRT80/TM6By⁺</i>	Satoko Suzuki
<i>Yw X; Pin/CyO; UAS-mCD8GFP</i>	Bloomington Stock Center
<i>GMR-KO tub-Gal80 FRT80/TM6By+ III</i>	Satoko Suzuki
<i>1xeyFLP/CyO; GMR-KO tub-Gal80 FRT80/TM6By+ III</i>	Satoko Suzuki
<i>ey3.5FLP</i>	Bloomington Stock Center
<i>yw; FRT42B fmi[E59]/ CyO, y⁺</i>	Kirsten Senti
<i>eyFLP2; Gal4[109-68]/CyO, y⁺;gogo[H1675], FRT80B/TM6B</i>	this thesis
<i>eyFLP2; Gal4[109-68]/CyO, y⁺; 3Lcl, FRT80B</i>	this thesis

<i>hs-FLP</i>	Bloomington Stock Center
<i>hs-FLP, elav-Gal4, UAS-mCD8GFP</i>	<i>Drosophila</i> genetic Resource Center
<i>Rh1-tlacZ</i>	Barry Dickson
<i>Rh1-tlacZ; mδ-Gal4, UASmCD8GFP/CyO, Kr-GFP</i>	this thesis

2.5 Dissections and Immunohistochemistry

Larval brain dissection

3rd instar larvae were washed for 30 sec in EtOH. The larvae were cut into half with scissors and cuticles were inverted. The brain was dissected out and transferred to PBT washing solution. After fixation and antibody staining the brains were transferred into Vectashield Mounting Medium (Vector Laboratories, California) and mounted onto a microscope slide.

Pupal lamina dissection

White pupae (0hrs APF) were collected into a separate food vial and raised at 25°C or 30, 42 or 51 hrs. For dissection, the anterior part of the pupal case was removed from pupae in PBS using sharp scissors. The brain was dissected out of the head capsule and transferred to PBT washing solution. After fixation and antibody staining, the retina and the lamina (30 and 42 hrs APF) were disconnected from the brain with fine dissection needles and mounted in Vectashield Mounting Medium (Vector Laboratories, California).

Agarose section

Adult *Drosophila* brains were anesthetized with CO₂ and washed in 70% EtOH for 30s. Fly heads were cut off from the body and the entire proboscis of each fly was removed in PBS using sharp scissors. Fly heads were fixed for 3 days in 4% formaldehyde in PBS. After fixation heads were rinsed 3 times and washed 3 times for 15 min in PBS. 7% agarose in PBS was cooked in a microwave until agarose has been dissolve. After cooking the agarose solution was cooled down at RT for 2 min. Washed fly heads were transferred into a Petri dish and covered with the hot agarose solution. Heads were arranged with scissors into a

preferred orientation. After the agarose was solidified small pyramids were cut from the gel with one fly head on the top of the pyramid in the preferred orientation. Agarose blocks were transferred into PBS. 75µm thick horizontal slices were cut from agarose blocks using a vibrating blade microtome (Leica VT1000S). Agarose slices were transferred in 24-well plates for standard antibody staining. Antibodies (0.5% PBT) were incubated for 2 days each.

Transmission electron microscopy (TEM)

(in collaboration with Marianne Braun)

Adult *Drosophila* flies were anesthetized with CO₂ and washed in 70% EtOH for 30s. Heads were cut off from the body using sharp scissors in PBS. The entire proboscis was removed from each fly to allow penetration of fixative. Prepared heads were fixed overnight in 2.5% glutaraldehyde in PBS. Fly heads were postfixed and dehydrated in Dalton solution (1% Osmiumtetroxide, 1% Kaliumbichromat and 0.85% Natriumchlorid) and embedded in Epon. Sections of 1 µm were stained with Toloidinblue. Ultra-thin sections of 70nm were counterstained with Uranylacetat and Leadcitrat. Images were taken on a Zeiss EM 10 and JEOL TEM 1230.

Whole mount immunostaining of larval, pupal and adult brains

After dissection brains were transferred into 0.1% PBT (0.1% Triton-X100 in PBS) on ice after dissection. Brains were fixed on a shaker in 4% Formaldehyde in 0.1% PBT for 45min. After fixation brains were rinsed for 3x and washed for 3x for 15min in 0.3% PBT at room temperature (RT). Brains were incubated at room temperature for 30min in 0.3% PBT with 10% NGS to block unspecific binding-sites. The primary antibodies were diluted in 0.3% PBT and brains were incubated in the antibody solution at 4°C overnight on a shaker. After primary antibody incubation brains were rinsed 3x and washed 3-5x for 15min. Fluorescent secondary antibodies in 0.3% PBT were applied and incubated 2 hrs at RT or overnight at 4°C. Secondary antibodies were discarded and brains rinsed 3x and washed for 3x for 15min. Brains were transferred into Vectashield Mounting Medium (Vector Laboratories, California) and mounted onto a microscope slide.

Table 4 Primary antibodies

Antibody	Host species	Dilution	Source
anti-GFP	rabbit	1:300	Torrey Pines Biolabse
anti-GFP Alexa Fluor488-conjugated	rabbit	1:200	Molecular Probes
anti- β -gal	mouse	1:300	Promega Madison, Wisconsin
anti- β -gal	chicken	1:1000	Abcam
anti-gogo	rabbit	1:1000	Takashi Suzuki
anti-c-Myc	rabbit	1:300	Gramsch Laboratories, Schwabhausen, Germany
anti-Myc (9E10)	mouse	1:300	Santa Cruz
anti-Myc (9E10) TRITC conjugated	mouse	1:300	Santa Cruz
anti-24B10	mouse	1:25	Developmental Studies Hybridoma Bank [DSHB]
anti-elav	rat	1:100	Developmental Studies Hybridoma Bank [DSHB]
anti-tau	mouse	1:200	Sigma
anti-mCD8	rat	1:300	Caltag
anti-Gogo	rabbit	1:50	Takashi Suzuki

Secondary antibodies

Alexa Fluor-conjugated secondary antibodies (488, 568, 633; Molecular Probes) were used at 1:300.

2.6 Molecular methods

Isolation of genomic *Drosophila* DNA

Buffer A

100mM Tris-HCl (pH 7,5)

100mM EDTA

100mM NaCl

0,5%SDS

LiCl/KAc-solution

5M KAc und 6M LiCl (1:2,5)

Flies were genotyped by polymerase chain reaction (PCR). 1-3 adult flies were collected in a 1.5ml Eppendorf-tube and froze at -80°C for at least 30 min. 400µl solution A per tube were added and flies were smashed using a plastic mortal to disrupt cells. Homogenized flies were incubated at 65°C for 30 min. 800µl LiCl/KAc-solution added and the solution was incubated for 10 min on ice. Proteins were precipitated by centrifuging the sample at 13,000 rpm for 15 min. 1ml of the supernatant was transferred into a new tube. The genomic DNA was precipitated by adding 600µl Isopropanol and spinning at 13,000rpm for 30 min. The supernatant was discard, and the dried pellet washed with 70% EtOH, once more dried, and resuspended in 100µl ddH₂O. The concentration of the DNA was measured with a Nanodrop1000 sepctrometer (peqlab).

2.7

Polymerase Chain Reaction

iProof polymerase mix and Taq Polymerase were mixed according to the companies manuals.

25µl assay (Taq Polymerase)

2.5µl 10x reaction buffer
0.4µl dNTPs (10mM)
0.6µl I primer sense (10mM)
0.6µl primer antisense (10mM)
0.25µl Taq Polymerase
0.5µl DNA (50ng/µl)
H₂O

25µl assay using iProof Polymerase

12.5µl 2x iProof Master Mix
0.6µl primer sense (10mM)
0.6µl primer antisense (10mM)
0.5 µl DNA (50ng/µl)
H₂O

Standard PCR program

1. 98°C 30sec
2. 98°C 10sec
3. 50-65°C 30sec
3. 72°C 30sec/kb
5. Step 2 to 4 for 34 more cycles

DNA Gel electrophoresis

DNA is negatively charged and can thus be separated by electrophoresis. Diluted DNA was mixed with 6x DNA loading dye and according on the fragment size separated in 0.7%-1% agarose gel. The according amount of agarose was diluted in 1x TAE(Tris-Acetate-EDTA) buffer and cooked until the agarose was melted. Ethidiumbromid was added to the melted agarose to a final concentration of 0.5µg/ml. The agarose gel was cured in the gel electrophoresis mold.

6x loading buffer

0.25% Bromphenol blue
 0.25% Xylene Cyanol
 30% Glycerol
 100mM Tris pH 7.5
 100mM EDTA pH 8.0 H₂O

50xTAE (2I)

484g Tris base
 50mM EDTA pH 8.0
 114.2ml glacial acetic acid
 H₂O
 adjust pH 8.5 with gl. ac. acid

2.8 Statistical tests and software**Statistical tests**

Statistical significances for two-tailed Student's t-test and chi test were assessed in Excel. Statistical significances for Kolmogorov–Smirnov test and Levene's test were assessed in Python using custom written scripts from SciPy. (Ascher et al., 2001, Jones et al., 2001)

Software

Name	use
FV10-ASW 2.0	Confocal imaging (Olympus) and image processing
ImageJ	Image analysis
Adobe Photoshop	Image processing
Adobe Illustrator	Illustration

Python	Statistical tests
Microsoft Excel	Statistical tests
Prism5	Statistical tests

2.9 Summary of experimental genotypes

Figure 4-1:

B: *ey3.5/ey3.5;; gogo[H1675], FRT80B/, FRT80B*

C: *ey3.5/ey3.5;; FRT80B/, FRT80B*

D: *eyFLP2/+;; gogo[H1675], FRT80B/ 3Lcl, FRT80B*

F: *eyFLP2/+;; gogo[H1675], FRT80B/ 3Lcl, FRT80B*

eyFLP2/+;; Gal4109-68/+; gogo[H1675], FRT80B, UASgogoFL; 3Lcl, FRT80B

ey3.5FLP/+;; gogo[H1675], FRT80B/ 3Lcl, FRT80B

G, F: *ey3.5FLP/ey3.5FLP;; FRT80B/, FRT80B*

H, J: *eyFLP2/+;; gogo[H1675], FRT80B/ 3Lcl, FRT80B*

Figure 4-2

A: *ey3.5FLP/ey3.5FLP;; FRT80B/3Lcl, FRT80B*

B: *ey3.5FLP/ey3.5FLP;; gogo[H1675], FRT80B/3Lcl, FRT80B*

Figure 4-3

A, D: *ey3.5/ey3.5; mδ-Gal4, UASmCD8-GFP/+; FRT80B/FRT80B*

B, E: *ey3.5/ey3.5; mδ-Gal4, UASmCD8-GFP/+; gogo[H1675], FRT80B/FRT80B*

Figure 4-4

A, B: *ey3.5/ey3.5; mδ-Gal4, UASmCD8-GFP/+; FRT80B/FRT80B*

C, D: *ey3.5/ey3.5; mδ-Gal4, UASmCD8-GFP/+; gogo[H1675], FRT80B/FRT80B*

E: *hsFLP, elav-Gal4, UAS-mCD8GFP/+; eyFLP1.Exel/+; FRT80B/GMR-mCD8mKOmyc, tub-Gal80 FRT80B*

F: E: *hsFLP, elav-Gal4, UAS-mCD8GFP/+; eyFLP1.Exel/+; gogo[H1675], FRT80B/GMR-mCD8mKOmyc, tub-Gal80 FRT80B*

G: *ey3.5FLP/ey3.5FLP;; FRT80B/3Lcl, FRT80B*

H: *ey3.5FLP/ey3.5FLP;; gogo[H1675], FRT80B/3Lcl, FRT80B*

Figure 4-5

C: *ey3.5/ey3.5; mδ-Gal4, UASmCD8-GFP/+; FRT80B/FRT80B*

D: *ey3.5/ey3.5; mδ-Gal4, UASmCD8-GFP/+; gogo[H1675], FRT80B/FRT80B*

Figure 4-6

C: *ey3.5/ey3.5; mδ-Gal4, UASmCD8-GFP/+; FRT80B/FRT80B*

D: *ey3.5/ey3.5; mδ-Gal4, UASmCD8-GFP/+; gogo[H1675], FRT80B/FRT80B*

Figure 4-7

C: *hs-Flp, elav-Gal4, UASmCD8-GFP/+;; FRT80B/Gal80, FRT80B*

D: *hs-Flp/elavGal4; UAS > CD2y⁺ > mCD8-GFP/+*

Figure 4-8

A-C: *hs-Flp, elav-Gal4, UASmCD8-GFP/+;; FRT80B/Gal80, FRT80B*

D-F: *hs-Flp, elav-Gal4, UASmCD8-GFP/+;; gogo[H1675], FRT80B/Gal80, FRT80B*

Figure 4-9

B-C: *hs-Flp, elav-Gal4, UASmCD8-GFP/+;; gogo[H1675], Gal80, FRT80B/ FRT80B*

Figure 4-10

A: *ey3.5/+; mδ-Gal4, UASmCD8-GFP/+; FRT80B, GmrKO /FRT80B, Gal80*

B: *ey3.5/+; mδ-Gal4, UASmCD8-GFP/+; FRT80B, gogo[H1675], GmrKO /FRT80B, Gal80*

C: *ey3.5/+; mδ-Gal4, UASmCD8-GFP/+; FRT80B, gogo[H1675], Gal80, GmrKO /FRT80B*

Figure 4-11

A: *eyFLP/eyFLP; Gal4-109-68/+; gogo[H1675], FRT80/3Lcl*
 B: *eyFLP/eyFLP; Gal4-109-68/UAS-gogo; gogo[H1675], FRT80/3Lcl*
 E: *eyFLP/eyFLP; mδ-Gal4, UASmCD8-GFP/+; gogo[H1675], FRT80/3Lcl*
 F: *eyFLP/eyFLP; mδ-Gal4, UASmCD8-GFP/UAS-gogo; gogo[H1675], FRT80/3Lcl*

Figure 4-12

A: *ey3.5/+; mδ-Gal4, UASmCD8-GFP/+; FRT80B, GmrKO /FRT80B, Gal80*
 B: *ey3.5/+; mδ-Gal4, UASmCD8-GFP/+; FRT80B, gogo[H1675], GmrKO /FRT80B, Gal80*
 F: *hs-FLP/+; Rh1-Gal4, UAS-lacZ/+; FRT80B/tub-Gal80, FRT80B*
 G: *hs-FLP/+; Rh1-Gal4, UAS-lacZ/+; gogo[H1675], FRT80B/tub-Gal80, FRT80B*

Figure 4-13

A: *hs-Flp, elav-Gal4, UASmCD8-GFP/+;; FRT80B/Gal80, FRT80B*
 B: *hs-Flp, elav-Gal4, UASmCD8-GFP/+;; gogo[H1675], FRT80B/Gal80, FRT80B*

Figure 4-14

A: *Rh1-lacZ/+;; FRT80B/FRT80B*
 B: *eyFLP2/Rh1-lacZ;;Gogo[H1675], FRT80B/FRT80B*
 C: *eyFLP2/Rh1-lacZ; fmi[E59], FRT42B/FRT42B*

2.10

Figure 4-15

A: *mδ-Gal4, UASmCD8-GFP/+*
 B: *mδ-Gal4, UASmCD8-GFP/UAS-gogo; UAS-gogo/+*
 C: *Rh1-lacZ/+; m δ-Gal4, UASmCD8-GFP/+*
 D: *Rh1-lacZ/+; m δ-Gal4, UASmCD8-GFP/UAS-gogo; UAS-gogo/+*

3 RESULTS

3.1 Gogo is required for proper cartridge assembly

(in collaboration with Tatiana Tomasi and Marianne Braun)

In the *Drosophila* visual system R1-R6 axons project to the first optic ganglion, the lamina, and form synaptic units, called cartridges, with lamina neurons. In order to identify the molecular rules that guide proper cartridge formation, I analyzed candidate gene mutants with phenotypes in the visual system. It was previously described that the transmembrane protein Golden goal (Gogo) is required specifically in R axons for correct cartridge assembly in adult *Drosophila* brains (Hakeda-Suzuki et al., 2011). While in wild-type each cartridge is innervated by 6 termini per cartridge (figure 4-1 A), the absence of Gogo causes strong hypo- and hyperinnervation defects.

As a first characterization of the Gogo phenotype, I performed a detailed analysis of cartridge formation in adult flies. To remove Gogo from R axons, I generated genetic mosaic eyes using the FLP/FRT system, which is a site-directed recombination method allowing recombination in the eye. The flipase (FLP) recombinase recognizes short flipase recognition target (FRT) sites. To flip out gogo specifically in photoreceptor cells, I expressed the flipase under the control of the eyeless promoter fragment 'ey3.5'. (Bazigou et al., 2007). In these flies, the majority of R cells but not the postsynaptic cells were *gogo* mutant. I visualized cartridges in adult flies by labeling with the pre-synaptic marker 6H4. In wild-type controls, cartridges appeared as uniform rings that formed an overall well-ordered pattern (figure 4-1 A-C). In *gogo*⁻ mosaic eyes, in which R cells are homozygous for a *gogo* null mutation (*gogo*[D1600]), the structure of adult laminae displayed strong defects. Cartridges varied in size and failed to arrange in a structured way. Transmission electron microscopy (TEM) of adult lamina allowed a more detailed characterization of the phenotype caused by the lack of Gogo. In wild-type controls, six axon termini surround a pair of two lamina neurons, L1 and L2 (figure 4-1, D, (Meinertzhagen and O'Neil, 1991). Termini can be identified by characteristic invaginations of glia cells (capitate junctions [cp]). Based on the position of L3/L4 lamina neurons and R7/R8 termini R cell subtypes can be classified (Meinertzhagen and O'Neil, 1991). Unlike the highly ordered array of even sized cartridges in the wild-type, the array was strongly disrupted when Gogo was absent in the majority of R cells (figure 4-1, C, E, E', (Hakeda-Suzuki et al., 2011). Cartridges varied in size, and were innervated by more or less than six termini. In some cases two cartridges were fused to a single one, containing two L1/L2 pairs of lamina neurons. In wild-type controls about 90% of all cartridges contained a normal number of 6 termini per cartridge and about 10% were

innervated by 5, 7, and 8 termini, respectively (figure 4-1 F). When FL-Gogo was removed using *ey3.5FLP* only about 34% of cartridges contained the normal number of six termini, while about 66% showed aberrant numbers, ranging from 1-14 termini (figure 1-4 C, E, E', F). However, these defects did not reflect errors in cell fate specification or differentiation since the number of termini correlated to the number of cartridges (6 termini per cartridge, data not shown). In a control experiment Gogo was removed by expressing the flipase under the control of the eyeless promotor *eyFLP*. *eyFLP* is expressed in higher number of R axons compared to *ey3.5FLP*, and additionally in a fraction of Lamina neurons (LNs). The observed phenotype showed 79% mis-innervation and was therefore stronger, but quantitatively indistinguishable from *ey3.5FLP* mosaic eyes (figure 1-4, F). Despite the mis-innervation defects mutant cartridges possessed characteristic invaginations of glia cells (capitate junctions, cp) and T-bar shaped dens structures (figure 1-4, D-E', G-J). The latter suggested the presence of functional synapses.

To exclude that the projection defects in the lamina are not reflecting an earlier role of *gogo* during R8 medulla targeting, FL-Gogo was specifically rescued in R8 in *gogo⁻* mosaic eyes. While the medulla phenotype was fully rescued in this genetic background (data not shown, Tomasi et al.), the R1-R6 projection pattern in the lamina was still abnormal and not significantly different from *eyFLP* and *ey3.5FLP* mosaics (figure 1-4, F, (Hakeda-Suzuki et al., 2011)). Taken together those results revealed a requirement of Gogo during cartridge assembly.

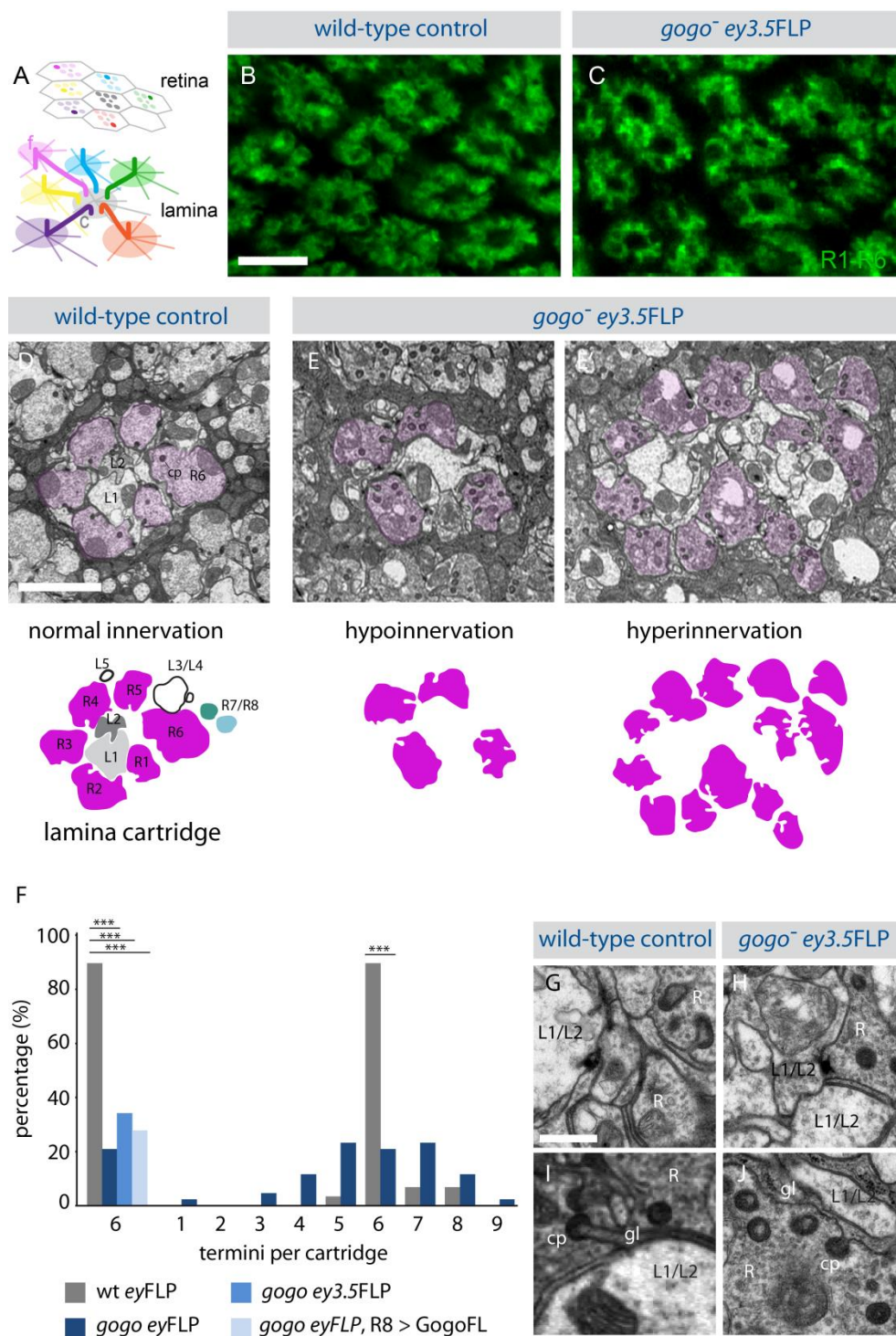


Figure 3-1 Retinotopic map formation is disrupted in the absence of Gogo

(A) Schematic of adult cartridge assembly. R1-R6 fascicles (f) separate at the lamina and project to different cartridges (c). Six R1-R6 axons from six different ommatidia in turn converge with one set of lamina neurons (not shown) to form a single cartridge. **(B, C)** Lateral sections of adult lamina cartridges visualized using presynaptic marker 6H4 in wild-type and mutant (green). **(B)** In control animals cartridges display uniform rings of six termini forming a regularly arranged pattern. **(C)** When

Gogo is absent cartridges are hypo- and hyperinnervated resulting in uneven sized and shape rings, and a strongly disordered pattern. **(D-E')** TEM of adult cartridge cross-sections in wt and in the absence of functional Gogo. **(D)** In control flies, each cartridge contains 6 termini per cartridge (highlighted in magenta, schematic) which are arranged in a circle around L1 and L2 lamina neurons. L3 and L4 are located in the periphery of each cartridge between R5 and R6. R7 and R8 termini lay on the outsider border of R6 and the diameter of their axons are small compared to R1-R6. **(E, E')** Absence of Gogo in the majority of R cells and in some target neurons results in a strong hypo- and hyperinnervation of lamina cartridges. Representative images show one cartridge which is innervated by only 4 R axon termini, and a second one in which originally two cartridges are fused to a single one, indicated by the presence of two L1/L2 pairs. The fused cartridge is innervated by 13 R1-R6 termini. **(G-J)** In both wild-type control and mutant R axons form T bar shaped synapses **(G, H)** and contain R termini characteristic capitate glia projections (cp) **(I, J)**. **(F)** Quantification of R termini per cartridge in wild-type, *gogo⁻eyFLP*, *gogo⁻eyFLP3.5* and R8 rescue. When Gogo is removed from R axons using either *eyFLP* or *eyFLP3.5* the number of termini per cartridge strongly differs from the wild-type control. Specific R8 expression of FL-Gogo in the mutant background does not result in significant differences from *gogo⁻eyFLP* or *gogo⁻eyFLP3.5*. In the wild-type *eyFLP* the majority of cartridges are innervated by 6 termini. In *gogo⁻eyFLP* the distribution of termini per cartridge is broadly distributed, ranging from 1-9 termini per cartridge. Scale bars: **B, C** = 5 μ m, **D-E'** = 2 μ m, **G-H** = 0.2 μ m.

3.2 Gogo is required for spatial distribution of R cell fascicles along the lamina plexus

To assess how Gogo regulates cartridge assembly, I examined the specific requirement of Gogo in R cells during different developmental time windows. To this aim, I first assessed if R1-R6 axons target to the correct layer in the brain. I visualized the overall projection pattern in a horizontal view using mAb24B10 staining of third instar eye-brain complexes. This antibody recognizes an antigen that is specifically expressed in R cells (Fujita et al., 1982). In wild-type control brains, R1-R6 growth cones targeted to a single layer in the lamina while R8 growth cones proceed to the medulla, forming a smooth topographic map (figure 4-2 A, B). The mAB24B10 staining in the medulla largely reflects R8 axons as only a few R7 axons express the antigen (Fujita et al., 1982). The pattern made by R1-R6 axons in *gogo*⁻ mosaic eyes was largely indistinguishable from wild-type: R1-R6 axons terminated the same layer at the lamina plexus and did not over- or undershoot (figure 4-2 C). In contrast, as previously described, R8 axons fail to form a smooth array in the medulla (figure 4-2 C, arrowheads, (Tomasi et al., 2008): R8 axons bundle and clump when entering the medulla.

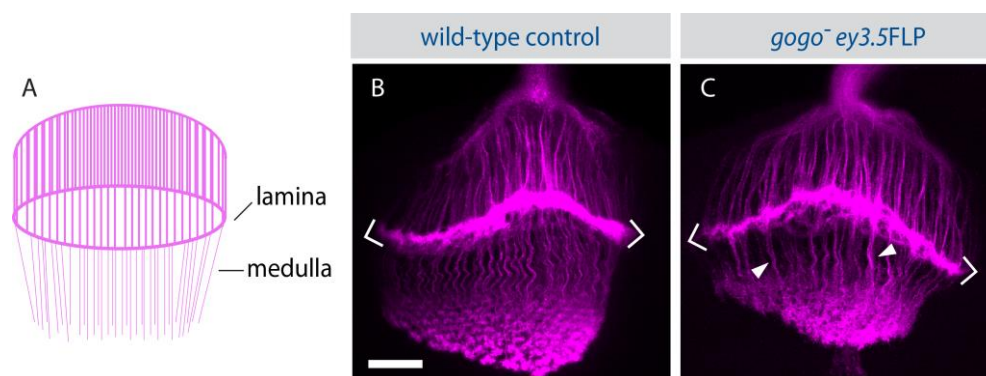


Figure 3-2 Initial R cell projections in Gogo mutants are normal

(A-C) Schematic (A) and horizontal view of confocal stacks of wild-type (B) and *gogo*⁻ eye specific mosaic (C) animals stained with mAb24B10 antibody (magenta). The developing brain was assessed at late third instar larval stages. Chevrons indicate the lamina plexus. (B) R1-R6 axons target to the lamina plexus which is seen as a smooth line of staining. R8 axons project through the lamina and their large growth cones form a well ordered pattern. (C) In *gogo*⁻ mosaic eyes the overall projection pattern of R1-R6 axons is largely normal. R1-R6 target to the same layer but their growth cones contain more filopodia-like structures compared to wild-type. In the medulla, the array of R8 axons is

slightly disrupted compared to wild-type. os: optic stalk; l: lamina; me: medulla; a: anterior; p: posterior; d: dorsal; v: ventral. Scale bar: 10 μ m.

Once R axon fascicles reach the lamina plexus, they terminate topographically with fixed relative positions to adjacent fascicles (Meinertzhagen and O'Neil, 1991, Clandinin and Zipursky, 2000). To examine retinotopic mapping in a *gogo*⁻ background, I assessed the lateral projection pattern of R1-R6 axons at the lamina plexus. I analyzed pupae at 30 hrs after puparium formation (APF). At this point, R axons are already positioned at their destination layer and pre-connected to lamina neuron columns but have not spread onto the surface of the lamina to innervate their final targets (Meinertzhagen and Hanson, 1993). This pre-connection between R1-R6 axons from a single ommatidium and lamina neurons is referred to as pre-cartridge. In addition to the mAB24B10 staining, I visualized R4 subtypes by expressing mCD8GFP under the control of the specific promoter *m̄-Gal4* (Prakash et al., 2009). While in larval stages *m̄-Gal4* drives expression also in R3 and R7 axons, in pupae at 30 hrs APF it is specifically expressed in R4 axons. In wild-type control brains, R1-R6 growth cones of each ommatidial bundle were seen as patches (pre-cartridges) (figure 4-3 A, C-D). They formed a regular checker-board pattern. The staining of R4 axons appeared as single dots, revealing that growth cones were extended but did not yet spread away from their original bundle in a specific direction. As individual R cell types have a defined and invariant location within their pre-cartridge (Meinertzhagen and Hanson, 1993), I examined the highly organized R4 projection pattern as a reference for topographic map formation. I illustrated the topographic regularity of R4 termini using DeLaunay triangulation and Voronoi diagrams (figure 4-3, G, see methods). In wild-type conditions, connections of R4 termini resulted in a net of equal triangles and polygons, respectively. When *Gogo* was absent in the majority of R cells (*ey3.5FLP*), the overall pattern of R1-R6 axons was severely disrupted and displayed an irregular arrangement of pre-cartridges (figure 4-3 B, E-F). This was also true on the level of R4 axons which fail to form a smooth pattern. Moreover, R4 growth cones seemed to be enlarged compared to wild-type (figure 4-3 C-F). The disruption of the uniform arrangement of the retinotopic map was also clearly visible in the DeLaunay and Voronoi diagrams that displayed triangles and polygons of unequal sizes (figure 4-3 G, H). Taken together these results reveal that *Gogo* function is required for the well-ordered arrangement of R1-R6 axon fascicles along the lamina plexus.

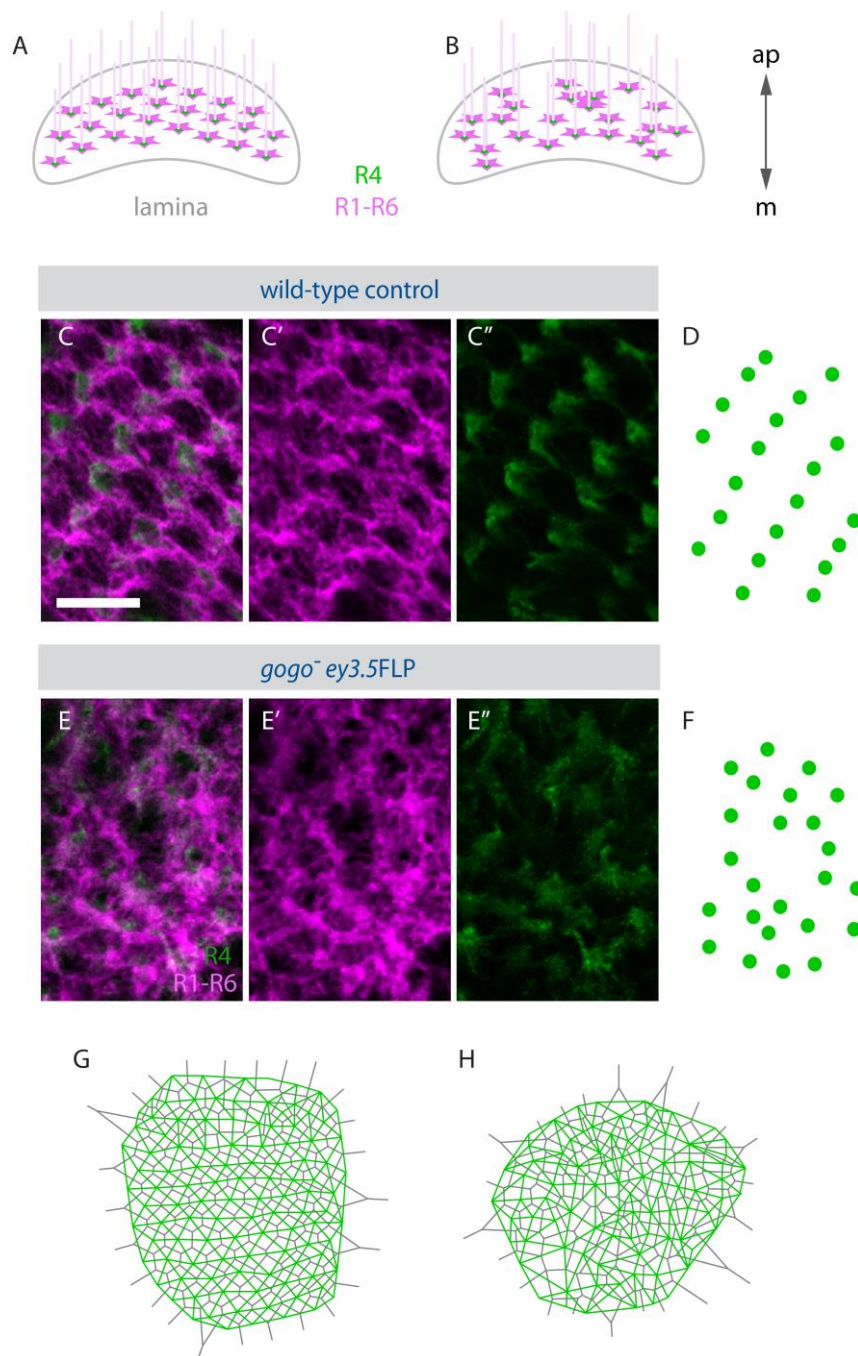


Figure 3-3 Retinotopic map formation is disrupted in the absence of Gogo

(A-F) Schematics and confocal stacks of R1-R6 fascicles in wild-type and *gogo*⁻ mosaic eyes from a lateral view. The overall projection pattern of R cells is visualized by mAB24B10 antibody staining (magenta) and R4 cells are specifically labeled by the expression of mCD8-GFP under the control of the specific driver *mδ-Gal4*. (A, C-D) Wild-type schematics and confocal images of the retinotopic map in early pupae (30 hrs APF). R1-R6 fascicles terminate at the lamina plexus maintaining equal spacing and spatial order of their ommatidia. R4 axons form an orderly pattern along the lamina

plexus. Their growth cones do not yet project away from their original fascicle. **(B, E-F)** In *gogo*⁻ mosaic eyes, R1-R6 fascicles fail to arrange in a correct position relative to neighboring axons. The pattern of R4 axons is disrupted and their growth cones display more filopodia-like structures compared to wild-type. **(G, H)** DeLaunay (green strokes) and Voronoi diagrams (grey strokes) demonstrate the uniform and irregular retinotopic mapping in wild-type **(G)** and mutant **(H)**, respectively. Scale bar: 10 μ m

3.3 R1-R8 axons do not displaying bundling defects

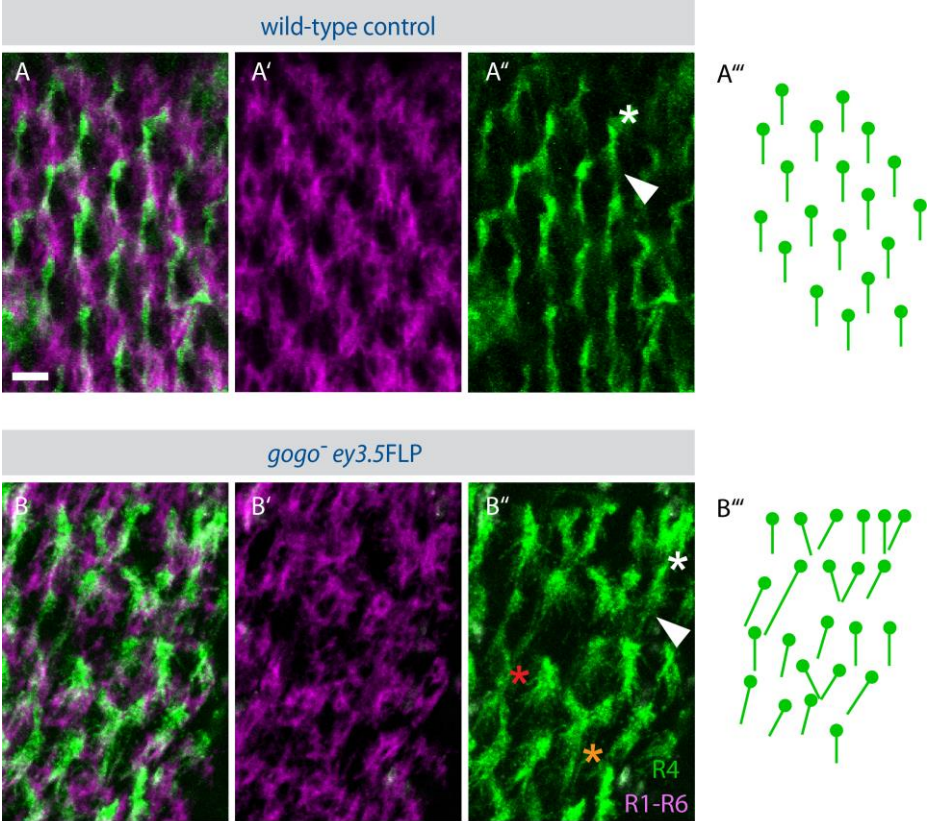
Defects in fascicle order described above could reflect a disruption of possible axon-target interactions, or, consistent with the role of Gogo during R8 medulla targeting, a disruption of interactions between R8 axons that occur before they exit the lamina (Tomasi et al., 2008). To assess how Gogo contributes to initial topographic mapping, I carried out a more detailed analysis of the phenotype during larval development. Three lines of evidence argue against axon-axon interactions between R8 axons or R1-R6 axons.

First, I labeled R4 axons by expressing mCD8-GFP under the control of the $m\delta$ -Gal4 driver and followed their projection within their original fascicle from the retina to the lamina plexus in wild-type and *gogo*⁻ mosaic late third instar larval brains. I observed that *gogo*⁻ R4 axons continue to grow within their original fascicle and did not intermingle with neighboring fascicles (figure 4-4 A-D'). Second, I generated small mCD8GFP labeled R cell clones in a wild-type background using mosaic analysis with a repressible cell marker (MARCM) method (Lee and Luo, 2001). Wild-type R1-R8 axons were labeled using *glass multiple reporter (gmr)*-mKOrange. In this construct, the marker gene mKOrange is directly fused to the *gmr* promoter that drives expression in all R cells. I followed GFP-labeled *gogo*⁻ axons within their original fascicles. Unlike during medulla targeting, R8 axons did not intermingle with R8 axons (or R1-R6 axons) of neighboring fascicles before exiting the lamina (figure 4-4 E-F'', I, J). Third, the lateral view of the developing lamina plexus in 3rd instar larvae revealed that R1-R8 fascicle did not clump but distributed along the entire dorso-ventral and anterior-posterior edge of the lamina plexus (figure G, H). Taken together, these findings suggest that Gogo is not playing a role in permitting R fascicles to separate from each other. I thus conclude that Gogo is not regulating axon-axon repulsion during lamina targeting but is rather mediating interactions between R axons and their target area within the lamina.

3.4

3.5 R4 target cartridge selection is disrupted when Gogo is absent in R axons

The findings above raised the interesting question whether altering the relative spatial position of R cell fascicles in the *gogo*⁻ background influences target cartridge selection. At a defined time-point during the first half of pupal development axons defasciculate simultaneously and extend across the lamina surface to select appropriate targets (Meinertzhagen and Hanson, 1993, Clandinin and Zipursky, 2000). The projection of each R cell subtype is characteristic in direction and length and as a result homologous R cell subtypes display a parallel projection pattern (Meinertzhagen and Hanson, 1993, Clandinin and Zipursky, 2000). Therefore, I examined the projection pattern of R4 axons at the onset of target cartridge selection (42 hrs APF). In the control situation, R4 axonal extensions were uniform in direction and length (figure 4-5 A-A''). They displayed a highly ordered pattern of equally arranged and parallel projections. Axon termini within the cartridges were visualized by mAB24B10 antibody staining. Single cartridges, appeared as donut-like structures that were equally in size and orderly arranged forming an overall smooth hexagonal pattern. In contrast, a lack of Gogo in R cell patches strongly disrupts the regularity of R4 projections (figure 4-5 B-B''). Their extensions were no longer parallel and axons differ in projection lengths. In some cases two R4 axons project to the same target cartridge. To analyze the differences in projection angles I measured orientation vectors for R4 axons in wild-type and *gogo*⁻ mosaic laminae. R4 axon extensions within *gogo*⁻ areas failed to project parallel and their distribution was significant higher than in the wild-type control (figure 4-5 C, D, two-sampled Kolmogorov–Smirnov (K-S) test $p < 0.0005$). Additionally, unlike in the wild-type control, R4 extensions differ significantly in length of their growth cones (Figure 4-5 E, F, levene's test, $p < 0.0005$). While in controls, R4 axons displayed a length between 4.3 and 6.5 μm , R4 axon lengths in the mutant background ranged from 1.8 to 9.6 μm . In the overall pattern, the normally uniform circular cartridges of R1-R6 axon termini were deformed and varied in size, reflecting a variant number of axons per target cartridge instead of the normal 6 (figure 4-5 A-B''). Furthermore, the defect of R axon order described above in pupae at 30 hrs APF was still present at this later developmental stage: The starting points (figure 4-5 A-B'', asterisks) of individual R4 extensions reflected the initial intrafascicular location at the lamina plexus. In the wild-type control, extension starting points of individual R4 axons were equally distributed along the lamina, while the pattern in the mutant background was completely disrupted (figure 4-5 A'', B'', green dots). Thus, when Gogo was absent in a large fraction of ommatidia, target cartridge selection of R1-R6 axons is altered.



R4 orientation vectors

R4 length in μm

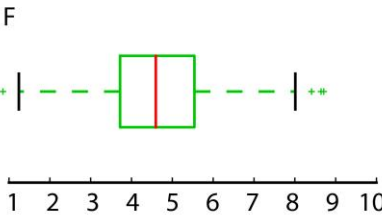
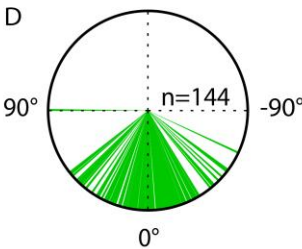
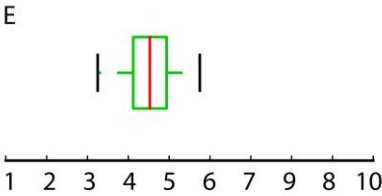
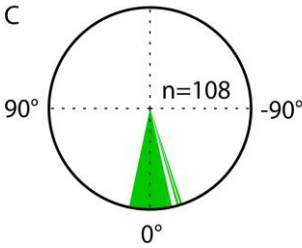


Figure 3-5 Target cartridge selection in the absence of Gogo

(A, B''') Horizontal sections of midpupal laminae at 42 hrs APF in wild-type control and in *gogo*⁻ background. At this time point R1-R6 axons have reached their target cartridges. Arrowheads **(A-A''')**, **(B-B''')** and dots **(A''', B''')** mark the start and asterisk **(A-A''', B-B''')** the end of R4 extensions. **(A-A''')** In control animals, R4 projection patterns (green) are uniform in direction and length and the overall pattern (magenta) displays orderly distributed and uniformly sized cartridges. Extension start displays the position where R4 axons reached the plexus. **(B-B''')** R4 extensions are not parallel and the overall pattern is highly disrupted. R4 cells form occasional long projections (red asterisk) and two R4 axons converge to a single target (orange asterisk). **(C, D)** Polar plots visualize orientation vectors of R4 axons in wild-type control and mutant conditions. **(E, F)** Boxplots displays significant variances in R4 axon length between the wild-type control **(E)** and the Gogo mutant **(F)**. Scale bar: 5µm.

3.6 Absence of Gogo in R cells disrupts lateral patterning of Lamina neurons

The extension of retinal axons towards the brain has been shown to be essential for the establishment of Lamina neurons (LNs) (Selleck and Steller, 1991, Meinertzhagen and Hanson, 1993, Huang and Kunes, 1996, 1998, Huang et al., 1998). In particular, arriving R cells induce proliferation and differentiation of LNs. LNs columns incorporate into pre-existing R axon fascicles in a one-to-one matching.

As in *gogo* mutant eyes, R axon fascicles were unevenly arranged along the lamina plexus, I examined if aberrant fascicle order could lead to defective lamina column assembly. I visualized LN cell bodies by antibody staining against the neuronal antigen Elav. Additionally, I visualized R4 axons by expressing mCD8GFP under the control of the *mδ*-Gal driver. I first analyzed the horizontal pattern of LNs in late third instar larval brains. In control flies, LNs formed columns of five cell bodies that intermingled between R4 axons (figure 4-6 A-A’). When Gogo was removed exclusively from the majority of R axons, the pattern of LN cell bodies was indistinguishable from wild-type controls (figure 4-6 A-B’): Columns perfectly integrated within R4 axons. I conclude that Gogo in R axons is not mediating proliferation or differentiation of LNs. To test if unevenly arranged R axon fascicles in *Gogo* mutant eyes affect the lattice of LNs, I analyzed the lateral distribution of LN neuron cell bodies in pupal stages at the onset of target cartridge selection (42hrs APF). In control animals LN cell bodies form an equal pattern above the lamina plexus (figure 4-6 E). However, when Gogo was absent in R axons but not in LNs, the well-ordered pattern of LN cell-bodies was disrupted (figure 4-6 F). This indicates that a disruption of R axon patterning along the lamina plexus can indirectly alter the lateral distribution of LN columns. As LNs serve as destination for R1-R6 axons during cartridge selection (Meinertzhagen and O’Neil, 1991, Meinertzhagen and Hanson, 1993), the results suggested that defective patterning of LNs could indirectly alter R1-R6 target cartridge selection.

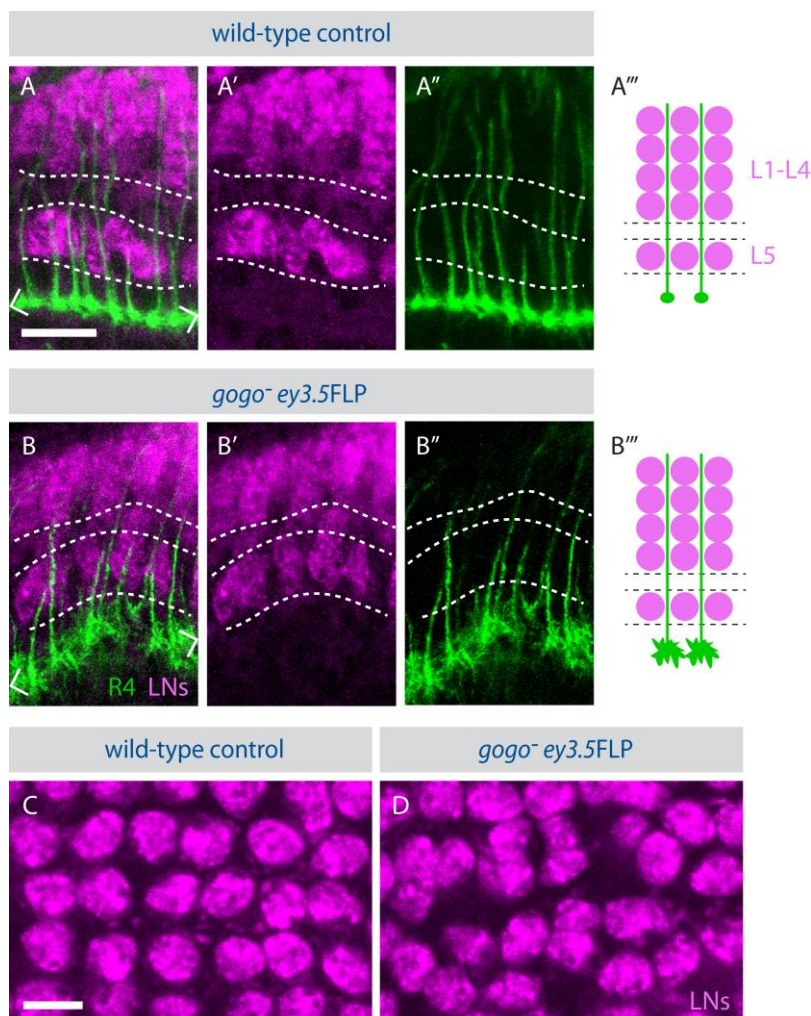


Figure 3-6 lamina column formation in *gogo* mosaic eyes

(A-B''') Horizontal sections of lamina neuron (LN) cell bodies and R4 axons in 3rd instar larvae in wild-type **(A-A'')** and *gogo* mutant **(B-B'')** brains, and corresponding schematics **(A''', B''')**. Chevrons indicate the lamina layer, and dashed lines separate LNs L1-L4 and L5 horizontally, respectively. R4 axons are labeled with GFP (green) and LNs are stained with the neuronal antibody anti-elav (magenta). **(A-A''')** In wild-type, LN cell bodies form columns of five neurons above the lamina plexus that intermingle between R axons (here only R4 is visible). **(B-B''')** The absence of Gogo does not influence column formation of LN and one-to-one incorporation of LNs and R axons. As described in the previous section, axon growth cones are enlarged compared to wild-type. **(C, D)** Lateral sections of LN cell bodies in pupal brains at 42hrs APF. In wild-type, LNs columns are equally distributed above the lamina plexus. In *Gogo* mosaic eyes LN columns fail to arrange orderly, resulting in an irregular pattern. Scale bars: A-B'': 10µm; C, D: 5 µm

3.7 Gogo is not required cell-autonomously in R cells for lateral cartridge selection

Aberrant target cartridge innervation of R4 axons could be caused by the disruption of the orderly arranged pattern of R1-R6 fascicles or LNs, respectively. However, defective target cartridge choice in pupae was shown to be mainly mediated by axon-axon interactions (Luo et al., 1997, Clandinin and Zipursky, 2000, Lee et al., 2001, Lee et al., 2003, Chen and Clandinin, 2008, Prakash et al., 2009). Thus, a reason of aberrant cartridge assembly and probably the most intuitive one of R1-R6 target defects described above could be a disruption of axon-axon interactions mediated by Gogo. To test this hypothesis, I assessed single cell analysis using the complementary (c) MARCM method (Lee and Luo, 1999, 2001, Prakash et al., 2005, Tomasi et al., 2008). This method allows generation of GFP labeled mutant cells in an otherwise wild-type background and uses a combination of the Gal4-UAS and the FLP/FRT system (figure 4-7 A). Mutant cells are generated in heterozygous animals via mitotic recombination induced by a heat-sensitive recombinase (hs-FLP). To selectively label homozygous mutant cells, the *gal80* gene is located in *cis* to the mutation. Gal80 suppresses Gal4-induced activation of the UAS promoter. After mitotic recombination, mutant cells lack the Gal80 repressor and UAS-activated GFP expression is no longer suppressed. Compared to the general MARCM method, in the cMARCM approach additionally the wild-type cells are labeled (Tomasi et al., 2008). This is achieved by recombining *gmr-mKOrange* in *cis* to the mutation. Each R cell type in the retina can be identified based on its morphology and position (Meinertzhagen and Hanson, 1993). Because axonal extensions of R cell types in the lamina are stereotypic with respect to the position of their cell bodies, the subtype and the behavior of individual axons can be analyzed in the wild-type labeled background (figure 4-7 B-D).

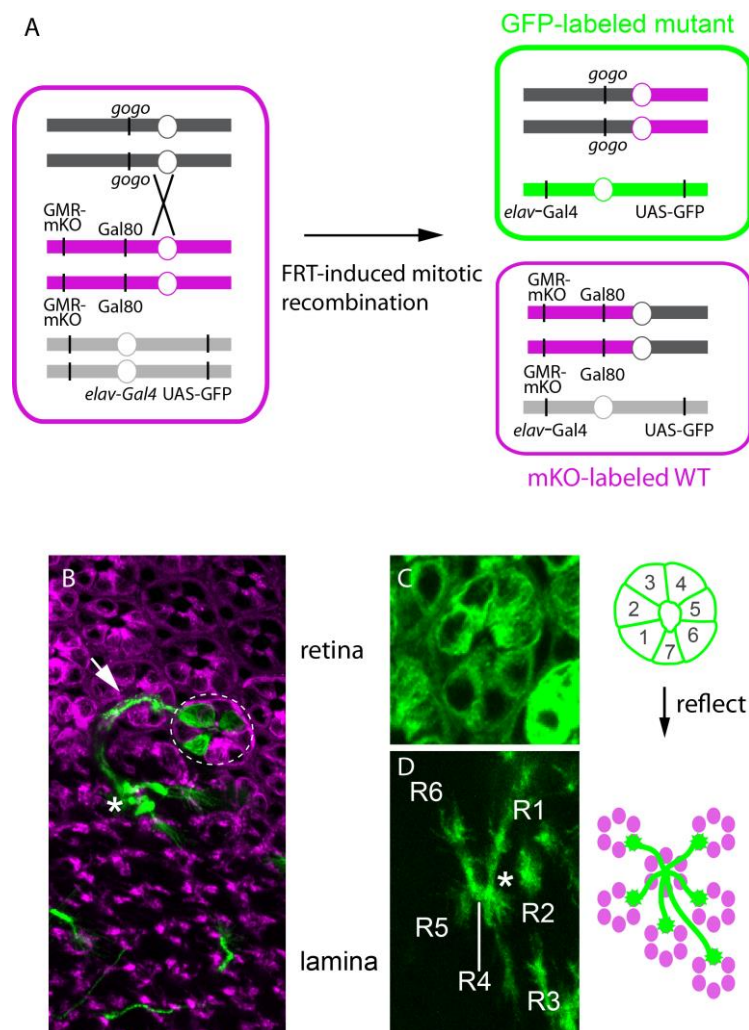


Figure 3-7 Strategy of cMARCM and presentation of analysis of single labeled R cells

Schematic of the complementary MARCM strategy. Left upper panel: Somatic cells are heterozygous for a *gogo* null allele and carry in *cis* to the mutant chromosome the Gal4 repressor Gal80 and the R cell marker GMR-KO. In heterozygous flies expression of UAS-mCD8-GFP by the neuronal driver *elav-Gal4* is repressed by Gal80. After DNA replication (G2) chromatids of the parental and the maternal chromatids undergo side-directed mitotic recombination mediated by FLP-FRT Recombination. Right upper panel: Upon mitotic recombination Gal80 repressor and *gmr-mKO* are lost and both chromatids carry the *gogo* null allele. Due to the lack of the Gal80 repressor the Gal4 protein can activate the UAS promoter via binding, and mCD8-GFP expression is no longer suppressed in homozygous mutant cells. Lower right panel: The second daughter cell is homozygous for *gmr-KO* and Gal80, and is therefore phenotypically indistinguishable from heterozygous cells. **(B)** mCD8-GFP labeled R cells can be traced from their cell bodies (dashed line) to the lamina (asterisk) by following their axons (arrow). **(C)** R1-R8 cell bodies form a flower shaped structure and each R cell subtype can be identified based on its position and morphology. **(D)** The lateral extension

made by R1-R6 axons is specific and invariant, and 180° rotated with respect to the position of R1-R6 cell-bodies.

I traced mutant axons from the retina to the lamina and followed their projections from their pre-cartridges to the target cartridges. R cells homozygous for the control chromosome defasciculated properly from their original ommatidial fascicle, spread upon the surface of the lamina and innervated correct cartridges (figure 4-8 A-C', n=23). Next, I analyzed ommatidia in which one R1-R6 cell was mutant for Gogo. Notably, all projections made by single mutant R axons, homozygous for *gogo* null mutation, were indistinguishable from the control experiment (figure 4-8 D, D'', n=20). I could not detect any defective target cartridge selection for either R1-R6 subtype. Additionally to single mutant cells, I analyzed ommatidia which contain two (figure 4-8 E, E', n=13) or more (figure 4-8 F, F', n=9) mutant cells. Remarkably, also under this conditions mutant axons were, as in wild-type, invariant and specified by their original ommatidium. These results revealed that Gogo is not required in a cell-autonomous way in R1-R6 cells to mediate target cartridge choice.

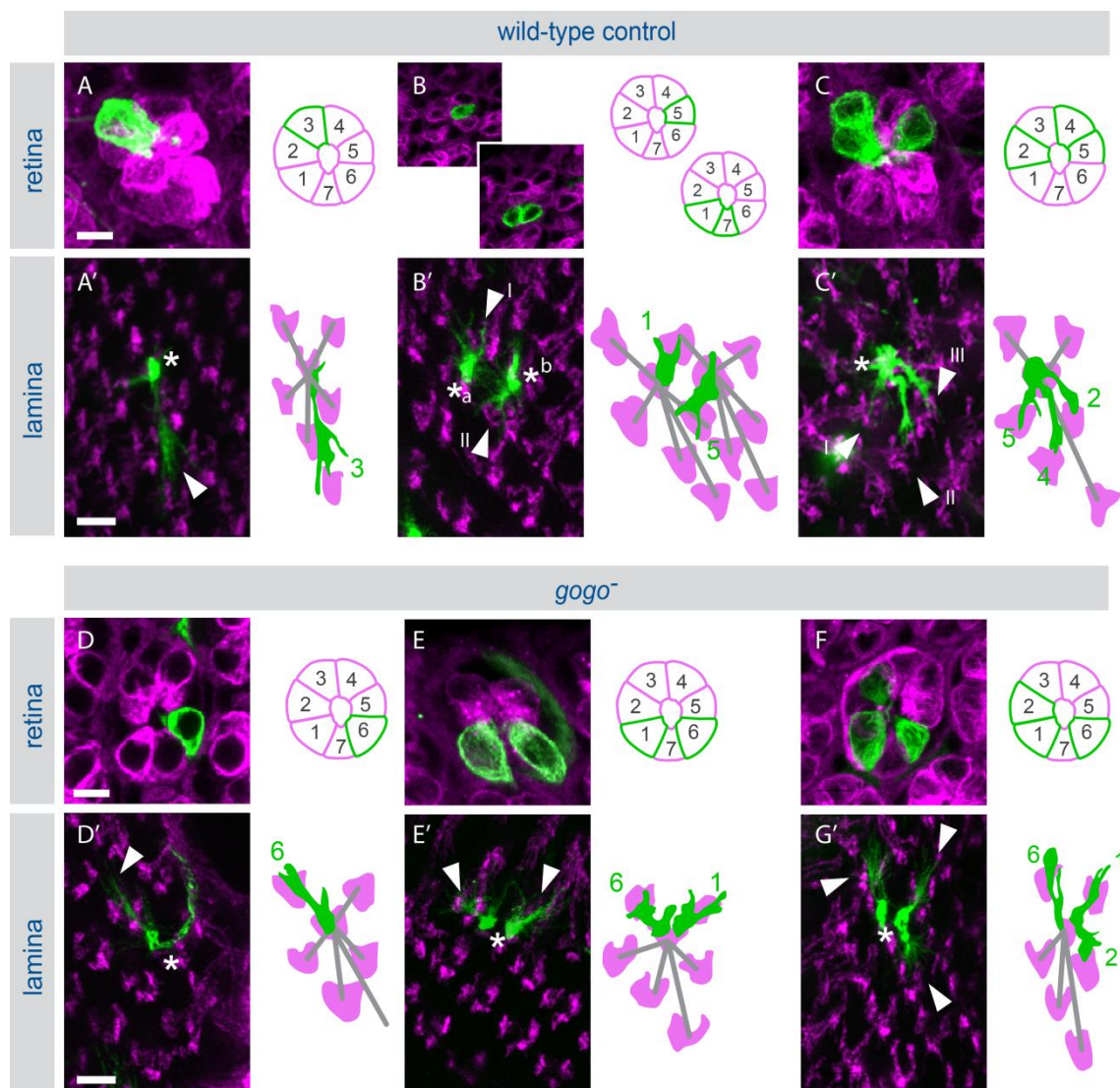


Figure 3-8 Gogo is not required in single R cells for lamina cartridge selection

(A-G') Cross sectional view of ommatidia (**A, B, C, D, E, F**), their lateral projection in the lamina and corresponding schematics (**A', B', C', D', E', F'**). Single cells were made homozygous for control chromosome or the *gogo*⁻ allele via mitotic recombination using cMARCM. Pupae were dissected at 42 hrs APF to visualize axonal target cartridge selection. Control or mutant R axons are labeled by mCD8-GFP (green) and remaining wild-type cells are labeled with GMR-KO (magenta). Asterisk marks start and arrowhead end of axon extensions. Wild-type and *gogo*⁻ R axons surrounded by wild-type cells choose correct targets in the lamina with respect to the position of their ommatidial cell bodies. Grey lines in schematic drawings indicate the expected projections of the remaining R1-R6 cells that are adjacent to mCD8-GFP labeled cells within the ommatidium.

3.8 Gogo is not required in neighboring axons for lateral cartridge selection

The finding that Gogo is not required cell-autonomously in R cells raised the question if Gogo could act non-autonomously and thereby supply a short-range signal for neighboring cells. In this way, the molecular mechanism of how Gogo mediates cartridge selection would be similar to the transmembrane protein Flamingo (Fmi (Chen and Clandinin, 2008)). To analyze the behavior of wild-type axons neighboring *gogo* mutant axons, I used the reverse (r) MARCM method (figure 4-9 A, (Chen and Clandinin, 2008)). In this approach the Gal80 repressor was located in *cis* to the *gogo* null mutation. Therefore all wild-type cells expressed KO and additionally, individual wild-type cells were labeled with mCD8-GFP. *gogo* mutant R cells did not express any marker and could therefore be detected in the labeled wild-type background, as they appear black. This allowed me to trace wild-type axons which are directly adjacent to *gogo* mutant axons. I analyzed axons which are directly neighboring to a mutant axon (n=46) and those which have either one (n=19) or two (n=9) wild-type cells between themselves and the mutant axon (figure 4-9 B-D'). Additionally, I analyzed ommatidia that contain more than one *gogo* mutant cell. However, all analyzed wild-type R axons selected appropriate target cartridges, independent of position and number of mutant neighbors. Taken together those results suggest that *gogo* is not mediating afferent-afferent interaction between axons which originate from the same ommatidium during target cartridge selection.

It has been described previously that within each ommatidium the R8 axons differentiate first. Thus, I considered the possibility that Gogo function in R8 single cells to provide a signal to R1-R6 axons for proper guidance. Thus, I additionally analyzed the behavior of wild-type R1-R6 axons when Gogo was absent in R8 axons. However, also in this experiment, the absence of Gogo was not influencing target selection (n=12, supplementary figure 1). Thus, a removal of Gogo in single cells was insufficient to result in the phenotype described above.

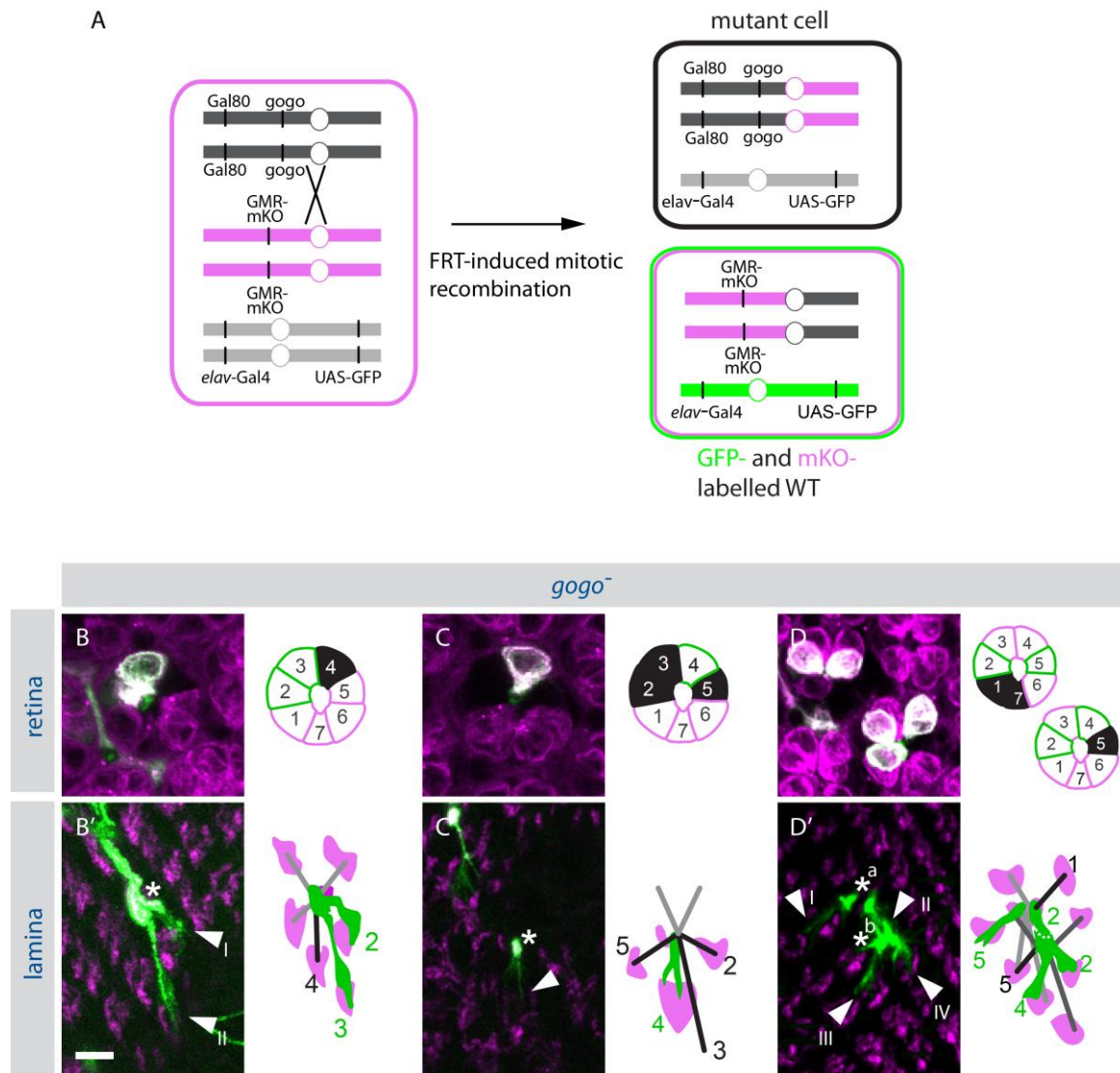


Figure 3-9 Gogo is not providing non-cellautonomous signals to R1-R6 axons.

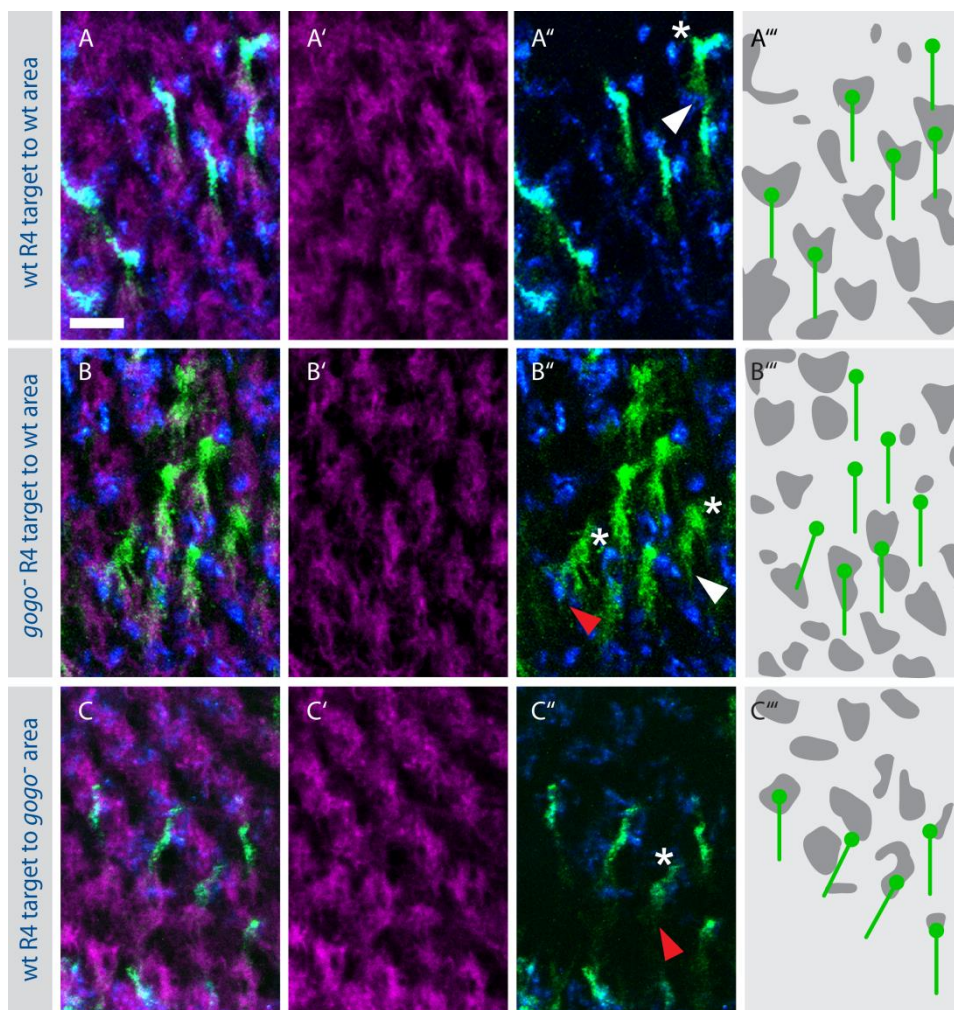
(A) Schematic of the reverse MARCM strategy. Left panel: Autosomal cells heterozygous for a *gogo* null allele carry in *cis* to the mutation the *Gal80* gene and in *trans* *gmr-KO* orange, which are all flanked by FRT sites. Heterozygous R cells are therefore marked with KO orange. Right upper panel: After FRT-induced mitotic recombination by heat sensitive flipase, one daughter cell carries the two wild-type alleles of *Gogo* and *Gmr-KO*. The cell lacks the Gal4 repressor *Gal80* and expresses mCD8-GFP. Right lower panel: Consequently, the second daughter cell is a homozygous mutant for *gogo⁻* and is neither expressing KO nor mCD8-GFP. **(B-D')** Target cartridge selection of mCD8GFP-labeled wild-type R1-R6 axons which are adjacent to *gogo⁻* R cells. Homozygous mutant cells express no marker and their cell bodies appear black within the KO-labeled wild-type ommatidial cell-bodies **(B, C, D)**. In corresponding regions in the lamina only extensions of mCD8-GFP expressing wild-type axons, but not of *gogo* mutant axons are visible **(B', C', D')**.

3.9 Gogo is required in R axons of neighboring ommatidia

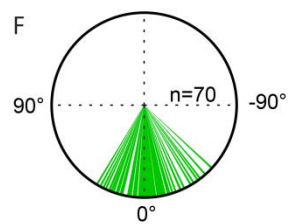
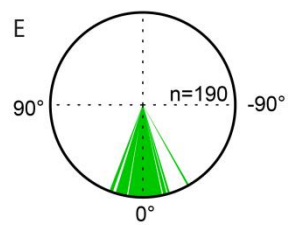
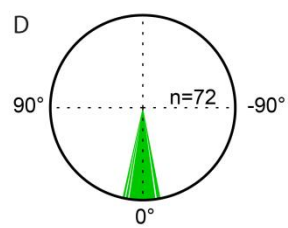
Single mutant R1-R6 cells did not display targeting defects in wild-type tissue. The same is true for wild-type R axons with mutant neighbors. Therefore, I next examined the phenotype when Gogo was absent in a small fraction of neighboring ommatidia, since the abnormal phenotype could reflect a community effect of a large fraction of misguided axons. I removed Gogo using only one copy of *ey3.5FLP* and analyzed mutant patches that span only a few neighboring ommatidia. I visualized only mutant R4 axons expressing mCD8-GFP under the control of the $m\delta$ -Gal4 driver and by recombining the Gal80 repressor in *trans* to the *gogo* mutation. Interestingly I found, that within these small clones target the overall pattern of cartridge assembly in pupal brains was not altered and R4 axons displayed an overall parallel and orderly arranged projection pattern (figure 4-10 A-B”). Thus, the phenotype seen in large clones did not appear. To assess the differences in R1-R6 target cartridge selection between large clones and small clones, I analyzed the behavior of mutant R4 axons that project from the mutant side of the clone border towards the wild-type side. I visualized only mutant R4 axons by combining the Gal4 repressor Gal80 in *trans* to the Gogo mutation (figure 4-10 B). I found that the projection pattern of mutant axons that project from the mutant side of the clone border towards the wild-type side is indistinguishable from wild-type control (figure 4-10 A-B); As expected, the overall projection pattern of mutant R4 axons was parallel at the border and vector angles distribution was not significantly different from the control (two-sampled K-S test, figure 4-10 D, E). There was also no significant variance between R4 axon length in mutant and control (levene’s test, figure 4-10 G, H). Nevertheless, mutant R4 growth cones showed an increase of filopodia like structures, as described also above. I conclude from this data that at the clone border the spatial distribution of R axon fascicles and therefore the position of R4 target areas was not altered. I conclude that Gogo has to be absent in a large fraction of neighboring ommatidia to disrupt the order of the retinotopic map. In the light of my findings described above on *gogo* single and large cell clones, these data strongly argue for a role of Gogo in R cell topography that can be compensated for in small mutant areas.

In small clones fascicle order was not disrupted and mutant R4 axons targeted to correct cartridges. Together with the finding that Gogo is not required in R1-R6 axons to mediate afferent-afferent interactions, this suggests that defective target cartridge choice in the absence of Gogo is only a secondary defect of fascicle order along the lamina plexus. However, I considered the possibility that Gogo could have a non-cell autonomous function in R cells of the target area for growing R1-R6 axon. To assess the behavior of wild-type

axons that project to a *gogo*⁻ area, I analyzed the reciprocal experiment. I visualized wild-type, but not mutant R4 axons by recombining the Gal80 repressor in *cis* to the *gogo* mutation. Interestingly, wild-type R4 axons failed to project in parallel when their target cartridge was mutant (figure 4-10 C-C’'). Vector angles of R4 axons were significantly different compared to wild-type controls (two-sampled K-S test, $p < 0.0016$) and to the reciprocal experiment ($p < 0.016$, figure 4-10 D-F)). In contrast, the length of wild-type R4 axons was invariant to the control groups (Levene’s test, figure 4-10 G-I). Thus, although the position of the target area was not altered, R4 axons fail to innervate correct targets when Gogo is absent in R cells of the target area. In the light of my findings described above, this led me suggest that Gogo could mediate R1-R6 target selection in two different ways: First, altering the lattice of LN targets could indirectly affect R1-R6 target selection. Second, Gogo in R cells within the target area could provide a direct signal to growing R1-R6 axons.



R4 orientation vectors



R4 length in μm

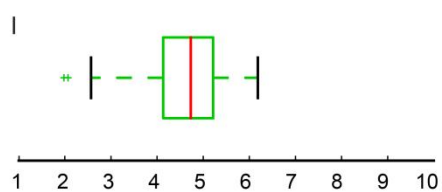
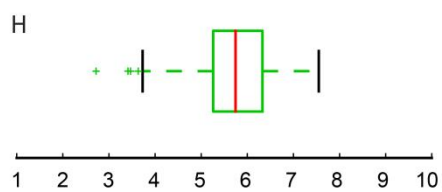
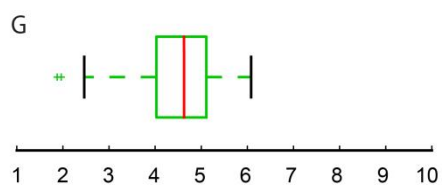


Figure 3-10 Gogo is required in R axons of neighboring ommatidia for target cartridge selection

(A-C''') Projection pattern of R4 axons at the clone border. **(A-A''')** Laminae of control animals display a uniform R4 and overall projection pattern. **(B-B''')** Mutant R4 axons express mCD8-GFP, whereas wild-type R4 axons are not visible. When R axons of the target cartridge area are wild-type the majority of *gogo*⁻ R4 axons project parallel to each other. However, the morphology of R4 mutant growth cones is changed. Growth cones are bigger and bear more filopodia-like structures compared to the wild-type control. **(C-C''')** Wild-type R4 axons express mCD8-GFP, whereas mutant R4 axons are not visualized. Wild-type R4 growth cones fail to target parallel and often fail to innervate appropriate targets. **(D-F)** Orientation vectors of controls **(D)**, *gogo*⁻ R4 axons that project to wild-type area **(E)**, and wild-type R4 axons that target to a *gogo*⁻ area **(F)**. **(G-I)** boxplots showing the variance in axonal length of R4 axons in controls **(G)**, mutant R4 axons that target to wild-type areas **(H)** and wild-type R4 axons that target to R axon mutant areas **(I)**. Scale bars: 5µm.

3.10 Gogo function in R8 is sufficient to form a smooth topographic map along lamina plexus

Gogo is required for the formation of a smooth topographic map at the level of the lamina. However, loss of Gogo in single cells or in small regions was insufficient to cause a defect in lamina topography. This suggests that Gogo is involved in a coordinator or pioneer fashion to set up the initial axon framework required to build the final map.

Therefore I next assessed, if Gogo is sufficient in only a subset of R cells to guide ommatidial fascicles to their correct positions at the lamina plexus. Within each ommatidium the R8 cell is the first to differentiate and send its axon towards the brain, followed by sequential outgrowth of R2& R5, R3& R4, R1& R6 and lastly R7 (Wolff and Ready, 1993). Interestingly it is proposed that R8 acts as a pioneer axon for the ommatidial fascicle. To address this question I performed rescue experiments with cell type specific drivers. I generated *gogo*⁻ mosaic eyes using *eyFLP* to remove Gogo from the majority of R cells and the target area. In pupal stages, at the onset of target cartridge selection the overall pattern of cartridges was severely disrupted (figure 4-11 A). I next expressed one copy of FL Gogo exclusively in R8 axons using the specific driver line Gal4 109-68 in the *gogo*⁻ *eyFLP* background. Interestingly, targeted expression of Gogo in R8 axons was sufficient to completely rescue the R1-R6 phenotype (figure 4-11 B): The overall pattern of the lamina was indistinguishable from wild-type: Cartridges were orderly arranged and sized. To visualize the regularity of the pattern, I generated plot profiles of 40µm (spans approximately 4 cartridges) and pooled the data. While I could not detect a periodicity in *gogo*⁻ mosaic flies, the pooled profiles of the R8 rescue displayed four regular peaks (figure 4-11 C, D). In a second approach, I expressed FL-Gogo using the *mδ*-Gal4 driver line. As mentioned above, expression of this Gal4 line is already seen in larval stages and is expressed not only in R4 but also in R3 and weakly in R7 cells at this developmental time-point. However, in contrast to the R8 rescue, I could not detect a comparable rescue (figure 4-11 E-H). I conclude that Gogo expression in R8 is sufficient for the orderly arrangement of R1-R6 fascicles and R1-R6 target selection.

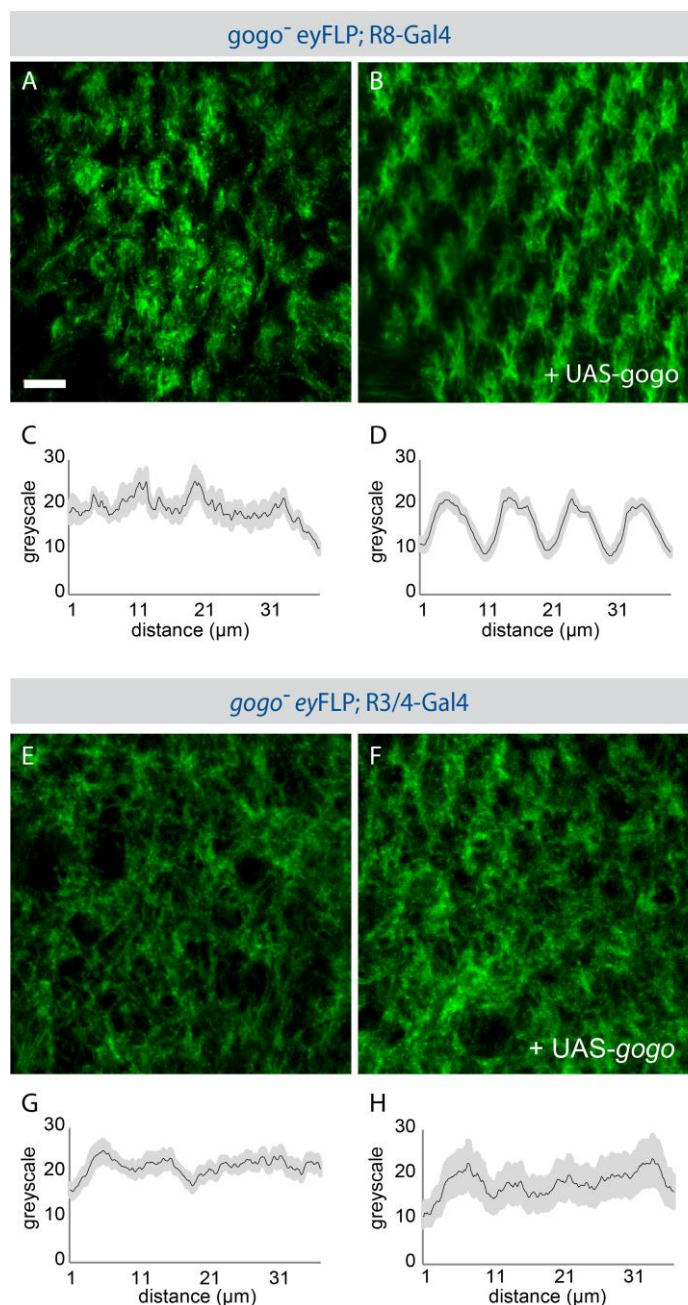


Figure 3-11 Gogo function in R8 is sufficient to maintain retinotopic map formation

(A-H) Pupal lamina in *gogo⁻* mosaic eyes (*eyFLP*) and specific rescue experiments stained with 24B10 antibody and plot profiles. (A, E) The absence of Gogo in the majority of R axons and the target area strongly disrupts the overall pattern of pupal lamina formation (42 hrs APF). (B) When FL Gogo is specifically re-expressed in R8 axons the ordered pattern of the topographic map is fully rescued. (F) However, FL Gogo expression in R4 and R3 axons in the mutant background is insufficient to restore the orderly arrangement of cartridges (B, D, F, H) Pooled plot profiles of 4 cartridges each in single experiments display the pattern regularity. The R8 rescue displays a periodic profile while in mutant controls and R4 rescue a periodicity is not detectable. Scale bars: 5 μ m

3.11 Gogo is crucial for centripetal elongation of R1-R6 axons

The presented results clearly suggest that Gogo function is mediating cartridge formation during the first half of pupal development. However, one result remains unresolved. Although expressing Gogo exclusively in R8 in a mutant background rescued the pupal phenotype, [Hakeda-Suzuki et al. \(2011\)](#) demonstrated that in adults a specific R8 rescue is not sufficient to rescue cartridge assembly. This indicates that Gogo is not only required for cartridge assembly during the first half of pupal development but must have also a different function after target cartridges are already selected. Therefore, I next tested the behavior of mutant axons during cartridge elongation.

Upon reaching their final target cartridges wild-type R1-R6 axons form a characteristic thick terminus that projects centripetally assembling the lamina neuropile ([Meinertzhagen, 1993](#)). R1-R6 growth cones extend parallel to neighboring axons and remain tightly associated with axons of their target cartridge. I analyzed the centripetal extension of R1-R6 axons within the developing lamina in the absence of Gogo. I first characterized the projections of R4 extensions within cartridges at 51 hrs APF. Axons of individual cartridges in a horizontal view can be clearly distinguished from neighbors at this developmental stage ([figure 4-12 A-A''](#)). As expected, I always found exactly one R4 axon within each cartridge projecting parallel to neighboring R4 axons, towards the brain. The position of R4 axons was not changed within the cartridges. I then examined the extensions of axons within target cartridges in the *gogo*⁻ mutant background (*ey3.5FLP*). In such conditions R4 did not extend straight but turns laterally ([figure 4-12 B-B''](#)). The m24B10 antibody staining of all R axons revealed that cartridge bundles project away from their appropriate paths. Surprisingly, I found that single R4 cells often do not stay in their initial target cartridge but project to neighboring cartridges following inappropriate tracts (*chi test*, $p > 0.0001$).

To examine if the bundling phenotype still occurs in adult flies, I performed a second experiment. I expressed mCD8-GFP under the control of Rh1-Gal4 and recombined the Gal4 repressor Gal80 in *trans* to the *gogo* mutation to visualize only mutant axons. In adult control brains R1-R6 wild-type axons form straight termini that are parallel ([figure 4-12 F](#)). R1-R6 axons that lack Gogo (*ey3.5FLP*) often bundled with mutant axons ([figure 4-12 G](#)). Thus, the absence of Gogo leads to strong defects in termini extension within cartridges. The bundling of R1-R6 axons indicate that Gogo mediates repulsive interactions between R1-R6 axons.

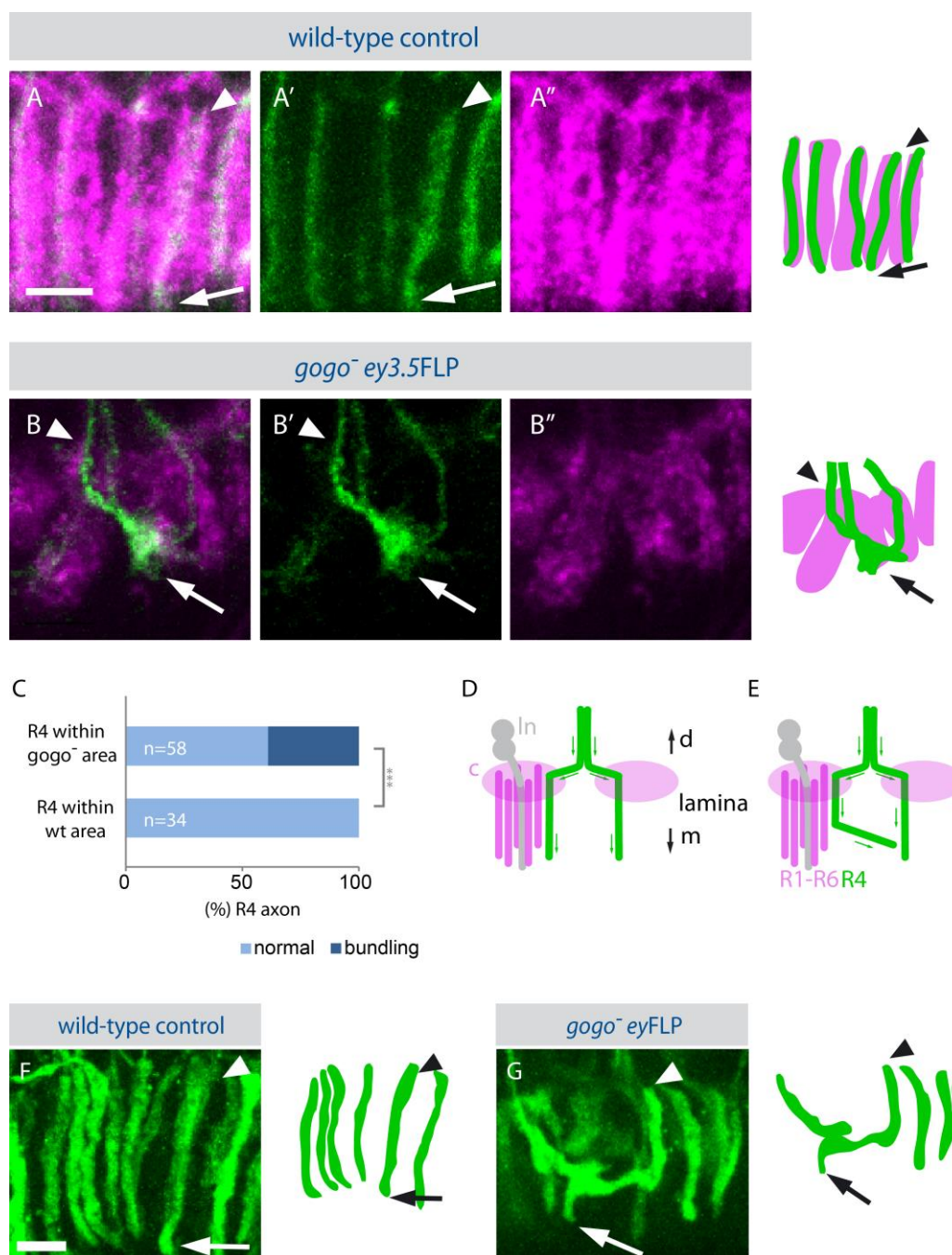


Figure 3-12 In *Gogo* mosaic eyes R axons bundle with R axons from neighboring cartridges

(A-B'') Horizontal sections showing the developing lamina in wild-type and *gogo⁻* mosaic eyes and corresponding schematics at 51 hrs APF. R1-R6 axons are labeled with Gmr-KO (magenta) and R4 axons are labeled with GFP (green). Arrowheads indicate an axon's start and arrows end of elongation. **(C, D)** Schematic drawings of wt R1-R6 axon extensions during cartridge formation in wt and mutant backgrounds. When axons arrive at the lamina plexus they extend lateral to the target cartridge (c), turn again and elongate parallel with lamina neurons (In). Synapses are formed along

the whole cartridges. In wild-type controls R axons elongate parallel in separate columns. **(B-B'', D)** When Gogo is absent in the majority of ommatidia R axons fail to project parallel to one another. Moreover, single R axons (R4) leave their original target cartridge and bundle with axons of adjacent cartridges. Note that axon termini are not yet fully extended at this developmental stage. **(E)** In the wild-type control all R4 axons follow the original tracts of their target cartridge. In the *gogo*⁻ background almost 40% of R4 axons project away from their target cartridge to join a neighboring column. **(F, G)** The phenotype still appears in adult flies. mCD8-GFP expressing R1-R6 axons are homozygous for a control **(F)** or *gogo*⁻ **(G)** allele. While in wild-type control flies R1-R6 axons project in parallel, they often bundle with adjacent *gogo*⁻ R axons. Scale bars: 5µm

3.12 Gogo is insufficient in single R axons to cause bundling during cartridge elongation

I next determined if Gogo function in single R cells would be sufficient to cause the phenotype described above. To visualize the behavior of single *gogo*⁻ R1-R6 axons within cartridges, I used the cMARCM method. I analyzed the structure and the projections of wild-type and *gogo*⁻ protusions. Like in wild-type controls ($n=25$), single mCD8-GFP-labeled *gogo* mutant R1-R6 ($n=29$) elongate straight within their original ommatidia (figure 4-13). However, like during earlier developmental stages, growth cones of mutant axons displayed abnormal increases in filopodia-like structures. Thus, similar to the phenotype described above, the absence of Gogo in single axons was insufficient to cause the phenotype described above.

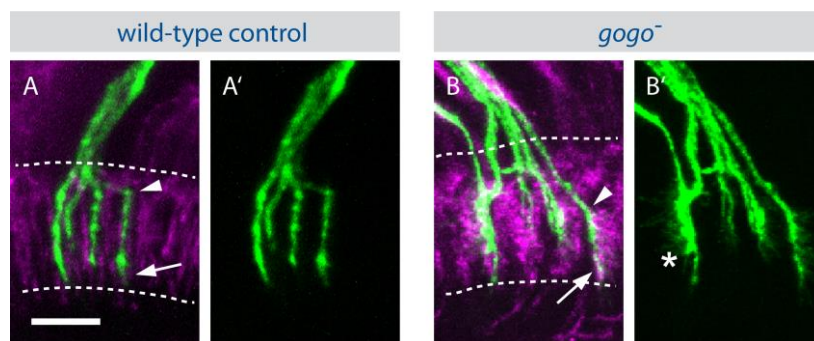


Figure 3-13 single mutant R1-R6 axons during cartridge elongation

(A-B') cMARCM in control flies **(A, A')** and in the absence of Gogo **(B, B')** in pupae at 51 hrs APF. Arrowheads indicate start (apical) and arrows end (medial) of extensions. Dashed lines indicate the lamina plexus. Single axons homozygous for a control chromosome or a *gogo* null allele are labeled by mCD8-GFP, while the wild-type background is labeled with *gmr-KOrange*. Dashed lines indicate the lamina plexus. In the wild-type control, R1-R6 termini extend straight within cartridges. When single *gogo* mutant axons are surrounded by wild-type axons they do not bundle but extend straight. Mutant R1-R6 extending termini display more filopodia-like structures compared to wild-type. Note that axon termini are not yet fully extended at this developmental stage. Scale bar = 5 μ m

3.13 R axon elongation within cartridges is directly regulated by Gogo function

The observed phenotype within the lamina plexus posed the question whether an inappropriate number of axons per cartridge caused bundling within the lamina plexus based on an unbalanced distribution of attractive and repulsive molecules in cartridges. Two lines of evidence demonstrated that the bundling of R1-R6 termini during centripetal axonal extension is due to a primary function of Gogo and not simply to a secondary effect of inappropriate cartridge choice during pupal development: First, as described above, the specific expression of Gogo in R8 could rescue the initial topographic map formation and as a consequence the lateral target choice of R1-R6. In contrast, the cartridge assembly in adult was not rescued although R8 medulla targeting was completely normal.

Second, the atypical cadherin Flamingo (Fmi) is required for proper target cartridge selection (Lee et al., 2003, Chen and Clandinin, 2008). In the absence of Fmi, axons choose inappropriate targets and thus cause a strong hypo- and hyperinnervation of cartridges. In a lateral view of the adult lamina the cartridges contain a variable number of axon termini (Lee et al., 2003). If bundling of R1-R6 axons within lamina cartridges would be due to axon guidance defects earlier in development, Fmi mutants should display defects comparable to Gogo mutants in elongation of R1-R6 termini within lamina cartridges. I therefore analyzed centripetal axon growth when Fmi was absent in R cells. In contrast to *gogo* mutants, the pattern of R1-R6 axons within cartridges in the Fmi mutant background was indistinguishable from wild-type (figure 4-14 A-C). However, the high density of the lamina made it difficult to analyze the horizontal lamina pattern in detail when all R1-R6 axons were labeled. Thus, I could not analyze if in the absence of Fmi the horizontal pattern of lamina cartridges displayed possible small deviations compared to wild-type. Due to time constraints and difficulties to generate the required genetic backgrounds, I could so far not visualize only small fraction of R1-R6 termini in the Fmi mutant background.

Together, the results suggest that strong bundling of R1-R6 axons within lamina cartridges is independent of (1) fascicle distribution and (2) aberrant target cartridge innervation. This indicates that Gogo function in R1-R6 axons is directly mediating the correct spacing of axons from neighboring cartridges during centripetal elongation.

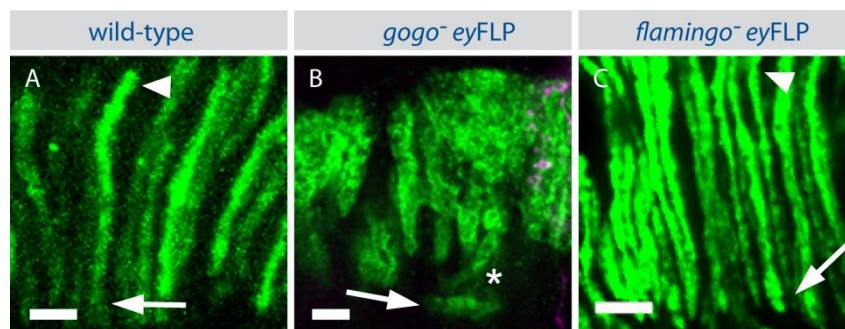


Figure 3-14 R1-R6 axon termini do not bundle in the absence of Fmi

(A-C) Horizontal view of adult cartridges in wild-type controls, *gogo*⁻ eyFLP and *fmi*⁻ eyFLP mosaic eyes in adult brains. Axon termini are visualized by expressing lacZ under the control of the R1-R6 specific Rh1 promoter. Arrowheads mark the start (apical) and arrows the end (medial) of R1-R6 axon extensions. Unlike in the absence of Gogo **(B)**, the lack of Fmi **(C)** is indistinguishable from the wild-type control **(A)**. Scale bars: 5 μ m

3.14 Gogo function is concentration-dependent during R axon elongation in target cartridges

To examine if differences in the Gogo concentration between R cell subtypes influence cartridge formation, I dissected brains in the Gogo *gain of function* background to analyze. I overexpressed two copies of FL Gogo using $m\delta$ -Gal4 driver line. I additionally expressed mCD8-GFP to visualize R4 axon extensions. I first analyzed pupal brains to examine target cartridge selection when Gogo is overexpressed. Increasing Gogo levels did not disrupt R4 target selection or the overall pattern of cartridges (figure 4-15 A-B'). This result was consistent with my loss of function data presented above: Neither a removal nor an increase of Gogo in R axons could influence target cartridge selection cell-autonomously.

Next I focused on cartridge assembly in adult brains to analyze if an increase of Gogo concentration in R4 axons would influence R1-R6 elongation within cartridges. Since the markers I used in pupal brains are difficult to detect in adult brains, I visualized R1-R6 termini by expressing lacZ under the control of the Rhodopsin1 (Rh1) promoter. The Rh1-promoter drives expression in all R1-R6 cells. In the wild-type control, cartridges displayed uniform rings of six axon termini per cartridge (figure 4-15 C). Interestingly, similar to the loss of function condition (chapter 4-1), increasing Gogo levels in a subset of R cells caused hypo- and hyperinnervation of cartridges (figure 4-15 D). In the mutant only around 50% of all cartridges were innervated by the normal number of 6 termini, compared to 100% in wild-type (figure 4-15 E). 50% of all cartridges varied from four to nine termini per cartridge. The mis-innervation indicates that bundling occurs between R1-R6 termini within cartridges when the amount of Gogo is increased in R3/R4 axons. I additionally examined the horizontal pattern of R1-R6 axons within the adult lamina to analyze if termini bundle when Gogo expression levels are altered. The $m\delta$ -Gal4 is not or only weakly expressed in R4 axons but displayed a strong expression in glia and/or LNs (figure 4-15 F-G", green channel). I visualized R axons by staining the pre-synaptic marker 6H4 (figure 4-15, F-G", magenta channel). When Gogo is overexpressed, extensions of R1-R6 termini display irregularities compared to wild-type that indeed could indicate bundling between axons. However, the phenotype seems to be less strong than in the loss of function background. As mentioned in the last chapter, it is difficult to analyze the horizontal pattern of axons within lamina cartridges when all R1-R6 axons are labeled. Due to the quality of the images, the results presented in figure 4-15, F-G" are preliminary.

As the $m\delta$ -Gal4 driver is not specific to a subset of R axons but is also expressed in glia cells and LNs from mid-pupal stages on, I expressed Gogo as a control using the *gcm*-Gal4 driver line. This promoter drives expression in glia cells and LNs during development.

However, I could not detect any mis-innervation defects in flies with *gogo* overexpression restricted to glia and LNs (data not shown).

This indicates that the relative amount of Gogo is crucial in R1-R6 axons during cartridge elongation. However, increasing Gogo levels in R3/4 cells is insufficient to induce defective target cartridge selection during pupal stages. Thus, the results are consistent with Gogo loss of function situation and show that Gogo is not required in R1-R6 axons to mediate target cartridge selection.

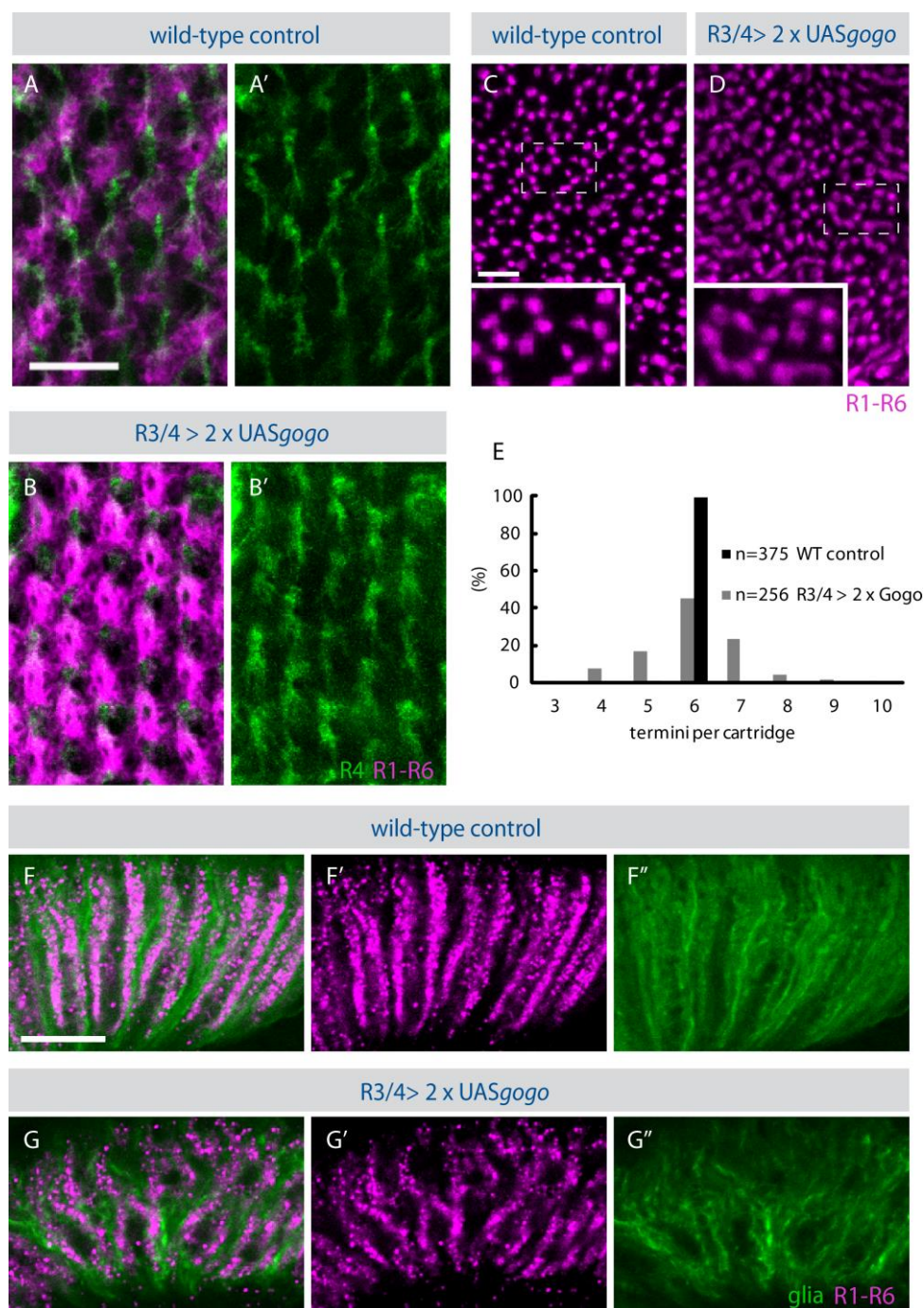


Figure 3-15 Overexpression Gogo in pupal and adult brains

(A-D) Confocal stacks of wild-type and overexpression of Gogo in R3/R4 using the $m\delta$ -Gal4 driver. **(A, B)** wild-type control and overexpression in pupal laminae. R1-R6 cells are labeled with mAB24B10 antibody staining and R4 axons are visualized by mCD8-GFP expression. Increasing Gogo level in R3/R4 axons is not influencing R4 target selection or the overall pattern of cartridges assembling. **(C, D)** Wild-type control and overexpression in adult laminae. Termini of R1-R6 axons are visualized using the direct fused construct Rh1-lacZ. While in wild-type cartridges are formed by six axon termini (rings) the number of termini per cartridges alters when Gogo levels are increased in R3/R4. **(E)**

Quantification of termini per cartridge in wild-type controls and overexpression. **(F-G'')** Horizontal pattern of wild-type control and overexpression of Gogo in adult brains. R1-R6 axons are visualized by 6H4 antibody staining (magenta). In adult stages, $m\delta$ -Gal4 is expressed in glia cells and/or LNs (green). Compared to wild-type **(F-F'')**, the pattern of R1-R6 axons in gain of function flies is disrupted **(G-G'')**. Scale bars: A-D = 5 μ m, F-G'': 10 μ m

4 DISCUSSION

Here I show that the transmembrane protein Golden goal (*gogo*) is required in the *Drosophila* visual system for R1-R6 photoreceptor retinotopic map formation, a principle of visual systems that allows for the continuous representation of visual fields in the brain. To maintain retinotopy in the *Drosophila* lamina, R1-R6 axons have to undergo a complex and precise axonal sorting during development, a principle called neural superposition; this enhances the signal-to-noise ratio (Meinertzhagen and Hanson, 1993). The precise connection pattern of R1-R6 axons ensure that R cells receiving the same light input form synapses with the same set of postsynaptic neurons. In *gogo* mutant mosaic eyes, R1-R6 axons fail to innervate their lamina cartridges properly, displaying strong hypo- and hyperinnervation defects. Motion vision is important for flies to navigate correctly in their environment and the visual system comprises more than half of the fly brain. It has been shown in behavioral assays that the motion perception of flies depends on proper R1-R6 function (Buchner and Heisenberg, 1977). In *Gogo* mosaic eyes, R1-R6 axons fail to innervate their lamina cartridges properly, displaying strong hypo- and hyperinnervation defects. Defective R1-R6 innervation in *Gogo* mosaic eyes should lead to a reduced or eliminated motion detection in the fly as cartridges are innervated by R axons that receive different light inputs. *Gogo* has been previously described to mediate synaptic layer targeting in R8 axons. In particular, *Gogo* mediates repulsive interactions between R8 axons during medulla targeting and axon-target interactions to maintain retinotopy. However, the function of *Gogo* during lamina targeting was not analyzed yet. Here I provide evidence that *Gogo* functions in 3 independent steps during visual system development. First, *Gogo* is required for the correct patterning of the initial topographic map during ganglion specific targeting. Second, in later developmental stages *Gogo* is required in the target field to guide growing R1-R6 axons to correct cartridges. Third, during centripetal elongation of R1-R6 axons within cartridges *Gogo* function restricts R axons within their bundle.

4.1 Initial R1-R6 patterning depends on pioneer-follower interactions

My results indicate that during early developmental stages (30hrs APF) Gogo is involved in initial topographic map formation of R1-R6 axons. In particular, R1-R6 fascicles target initially to the correct ganglion, the lamina, and do not over- or undershoot but display defects in their spatial distribution along the plexus. The irregular spacing of R1-R6 fascicles disrupts initial retinotopy. How is the smooth initial topographic mapping of R axon fascicles instructed by Gogo function? I have shown that Gogo function in R8 axons is sufficient to mediate target specificity of R1-R6 axon fascicles. Targeted expression of Gogo in R8 axons in the mutant background is sufficient to fully rescue topographic ordering: the lamina displays a regularity which is indistinguishable from wild-type. This provides evidence for a pioneer role of R8 axons for R1-R7 axons. Contrary, when Gogo was expressed in later differentiating R3 and R4 subtypes, I did not observe a similar rescue. Thus, the pathfinding of R1-R6 follower axons is strongly influenced by the genotype of R8 pioneers. The principle of pioneer-follower interactions is often found in sensory systems throughout species and is an essential mechanism of axon guidance processes in any developing nervous system (Raper and Mason, 2010). In general, pioneer axons are born early in development when axons only have to grow over small distances. Pioneer axons are thought to provide a scaffold to follower axons that are later born in development. Especially in visual systems, it has been shown that pioneer-follower interactions are involved in the establishment of retinotopic organization in *Xenopus* and *Danio rerio* (zebrafish) (Holt, 1984, Pittman et al., 2008).

In *Drosophila*, pioneer follower interactions between R8 and R1-R6 axons have been proposed in previous studies (Tomlinson and Ready, 1987, Lee et al., 2003): 25 years ago a study from Tomlinson and Ready revealed that within each ommatidium the R8 axons differentiate first, followed by sequential outgrowth of R1-R7 axons. This suggests a pioneer role of R8 for photoreceptor patterning. On a molecular level, the atypical cadherin Flamingo (Fmi) has been shown to be sufficient in R8 axons for correct initial topographic mapping of R1-R6 axons across the lamina plexus (Lee et al., 2003). Flamingo mediates repulsive interactions between R8 axons and when this molecular cue is missing, neighboring R1-R8 fascicles fail to maintain their correct column and bundle. A function of Gogo that is restricted to R8 axons during initial topographic mapping is also consistent with the protein's spatial expression pattern: In third instar larval stages, when R axons differentiate and grow towards the brain, Gogo is expressed specifically at the tips of R8 axons but not in R1-R6 (Tomasi et al., 2008). From 24 hrs APF Gogo protein is detected in R1-R6 axons.

What distinguishes pioneer R8 axons from follower R1-R7 axons? Gogo functions in early differentiating R8 axons is sufficient for proper retinotopic map formation, while Gogo

function in late differentiating R3 and R4 does not show a similar rescue. This led me to suggest a model in which the timing and/or the position of axon outgrowth rather than the cell identity is crucial for pathfinding. How do follower axons interact with R8 axons? The simplest interpretation is that R1-7 axons directly follow the axons through fasciculation with R8. It is previously described that in vertebrates, cell adhesion molecules (CAMs) of the immunoglobulin superfamily (IgSF) are involved in navigating retinal ganglion cells (Pollerberg and Beck-Sickinger, 1993, Brittis et al., 1995, Avci et al., 2004, Zelina et al., 2005). Future studies could reveal if disruption of CAMs in *Drosophila* R axons could lead to similar guidance defects. In zebrafish, pioneer axons have been shown to be essential to initiate the outgrowth of follower axons (Pittman et al., 2008). Selective laser or genetic ablation of R8 axons could be helpful to further examine if suppressing the outgrowth of R8 axons would subsequently block R1-R7 outgrowth. Diphtheria toxin-mediated ablation of all R cells revealed that in principle R cells can be ablated during development (Kunes and Steller, 1991). However, the specific ablation of R8 is challenging as R8 induces the determination of R1-R7 cell-fate and thus the time window for ablation is short.

4.2 Axon-target vs. axon-axon interactions

How does Gogo in R8 pioneer axons mediate R1-6 initial topographic mapping? To explore how Gogo determines correct spacing of ommatidial bundles at the lamina plexus, I assessed whether Gogo could provide repellent or competitive interactions to restrict the intermediate target area. While during medulla targeting Gogo indeed mediates repulsive interactions between R8 axons (Tomasi et al., 2008), I did not find evidence that lamina targeting is similarly regulated. In the absence of Gogo, R8 axons do not bundle or clump with R8 neighbors before exiting the lamina plexus, and R1-R6 axon bundles distribute across the entire dorso-ventral axis. Moreover, R4 axons continue to grow in their original fascicle, indicating that Gogo is not mediating fasciculation among R1-R8 axons. This suggests that Gogo is not involved in self-assembly of the initial retinotopic map but rather in an axon-target process.

It has been proposed in many studies in vertebrates and invertebrates that two guidance mechanisms are mainly involved in the establishment of retinotopic map formation during development. First, retinal cells are guided by the existence of molecular labels that are expressed in gradients across the target areas as shown for Ephrins (McLaughlin and O'Leary, 2005). Second, in addition to axon-target interactions, retinotopic map formation requires axon-axon competition (Reber et al., 2004). In the *Drosophila* visual system both, long-range guidance via positional cues and axon-axon competition are required for retinotopic mapping. Gradients of Ephrin (Eph) receptor tyrosine kinases and dWnt4 molecular cues are required for map formation (Dearborn et al., 2002, Sato et al., 2006, Dearborn et al., 2012). Additionally, a number of mutants revealed that targeting of R axon fascicles can be independent of axon-axon competition (Kunes et al., 1993). In the absence of the transcription factor *sine oculis* (*so*) and the *Epidermal growth factor receptor* (*Egfr*, also known as *Ellipse*), neighboring wild-type fascicle target correctly although neighboring fascicles are absent. Furthermore, wild-type axons adjacent to mis-routed glass mutant R axons do not show targeting defects, indicating that indeed axon-target interactions are involved in retinotopic map formation in *Drosophila* (Kunes et al., 1993). Still, target independent guidance of R axons mediated by axon-axon interaction and competition has been proposed during medulla targeting (Lee et al., 2003, Senti et al., 2003, Bazigou et al., 2007, Tomasi et al., 2008).

Could Gogo provide a positional guidance cue within R8 axons to mediate axon-target interactions? Gogo antibody staining revealed that in the developing visual system the protein localization is higher in younger R8 axons (Tomasi et al., 2008). This could indicate that Gogo is expressed in a gradient across all R8 axons and supports the idea that Gogo mediates axon-target interactions. In cell aggregation assays it has been shown previously

that the extracellular domain of Gogo is not promoting homophilic binding. Furthermore, during medulla targeting homophilic bindings are not required for axon-axon or axon-target interactions between R8 axons and R8 axons and target neurons, respectively (Tomasi et al., 2008). Thus, Gogo is likely to mediate axon guidance via heterophilic binding. However, possible candidates for binding partners are not yet identified.

How could the relative position of R cells bundles be determined via Gogo receptor signaling? Lamina neurons can not fulfill this function as they are integrated into columns only after R cells are positioned at their intermediate target. The destination zone of ommatidial bundles is highly populated by glia cells which are in close contact to the growth cones and which provide a stop signal to R1-R6 axons. Could correct fascicle positioning also be regulated via glia-axon interactions? Such a mechanism has been already suggested by Yoshida et al. (2005) (Yoshida et al., 2005). When glia cells fail to differentiate, R cells are not able to find their intermediate targets and mis-target, resulting in the irregular patterning of lamina neurons. Moreover, in the *Drosophila* embryo the absence of midline or longitudinal glia leads to defasciculation defects or misrouting of axons, respectively (Klammt et al., 1991, Hidalgo et al., 1995, Hidalgo and Booth, 2000).

4.3 The role of Gogo during R1-R6 target cartridge selection

Beside the defects in fascicle distribution along the lamina plexus, I observed that at a later developmental time point, R1-R6 axons fail to select appropriate target partners when Gogo is absent in a large fraction of ommatidia. Previous investigations elucidate that R1-R6 target selection depends on three sequential steps: First, the orientation of R1-R6 axonal projections is influenced by the orientation of the ommatidium from which they originated in the retina along the dorso-ventral axis (Clandinin and Zipursky, 2000). Second, interactions among R1-R6 growth cones regulate the direction of growth cone extension of individual R cell types, and hence, the trajectory paths (Meinertzhagen and Hanson, 1993, Luo et al., 1997, Clandinin and Zipursky, 2000, Clandinin et al., 2001a, Lee et al., 2003). Intense studies revealed molecules that are required for afferent-afferent interactions among R cells. Fmi regulates interactions among R1-R6 growth cones in a level-dependent non-cell autonomous way (Lee et al., 2003). By contrast, the receptor tyrosine phosphatase LAR is required for R axons to leave their fascicle (Clandinin et al., 2001a). In a final third step, axon-target interactions between R1-R6 axons and lamina neurons play a putative role. N-Cad in lamina neurons has been shown to mediate the recognition or projections towards the specific targets (Clandinin et al., 2001a, Lee et al., 2001).

Interestingly, my results reveal that Gogo is not involved in any of the three proposed steps of target cartridge selection. First, the absence of Gogo does not influence the orientation of the ommatidia in early development. Second, at a later developmental stage, single mutant R axons defasciculate properly from the ommatidial fascicles and choose correct target cartridges, suggesting that Gogo is not mediating cell-autonomous interactions between growth cones. Moreover, wild-type axons are not influenced by the absence of Gogo in adjacent R cells. This excludes the possibility that Gogo is regulating R1-R6 target selection in a non-cell autonomous way. The result is rather surprising as most genes described to be required for cartridge formation are directly mediating afferent-afferent interactions between R1-R6 axons. Third, as described above, re-expressing Gogo in R8 axons in the mutant background rescued the entire retinotopic map at the onset of target cartridge selection. This clearly indicates that although Gogo is expressed in R1-R6 axons and in lamina neurons, Gogo function in R8 axons is sufficient for correct retinotopic mapping until midpupal stages.

How does Gogo function in R8 axons contribute to R1-R6 target specificity during pupal development? My results provide evidence that Gogo is required within the target area for guiding R1-R6 axons. I show that in small *gogo* mutant clones and at the clone border distribution of R1-R6 fascicles appears normally. I analyzed the projections of R4 axons from the mutant side of the clone border towards the wild-type side, and find that at clone borders,

mutant R4 axons project normally when they innervate areas in which R1-R8 fascicles are wild-type. This result is consistent with my finding that Gogo is not required for afferent-afferent interactions between R1-R6 axons. In contrast, in the reciprocal experiment, wild-type axons navigate incorrectly to areas that are initially innervated by mutant R cells. This provides evidence that Gogo is required non-cell autonomously in neighboring R8 axons of the target field to guide R1-R6 growth cones. It has been shown previously that molecular labels in lamina neurons are necessary for correct R1-R6 targeting (Prakash et al., 2005, Prakash et al., 2009). However, to my knowledge, it has been not described before that a molecular label is required for target cartridge selection in R axons within the target area. I propose a model in which Gogo in R8 axons provides a signal to navigate R1-R6 growth cones (figure 5-1 A, B). However, this surprising result leaves open several possibilities regarding the precise role of Gogo in R8 in controlling R cell target choice. On one hand, incorrect pattern formation of R axons could be due to the requirement of Gogo in R8 axons that could provide a signal to growing R1-R6 axons. In an alternative model, R8 could pattern the target in a Gogo-dependent fashion by providing a signal to the target area. In the absence of Gogo signal in R8 axons the target develops abnormally and this resulting deviations in cartridge organization may lead to defects in R1-R6 targeting.

Since within large *gogo* mutant clones fascicle distribution is altered, my results also stresses the importance of proper spacing between axon fascicles for R-cell targeting and extension. Although R1-R6 axonal extensions are cell-type specific and asymmetric during cartridge selection, R1-R6 fascicles and lamina neuron targets are identical (Clandinin and Zipursky, 2002). They only differ in their anterior-posterior and dorso-ventral position at the lamina plexus. A lack of Gogo alters the positional map of axon fascicles, and thereby the horizontal position of the lamina target neurons. I compared R4 pattern formation at the clone border, where R1-R6 fascicle distribution appears normally, and within large *gogo* mutant clones. I found that in the latter, R4 axons are not only shifted in projection direction but vary significantly in their axonal length compared to R4 axons at the clone border. Thus, I propose that by shifting the target R cell field, the R-axon continues to grow until reaching its target (figure 5-1 C, D). In this model, Gogo is only indirectly influencing target cartridge selection. My results complement an earlier study, where diagonal but not mirror-reflecting rotation of ommatidia disrupts the axon extension in regards to the position of its cell body, suggesting that both, the orientation of ommatidia and the proper assembly of neurons in the target field play a crucial role correct R1-R6 target innervation (Clandinin and Zipursky 2000).

Taken together, my results suggest two distinct models of R1-R6 target selection. First, Gogo in R8 axons provides a signal to the target area that reinstructs patterning of the target field later guiding R1-R6 growth cones towards their final target. Second, altered

fascicle spacing shifts the position of the target field that indirectly alters the extension of R1-6 axons towards the target.

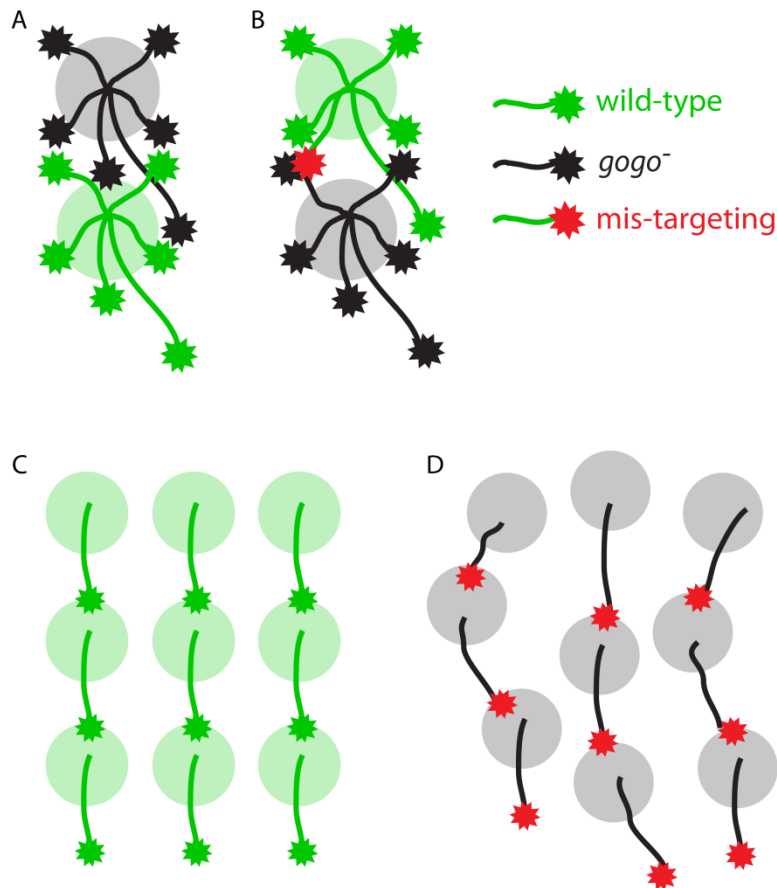


Figure 4-1 Target cartridge selection in the absence of Gogo

(A,B) Model 1: **(A)** *gogo* mutant R1-R6 axons target correctly to wild-type areas. **(B)** Wild-type axons fail to project correctly to areas that are initially innervated by mutant R axons.

(C, D) Model 2: **(C)** In the wild-type, target fields form a well arranged pattern. **(D)** When Gogo is absent in R axons the pattern of the target field is disrupted and thus R axons vary in the length of their extensions.

4.4 Redundancy compensates for the loss of Gogo in small fractions of R cells

Another interesting finding of the presented work is that a collapse of the initial retinotopic map occurs only when Gogo is absent in a group of neighboring neurons. A loss of Gogo function in single R8 axons or in only a few neighboring ommatidia reduces the phenotype to a nearly undetectable level. This led me to suggest a model in which redundant mechanisms compensate for the loss of Gogo in single R axons or very small regions of mutant fascicles (figure 5-2). Genetic redundancy is a common principle that refers to situations where the loss of function of a gene can be compensated for by the presence of other genes and is important to higher the robustness of an organism (Zhang, 2012).

Interestingly, a study in zebrafish proposed that the phenotype of a guidance molecule can be compensated for by complementary guidance mechanisms (Pittman et al, 2008). One possible explanation could be a model in which guidance by neighboring axons or fascicles narrows the area that can be occupied by each fascicle and thereby compensates for the loss of *gogo* in single R axons or very small regions of mutant neighboring fascicles. When the molecular cue Gogo is missing in only one or a few cells, their degree of freedom is still restricted by the fact that the surrounding axons follow their proper guidance target. Interestingly, computational and *in vivo* models addressed the co-dependence of spatial competition and axon-target interactions in the mouse visual system. The study on these models concluded that chemical labels are insufficient to specify the retinocollicular projection, but instead competition for space is required during map formation (Triplett and Feldheim, 2012).

Based on my data, I propose that the extraordinary precision of connection pattern in the *Drosophila* lamina is achieved through a combination of Gogo-dependent and Gogo-independent guidance by neighboring axons and fascicles. Gogo function can be partially compensated for by the presence of neighboring, correctly targeting wild-type R axons or axon fascicles that provide spatial restriction and guidance within the limited space of the fly retina. The combination of several complementary mechanisms or guidance molecules allows for extraordinary precision in the formation of nervous systems.

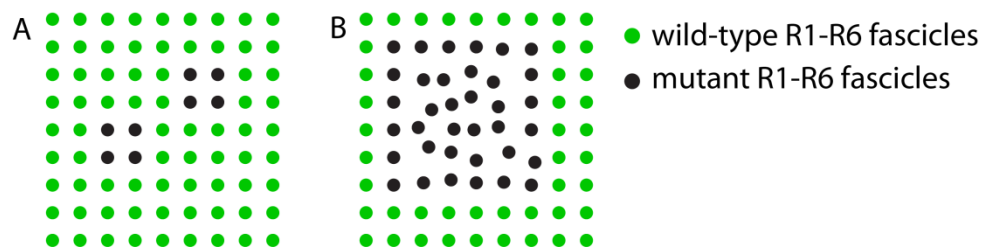


Figure 4-2 Redundancy in the absence of Gogo

(A) When Gogo is absent in only a small fraction of R cells, the pattern formation of the retinotopic map is not altered. **(B)** In large *gogo* mutant cell clones, R1-R6 fascicle fail to orderly arrange and the retinotopic map is disrupted.

4.5 Defining a new phenotype in the *Drosophila lamina*

In addition to Gogo function during 3rd instar larval stages and the first half of pupal development, I determined that Gogo is also required for the last step of cartridge formation. During this developmental step, R1-R6 axons have already terminated at their target cartridges, but turn again 90° and elongate the cartridge deepening the neuropil. Unlike in wild-type, R1-R6 axons fail to extend parallel within their original cartridge, but bundle within termini from neighboring cartridges. Three lines of evidence suggest that abnormal centripetal elongation in the Gogo mutant background are a result of a primary function of Gogo and not a secondary consequence of aberrant target cartridge innervation: First, unlike Gogo, the absence of the transmembrane protein Flamingo does not cause a phenotype, although both proteins display strong target cartridge innervation defects. Second, targeted expression of Gogo in R8 axons in the mutant background fully rescued initial topographic mapping and R1-R6 target cartridge innervation defects during pupal stages, but not aberrant cartridge formation in the adult. Lastly, increasing Gogo level seems to cause abnormal cartridge innervation and bundling in the adult but does not affect initial topographic mapping or target cartridge selection in pupae. Thus, Gogo function in R1-R6 is required for cartridge elongation.

How does Gogo prevent abnormal bundling during centripetal elongation of R1-R6 axons within cartridges? The *gogo* mutant phenotype led me to suggest that during the cartridge elongation phase *gogo* mutant axons lose repulsive interactions within the lamina neuropil causing strong bundling between R axons. The phenotype is similar to the one described during R8 medulla targeting (Tomasi et al., 2008), suggesting a similar molecular mechanisms during both developmental stages. In the R8 model, Gogo acts as a heterotypic receptor molecule that mediates repulsion between R axons. When Gogo as a repulsive cue is missing competitive adhesive interactions could cause bundling. Adhesive interactions that can be mediated by cell adhesion molecules are required for fasciculation or layer-specific targeting (Sanes and Zipursky, 2010). In the medulla, *gogo* mutant R8 axons only bundle with mutant R8 axons but not with wild-type axons. I could not examine if this is also true for R1-R6 axons. Like R8 axons, single mutant R1-R6 axons project without defects during cartridge elongation. However, I could not analyze if neighboring mutant R1-R6 axons only bundle with neighboring mutant but not wild-type axons. This is due to the high density of R1-R6 axons within the lamina, which makes it so far impossible to analyze two neighboring axons. One possibility would be to individually label subsets of wild-type and mutant axons with different markers. Preliminary results suggest that the intracellular domain is required for the elongation of R1-R6 axons within cartridges (unpublished data), and

indicates that the underlying function of Gogo is to permit R axons to separate from each other and may be the same in R8 and R1-R6 axons.

The *Drosophila* lamina is one of the best characterized synaptic regions across species. Several works have characterized different cell types within cartridges, the number of synapses and post- and presynaptic neurotransmitters (Meinertzhagen and O'Neil, 1991, Meinertzhagen and Sorra, 2001, Hamanaka and Meinertzhagen, 2010). Interestingly, a recent computational model demonstrated that assembly of lamina cartridges might be explained by wiring economy and volume exclusion (Rivera-Alba et al., 2011). However, it is still unknown how cartridge elongation of R1-R6 axons is regulated during development on a molecular level. Here, I give for the first time evidence that parallel extension of R1-R6 axons requires the action of molecular cues, specifically Gogo. In the absence of Gogo R1-R6 axons fail to stay in their appropriate cartridge and intermingle with axons of neighboring cartridges.

It would be interesting to analyze if other known regulators of the *Drosophila* visual system are also involved in cartridge elongation in the neuropile. For instance, it has been described previously that the absence of the receptor tyrosine phosphatase LAR and N-cadherin in single R1-R6 cells elongate normally within the cartridge although axonal morphology is slightly disrupted (Clandinin et al., 2001a).

4.6 Similarities and differences of Gogo function during medulla and lamina targeting

Gogo is a multifunctional protein that mediates axon-axon and axon-target interactions in R8. I have discussed in the last chapter the similarities between Gogo function during R8 medulla targeting and R1-R6 axon extension within cartridges. However, I can also observe some differences in the way Gogo mediates lamina and medulla targeting. While Gogo is required for guiding R8 axons to their correct layer in the medulla, R1-R6 axons stop at their appropriate layer in the lamina independent of Gogo function. Interestingly, similar to Gogo, the transmembrane protein capricious (caps) and Fmi play a striking role in R8 but not in R1-R6 or R7 for layer-specific targeting (Lee et al., 2003, Senti et al., 2003, Shinza-Kameda et al., 2006). Layer-specificity in the lamina has been shown to depend on the presence of the receptor tyrosine phosphatase PTP69D and the Leukogen-antigen-related-link (LAR) (Newsome et al., 2000a, Clandinin et al., 2001a).

During medulla targeting Gogo permits R8 axons to separate from each other (Tomasi et al., 2008). I could not find evidence that Gogo is mediating axon-axon interactions between R axons before exiting the lamina and favor the idea that column-specificity of R1-R6 axons requires Gogo for interactions between R8 axons and their target.

It has been previously described that R8 axon-target interactions in the medulla depend on the interaction of Gogo and the transmembrane protein Flamingo (Fmi) (Hakeda-Suzuki et al., 2011). While Gogo alone is sufficient to promote targeting to the M1 intermediate layer, final targeting to the M3 layer requires the combined action of Gogo and Fmi. Although the phenotypes of Gogo and Fmi in the adult lamina are similar, my analysis suggests that they do not collaborate during R1-R6 axon guidance. First, while Gogo is not mediating repulsion between R8 axons before exiting the lamina, R1-R8 fascicles bundle in the absence of Fmi in R8 axons, suggesting that Fmi mediates axon-axon and not axon-target interactions during larval stages (Lee et al., 2003). Second, during target-cartridge selection Fmi regulates afferent-afferent interactions between R1-R6 axons in a non-cell autonomous way (Chen and Clandinin, 2008). In contrast, my analysis revealed that Gogo is not required for R1-R6 axon-axon interactions. Third, Gogo regulates centripetal elongation of R1-R6 termini within cartridges, whereas the absence of Fmi does not affect R1-R6 axon guidance during this developmental stage. Thus, the underlying mechanisms of Fmi and Gogo during R8 and R1-R6 pathfinding are likely to be different.

During medulla targeting, Gogo function strictly requires the presence of the cytoplasmic domain, suggesting it functions as a receptor rather than a cell adhesion molecule (Tomasi et al., 2008, Mann et al., 2012). Future experiment could elucidate whether lamina targeting depend on Gogo signaling via the cytoplasmic domain.

Interestingly, it has been shown that the cytoplasmatic domain of Gogo physically interacts with *hu li tai shao* (*hts*), the *Drosophila* homologue of the mammalian Adducin, a molecule involved in the assembly of the Actin-Spectrin cytoskeleton (Matsuoka et al., 2000, Ohler et al., 2011). Gogo has been proposed to positively and negatively regulate Hts during R8 axon targeting. Recent data indicate that the absence of Hts also affects cartridge assembly in the adult lamina (oral communication from S. Ohler, unpublished data). A possible interaction of Gogo and Hts could also explain the abnormal morphology of *gogo* mutant R1-R6 growth cones. In particular, *gogo* mutant growth cones are enlarged and develop more filopodia-like structures compared to wild-type. Similarly it has been reported that in the absence of Gogo or *hts* R8 growth cones display large swellings (Hakeda-Suzuki et al., 2011, Ohler et al., 2011, Mann et al., 2012). It might thus be possible that lamina targeting requires the combined interaction of Gogo and Hts.

5 CONCLUSION

Understanding the molecular basis for the establishment of retinotopic maps has been one of the major issues of axon guidance research. The transmembrane protein Golden goal has already been described to be required for the establishment of the *Drosophila* visual system. While several studies have addressed how Gogo mediates R8 medulla targeting, the underlying function during lamina cartridge formation was unclear. Here I define three distinct and specific functions for Gogo during R1-R6 axon targeting which provide new insights into how the wiring of the *Drosophila* lamina is achieved throughout development.

During ganglion-specific targeting Gogo is required in R8 axons for the correct patterning of R1-R6 fascicles along the lamina plexus. My results provide evidence that in this context Gogo is mediating axon-target interactions between R8 and a yet unidentified ligand in the target. Thus, it will be important to identify the Gogo ligand. It will be also interesting to analyze if Gogo uses the same ligand in R8 axons during medulla and lamina targeting.

My results provide evidence that at the onset of target cartridge selection Gogo is required in R8 axons within the target area to guide R1-R6 axons. However, the molecular details of Gogo function in this context remains unclear. Future experiments should address whether Gogo has a permissive or an instructive role in R8 to guide R1-R6 axons. In a permissive model, Gogo would act as a direct cue to guide R1-R6 axons, while in the instructive model Gogo would be required for the correct patterning of the target area. Thus, it would be necessary to establish methods which allow a detailed visualization and analysis of the target area.

The *gogo* bundling phenotype within lamina cartridges provides the first step towards our understanding of how R1-R6 axon elongation is regulated during development. My results suggest that elongation of R1-R6 termini is mediated via repulsive axon-axon interactions. Further experiments addressing the requirement of different Gogo domains could reveal if the mechanism of how Gogo permits R1-6 axons to separate from each other is similar to R8. A more detailed analysis of cartridge elongation suffers from a lack of methods to visualize individual R cell types. In the future it might be helpful to discover R cell type specific markers to improve the visualization of the adult lamina structure.

Finally, Gogo function can be partially compensated for by the presence of neighboring, correctly targeting wild-type R axons fascicles that provide spatial restriction and guidance within the limited space of the fly retina. I suggest that this may reflect a

general mechanism to balance minor molecular differences in expression levels to ensure the high precision of circuit formation in the *Drosophila* lamina.

The genetic tools available in *Drosophila* and the precise knowledge of its anatomy of the visual system provide a powerful system to study the development and function of neuronal circuits. Together with the new functions I presented in this thesis, the Gogo receptor remains an interesting and promising molecule for future studies in axon guidance in the visual system.

REFERENCES

- Ascher D, Dubois PF, Hinsen K, Hugunin J, Oliphant T (2001) Numerical Python, Lawrence Livermore National Laboratory, Livermore, California, USA.
- Avci HX, Zelina P, Thelen K, Pollerberg GE (2004) Role of cell adhesion molecule DM-GRASP in growth and orientation of retinal ganglion cell axons. *Dev Biol* 271:291-305.
- Bate CM (1976) Pioneer neurones in an insect embryo. *Nature* 260:54-56.
- Bazigou E, Apitz H, Johansson J, Loren CE, Hirst EM, Chen PL, Palmer RH, Salecker I (2007) Anterograde Jelly belly and Alk receptor tyrosine kinase signaling mediates retinal axon targeting in *Drosophila*. *Cell* 128:961-975.
- Berger J, Senti KA, Senti G, Newsome TP, Asling B, Dickson BJ, Suzuki T (2008) Systematic identification of genes that regulate neuronal wiring in the *Drosophila* visual system. *PLoS Genet* 4:e1000085.
- Brand AH, Perrimon N (1993) Targeted gene expression as a means of altering cell fates and generating dominant phenotypes. *Development* 118:401-415.
- Brittis PA, Lemmon V, Rutishauser U, Silver J (1995) Unique changes of ganglion cell growth cone behavior following cell adhesion molecule perturbations: a time-lapse study of the living retina. *Mol Cell Neurosci* 6:433-449.
- Buchner E, Heisenberg M (1977) The role of retinula cell types in visual behavior of *Drosophila melanogaster*. *J comp Physiol* 117:127-162.
- Cafferty P, Yu L, Rao Y (2004) The receptor tyrosine kinase Off-track is required for layer-specific neuronal connectivity in *Drosophila*. *Development* 131:5287-5295.
- Chae J, Kim MJ, Goo JH, Collier S, Gubb D, Charlton J, Adler PN, Park WJ (1999) The *Drosophila* tissue polarity gene starry night encodes a member of the protocadherin family. *Development* 126:5421-5429.
- Chen PL, Clandinin TR (2008) The cadherin Flamingo mediates level-dependent interactions that guide photoreceptor target choice in *Drosophila*. *Neuron* 58:26-33.
- Cheng HJ, Nakamoto M, Bergemann AD, Flanagan JG (1995) Complementary gradients in expression and binding of ELF-1 and Mek4 in development of the topographic retinotectal projection map. *Cell* 82:371-381.
- Chevais S (1937) Sur la structure des yeux implantés de *Drosophila melanogaster*. *Archs Anat Microsc* 33:107-112.
- Choe KM, Prakash S, Bright A, Clandinin TR (2006) Liprin-alpha is required for photoreceptor target selection in *Drosophila*. *Proc Natl Acad Sci U S A* 103:11601-11606.
- Chotard C, Leung W, Salecker I (2005) glial cells missing and gcm2 cell autonomously regulate both glial and neuronal development in the visual system of *Drosophila*. *Neuron* 48:237-251.
- Chou WH, Hall KJ, Wilson DB, Wideman CL, Townson SM, Chadwell LV, Britt SG (1996) Identification of a novel *Drosophila* opsin reveals specific patterning of the R7 and R8 photoreceptor cells. *Neuron* 17:1101-1115.
- Clandinin TR, Lee CH, Herman T, Lee RC, Yang AY, Ovasapyan S, Zipursky SL (2001a) *Drosophila* LAR regulates R1-R6 and R7 target specificity in the visual system. *Neuron* 32:237-248.
- Clandinin TR, Lee CH, Herman T, Lee RC, Yang AY, Ovasapyan S, Zipursky SL (2001b) *Drosophila* LAR regulates R1-R6 and R7 target specificity in the visual system. In: *Neuron*, vol. 32, pp 237-248.
- Clandinin TR, Zipursky SL (2000) Afferent growth cone interactions control synaptic specificity in the *Drosophila* visual system. *Neuron* 28:427-436.

- Dearborn R, Jr., He Q, Kunes S, Dai Y (2002) Eph receptor tyrosine kinase-mediated formation of a topographic map in the *Drosophila* visual system. *J Neurosci* 22:1338-1349.
- Dearborn R, Jr., Kunes S (2004) An axon scaffold induced by retinal axons directs glia to destinations in the *Drosophila* optic lobe. *Development* 131:2291-2303.
- Dearborn RE, Jr., Dai Y, Reed B, Karian T, Gray J, Kunes S (2012) Reph, a Regulator of Eph Receptor Expression in the *Drosophila melanogaster* Optic Lobe. *PLoS One* 7:e37303.
- Dickson BJ (2002) Molecular mechanisms of axon guidance. *Science* 298:1959-1964.
- Drescher U, Kremoser C, Handwerker C, Loschinger J, Noda M, Bonhoeffer F (1995) In vitro guidance of retinal ganglion cell axons by RAGS, a 25 kDa tectal protein related to ligands for Eph receptor tyrosine kinases. *Cell* 82:359-370.
- Feldheim DA, Kim YI, Bergemann AD, Frisen J, Barbacid M, Flanagan JG (2000) Genetic analysis of ephrin-A2 and ephrin-A5 shows their requirement in multiple aspects of retinocollicular mapping. *Neuron* 25:563-574.
- Fischbach KF, Dittrich AP (1989) The optic lobe of *Drosophila melanogaster*. I. A Golgi analysis of wild-type structure. *Cell Tissue Res* 258:441-475.
- Freeman M (1996) Reiterative use of the EGF receptor triggers differentiation of all cell types in the *Drosophila* eye. *Cell* 87:651-660.
- Frisen J, Yates PA, McLaughlin T, Friedman GC, O'Leary DD, Barbacid M (1998) Ephrin-A5 (AL-1/RAGS) is essential for proper retinal axon guidance and topographic mapping in the mammalian visual system. *Neuron* 20:235-243.
- Fryxell KJ, Meyerowitz EM (1987) An opsin gene that is expressed only in the R7 photoreceptor cell of *Drosophila*. *EMBO J* 6:443-451.
- Fuerst PG, Harris BS, Johnson KR, Burgess RW (2010) A novel null allele of mouse DSCAM survives to adulthood on an inbred C3H background with reduced phenotypic variability. *Genesis* 48:578-584.
- Fuerst PG, Koizumi A, Masland RH, Burgess RW (2008) Neurite arborization and mosaic spacing in the mouse retina require DSCAM. *Nature* 451:470-474.
- Fujita SC, Zipursky SL, Benzer S, Ferrus A, Shotwell SL (1982) Monoclonal antibodies against the *Drosophila* nervous system. *Proc Natl Acad Sci U S A* 79:7929-7933.
- Gao FB, Kohwi M, Brenman JE, Jan LY, Jan YN (2000) Control of dendritic field formation in *Drosophila*: the roles of flamingo and competition between homologous neurons. *Neuron* 28:91-101.
- Garrity PA, Lee CH, Salecker I, Robertson HC, Desai CJ, Zinn K, Zipursky SL (1999) Retinal axon target selection in *Drosophila* is regulated by a receptor protein tyrosine phosphatase. *Neuron* 22:707-717.
- Garrity PA, Rao Y, Salecker I, McGlade J, Pawson T, Zipursky SL (1996) *Drosophila* photoreceptor axon guidance and targeting requires the dreadlocks SH2/SH3 adapter protein. *Cell* 85:639-650.
- Gaze RM, Sharma SC (1968) Axial Differences in Reinnervation of Optic Tectum by Regenerating Optic Nerve Fibres. *Journal of Physiology-London* 198:P117-&.
- Gibbs SM, Truman JW (1998) Nitric oxide and cyclic GMP regulate retinal patterning in the optic lobe of *Drosophila*. *Neuron* 20:83-93.
- Golic KG, Lindquist S (1989) The FLP recombinase of yeast catalyzes site-specific recombination in the *Drosophila* genome. *Cell* 59:499-509.
- Gong Q, Rangarajan R, Seeger M, Gaul U (1999) The netrin receptor frazzled is required in the target for establishment of retinal projections in the *Drosophila* visual system. *Development* 126:1451-1456.
- Gontang AC, Hwa JJ, Mast JD, Schwabe T, Clandinin TR (2011) The cytoskeletal regulator Genghis khan is required for columnar target specificity in the *Drosophila* visual system. *Development* 138:4899-4909.
- Hadjieconomou D, Timofeev K, Salecker I (2011) A step-by-step guide to visual circuit assembly in *Drosophila*. *Curr Opin Neurobiol* 21:76-84.

- Hakeda-Suzuki S, Berger-Muller S, Tomasi T, Usui T, Horiuchi SY, Uemura T, Suzuki T (2011) Golden Goal collaborates with Flamingo in conferring synaptic-layer specificity in the visual system. *Nat Neurosci* 14:314-323.
- Halder G, Callaerts P, Gehring WJ (1995) New perspectives on eye evolution. *Curr Opin Genet Dev* 5:602-609.
- Hamanaka Y, Meinertzhagen IA (2010) Immunocytochemical localization of synaptic proteins to photoreceptor synapses of *Drosophila melanogaster*. *J Comp Neurol* 518:1133-1155.
- Hansen MJ, Dallal GE, Flanagan JG (2004) Retinal axon response to ephrin-as shows a graded, concentration-dependent transition from growth promotion to inhibition. *Neuron* 42:717-730.
- Hardie RC (1979) Electrophysiological analysis of the fly retina: I Comparative properties of R1-R6 and R7 and 8. *J Comp Physiol* 129:19-33.
- Hardie RC (1987) Is histamine a neurotransmitter in insect photoreceptors? *J Comp Physiol A* 161:201-213.
- Hay BA, Wolff T, Rubin GM (1994) Expression of baculovirus P35 prevents cell death in *Drosophila*. *Development* 120:2121-2129.
- Hidalgo A, Booth GE (2000) Glia dictate pioneer axon trajectories in the *Drosophila* embryonic CNS. *Development* 127:393-402.
- Hidalgo A, Urban J, Brand AH (1995) Targeted ablation of glia disrupts axon tract formation in the *Drosophila* CNS. *Development* 121:3703-3712.
- Hiesinger PR, Zhai RG, Zhou Y, Koh TW, Mehta SQ, Schulze KL, Cao Y, Verstreken P, Clandinin TR, Fischbach KF, Meinertzhagen IA, Bellen HJ (2006) Activity-independent prespecification of synaptic partners in the visual map of *Drosophila*. *Curr Biol* 16:1835-1843.
- Hing H, Xiao J, Harden N, Lim L, Zipursky SL (1999) Pak functions downstream of Dock to regulate photoreceptor axon guidance in *Drosophila*. *Cell* 97:853-863.
- Ho RK, Goodman CS (1982) Peripheral pathways are pioneered by an array of central and peripheral neurones in grasshopper embryos. *Nature* 297:404-406.
- Holt CE (1984) Does timing of axon outgrowth influence initial retinotectal topography in *Xenopus*? *J Neurosci* 4:1130-1152.
- Huang Z, Kunes S (1996) Hedgehog, transmitted along retinal axons, triggers neurogenesis in the developing visual centers of the *Drosophila* brain. *Cell* 86:411-422.
- Huang Z, Kunes S (1998) Signals transmitted along retinal axons in *Drosophila*: Hedgehog signal reception and the cell circuitry of lamina cartridge assembly. *Development* 125:3753-3764.
- Huang Z, Shilo BZ, Kunes S (1998) A retinal axon fascicle uses spitz, an EGF receptor ligand, to construct a synaptic cartridge in the brain of *Drosophila*. *Cell* 95:693-703.
- Hummel T, Attix S, Gunning D, Zipursky SL (2002) Temporal control of glial cell migration in the *Drosophila* eye requires gilgamesh, hedgehog, and eye specification genes. *Neuron* 33:193-203.
- Hutson LD, Chien CB (2002) Pathfinding and error correction by retinal axons: the role of astray/robo2. *Neuron* 33:205-217.
- Inoue A, Sanes JR (1997) Lamina-specific connectivity in the brain: regulation by N-cadherin, neurotrophins, and glycoconjugates. *Science* 276:1428-1431.
- Jarman AP, Ahmed I (1998) The specificity of proneural genes in determining *Drosophila* sense organ identity. *Mech Dev* 76:117-125.
- Joesch M, Schnell B, Raghu SV, Reiff DF, Borst A (2010) ON and OFF pathways in *Drosophila* motion vision. *Nature* 468:300-304.
- Jones E, Oliphant T, Peterson P, others a (2001) SciPy: Open Source Scientific Tools for Python.
- Kaminker JS, Canon J, Salecker I, Banerjee U (2002) Control of photoreceptor axon target choice by transcriptional repression of Runt. *Nat Neurosci* 5:746-750.
- Katsov AY, Clandinin TR (2008) Motion processing streams in *Drosophila* are behaviorally specialized. *Neuron* 59:322-335.

- Klambt C, Jacobs JR, Goodman CS (1991) The midline of the *Drosophila* central nervous system: a model for the genetic analysis of cell fate, cell migration, and growth cone guidance. *Cell* 64:801-815.
- Kunes S, Steller H (1991) Ablation of *Drosophila* photoreceptor cells by conditional expression of a toxin gene. *Genes Dev* 5:970-983.
- Kunes S, Wilson C, Steller H (1993) Independent guidance of retinal axons in the developing visual system of *Drosophila*. *J Neurosci* 13:752-767.
- Lee CH, Herman T, Clandinin TR, Lee R, Zipursky SL (2001) N-cadherin regulates target specificity in the *Drosophila* visual system. *Neuron* 30:437-450.
- Lee RC, Clandinin TR, Lee CH, Chen PL, Meinertzhagen IA, Zipursky SL (2003) The protocadherin Flamingo is required for axon target selection in the *Drosophila* visual system. *Nat Neurosci* 6:557-563.
- Lee T, Luo L (1999) Mosaic analysis with a repressible cell marker for studies of gene function in neuronal morphogenesis. *Neuron* 22:451-461.
- Lee T, Luo L (2001) Mosaic analysis with a repressible cell marker (MARCM) for *Drosophila* neural development. *Trends Neurosci* 24:251-254.
- Liu Y, Berndt J, Su F, Tawarayama H, Shoji W, Kuwada JY, Halloran MC (2004) Semaphorin3D guides retinal axons along the dorsoventral axis of the tectum. *J Neurosci* 24:310-318.
- Lu B, Usui T, Uemura T, Jan L, Jan YN (1999) Flamingo controls the planar polarity of sensory bristles and asymmetric division of sensory organ precursors in *Drosophila*. *Curr Biol* 9:1247-1250.
- Luo L, Flanagan JG (2007) Development of continuous and discrete neural maps. *Neuron* 56:284-300.
- Luo L, Lee T, Tsai L, Tang G, Jan LY, Jan YN (1997) Genghis Khan (Gek) as a putative effector for *Drosophila* Cdc42 and regulator of actin polymerization. *Proc Natl Acad Sci U S A* 94:12963-12968.
- Mann K, Wang M, Luu SH, Ohler S, Hakeda-Suzuki S, Suzuki T (2012) A putative tyrosine phosphorylation site of the cell surface receptor Golden goal is involved in synaptic layer selection in the visual system. *Development* 139:760-771.
- Matsuoka Y, Li X, Bennett V (2000) Adducin: structure, function and regulation. *Cell Mol Life Sci* 57:884-895.
- McLaughlin T, O'Leary DD (2005) Molecular gradients and development of retinotopic maps. *Annu Rev Neurosci* 28:327-355.
- Meinertzhagen I, Hanson T (1993) The development of the optic lobe. In: *The Development of Drosophila melanogaster*, vol. Cold Spring Harbor Laboratory Press, NY, pp pp. 1363-1491: M Bate, A Martinez-Arias (Eds.).
- Meinertzhagen IA, O'Neil SD (1991) Synaptic organization of columnar elements in the lamina of the wild type in *Drosophila melanogaster*. *J Comp Neurol* 305:232-263.
- Meinertzhagen IA, Sorra KE (2001) Synaptic organization in the fly's optic lamina: few cells, many synapses and divergent microcircuits. *Prog Brain Res* 131:53-69.
- Meinertzhagen IA, Hanson T. E. (1993) The Development of the Optic Lobe. In *The Development of Drosophila melanogaster*, M Bate, and A Martinez-Arias, eds (Cold Spring Harbor: Cold Spring Harbor Laboratory Press) pp. 1363-1491.
- Millard SS, Lu Z, Zipursky SL, Meinertzhagen IA (2010) *Drosophila* dscam proteins regulate postsynaptic specificity at multiple-contact synapses. *Neuron* 67:761-768.
- Misner D, Rubin GM (1987) Analysis of the promoter of the *ninaE* opsin gene in *Drosophila melanogaster*. *Genetics* 116:565-578.
- Monnier PP, Sierra A, Macchi P, Deitinghoff L, Andersen JS, Mann M, Flad M, Hornberger MR, Stahl B, Bonhoeffer F, Mueller BK (2002) RGM is a repulsive guidance molecule for retinal axons. *Nature* 419:392-395.
- Montell C, Jones K, Zuker C, Rubin G (1987) A second opsin gene expressed in the ultraviolet-sensitive R7 photoreceptor cells of *Drosophila melanogaster*. *J Neurosci* 7:1558-1566.

- Morata G, Ripoll P (1975) Minutes: mutants of drosophila autonomously affecting cell division rate. *Dev Biol* 42:211-221.
- Newsome TP, Asling B, Dickson BJ (2000a) Analysis of Drosophila photoreceptor axon guidance in eye-specific mosaics. *Development* 127:851-860.
- Newsome TP, Schmidt S, Dietzl G, Keleman K, Asling B, Debant A, Dickson BJ (2000b) Trio combines with dock to regulate Pak activity during photoreceptor axon pathfinding in Drosophila. *Cell* 101:283-294.
- Niederkofler V, Salie R, Sigrist M, Arber S (2004) Repulsive guidance molecule (RGM) gene function is required for neural tube closure but not retinal topography in the mouse visual system. *J Neurosci* 24:808-818.
- O'Tousa JE, Baehr W, Martin RL, Hirsh J, Pak WL, Applebury ML (1985) The Drosophila ninaE gene encodes an opsin. *Cell* 40:839-850.
- Ohler S, Hakeda-Suzuki S, Suzuki T (2011) Hts, the Drosophila homologue of Adducin, physically interacts with the transmembrane receptor Golden goal to guide photoreceptor axons. *Dev Dyn* 240:135-148.
- Papatsenko D, Sheng G, Desplan C (1997) A new rhodopsin in R8 photoreceptors of Drosophila: evidence for coordinate expression with Rh3 in R7 cells. *Development* 124:1665-1673.
- Pittman AJ, Law MY, Chien CB (2008) Pathfinding in a large vertebrate axon tract: isotypic interactions guide retinotectal axons at multiple choice points. *Development* 135:2865-2871.
- Poeck B, Fischer S, Gunning D, Zipursky SL, Salecker I (2001) Glial cells mediate target layer selection of retinal axons in the developing visual system of Drosophila. *Neuron* 29:99-113.
- Pollerberg GE, Beck-Sickinger A (1993) A functional role for the middle extracellular region of the neural cell adhesion molecule (NCAM) in axonal fasciculation and orientation. *Dev Biol* 156:324-340.
- Poskanzer K, Needleman LA, Bozdagi O, Huntley GW (2003) N-cadherin regulates ingrowth and laminar targeting of thalamocortical axons. *J Neurosci* 23:2294-2305.
- Prakash S, Caldwell JC, Eberl DF, Clandinin TR (2005) Drosophila N-cadherin mediates an attractive interaction between photoreceptor axons and their targets. *Nat Neurosci* 8:443-450.
- Prakash S, McLendon HM, Dubreuil CI, Ghose A, Hwa J, Dennehy KA, Tomalty KM, Clark KL, Van Vactor D, Clandinin TR (2009) Complex interactions amongst N-cadherin, DLAR, and Liprin-alpha regulate Drosophila photoreceptor axon targeting. *Dev Biol* 336:10-19.
- Ramon y Cajal S (1923) *Recollection of my life*. The MIT press.
- Rao Y, Pang P, Ruan W, Gunning D, Zipursky SL (2000) brakeless is required for photoreceptor growth-cone targeting in Drosophila. *Proc Natl Acad Sci U S A* 97:5966-5971.
- Raper J, Mason C (2010) Cellular strategies of axonal pathfinding. *Cold Spring Harb Perspect Biol* 2:a001933.
- Raper JA, Bastiani MJ, Goodman CS (1983) Guidance of neuronal growth cones: selective fasciculation in the grasshopper embryo. *Cold Spring Harb Symp Quant Biol* 48 Pt 2:587-598.
- Reber M, Burrola P, Lemke G (2004) A relative signalling model for the formation of a topographic neural map. *Nature* 431:847-853.
- Rister J, Pauls D, Schnell B, Ting CY, Lee CH, Sinakevitch I, Morante J, Strausfeld NJ, Ito K, Heisenberg M (2007) Dissection of the peripheral motion channel in the visual system of Drosophila melanogaster. *Neuron* 56:155-170.
- Rivera-Alba M, Vitaladevuni SN, Mischenko Y, Lu Z, Takemura SY, Scheffer L, Meinertzhagen IA, Chklovskii DB, de Polavieja GG (2011) Wiring economy and volume exclusion determine neuronal placement in the Drosophila brain. *Curr Biol* 21:2000-2005.

- Ruan W, Long H, Vuong DH, Rao Y (2002) Bifocal is a downstream target of the Ste20-like serine/threonine kinase misshapen in regulating photoreceptor growth cone targeting in *Drosophila*. *Neuron* 36:831-842.
- Sanes JR, Zipursky SL (2010) Design principles of insect and vertebrate visual systems. *Neuron* 66:15-36.
- Sarthy PV (1991) Histamine: a neurotransmitter candidate for *Drosophila* photoreceptors. *J Neurochem* 57:1757-1768.
- Sato M, Umetsu D, Murakami S, Yasugi T, Tabata T (2006) DWnt4 regulates the dorsoventral specificity of retinal projections in the *Drosophila melanogaster* visual system. *Nat Neurosci* 9:67-75.
- Schmitt AM, Shi J, Wolf AM, Lu CC, King LA, Zou Y (2006) Wnt-Ryk signalling mediates medial-lateral retinotectal topographic mapping. *Nature* 439:31-37.
- Selleck SB, Steller H (1991) The influence of retinal innervation on neurogenesis in the first optic ganglion of *Drosophila*. *Neuron* 6:83-99.
- Senti K, Keleman K, Eisenhaber F, Dickson BJ (2000) brakeless is required for lamina targeting of R1-R6 axons in the *Drosophila* visual system. *Development* 127:2291-2301.
- Senti KA, Usui T, Boucke K, Greber U, Uemura T, Dickson BJ (2003) Flamingo regulates R8 axon-axon and axon-target interactions in the *Drosophila* visual system. *Curr Biol* 13:828-832.
- Shapiro L, Love J, Colman DR (2007) Adhesion molecules in the nervous system: structural insights into function and diversity. *Annu Rev Neurosci* 30:451-474.
- Shinza-Kameda M, Takasu E, Sakurai K, Hayashi S, Nose A (2006) Regulation of layer-specific targeting by reciprocal expression of a cell adhesion molecule, capricious. *Neuron* 49:205-213.
- Shishido E, Takeichi M, Nose A (1998) *Drosophila* synapse formation: regulation by transmembrane protein with Leu-rich repeats, CAPRICIOUS. *Science* 280:2118-2121.
- Sperry RW (1963) Chemoaffinity in the Orderly Growth of Nerve Fiber Patterns and Connections. *Proc Natl Acad Sci U S A* 50:703-710.
- Su YC, Maurel-Zaffran C, Treisman JE, Skolnik EY (2000) The Ste20 kinase misshapen regulates both photoreceptor axon targeting and dorsal closure, acting downstream of distinct signals. *Mol Cell Biol* 20:4736-4744.
- Sugie A, Umetsu D, Yasugi T, Fischbach KF, Tabata T (2010) Recognition of pre- and postsynaptic neurons via nephrin/NEPH1 homologs is a basis for the formation of the *Drosophila* retinotopic map. *Development* 137:3303-3313.
- Suh GS, Poeck B, Chouard T, Oron E, Segal D, Chamovitz DA, Zipursky SL (2002) *Drosophila* JAB1/CSN5 acts in photoreceptor cells to induce glial cells. *Neuron* 33:35-46.
- Takeichi M (2007) The cadherin superfamily in neuronal connections and interactions. *Nat Rev Neurosci* 8:11-20.
- Tessier-Lavigne M, Goodman CS (1996) The molecular biology of axon guidance. *Science* 274:1123-1133.
- Tomasi T, Hakeda-Suzuki S, Ohler S, Schleiffer A, Suzuki T (2008) The transmembrane protein Golden goal regulates R8 photoreceptor axon-axon and axon-target interactions. *Neuron* 57:691-704.
- Tomlinson A, Ready DF (1987) Neuronal differentiation in *Drosophila* ommatidium. *Dev Biol* 120:366-376.
- Triplett JW, Feldheim DA (2012) Eph and ephrin signaling in the formation of topographic maps. *Semin Cell Dev Biol* 23:7-15.
- Umetsu D, Murakami S, Sato M, Tabata T (2006) The highly ordered assembly of retinal axons and their synaptic partners is regulated by Hedgehog/Single-minded in the *Drosophila* visual system. *Development* 133:791-800.

- Walter J, Kern-Veits B, Huf J, Stolze B, Bonhoeffer F (1987) Recognition of position-specific properties of tectal cell membranes by retinal axons in vitro. *Development* 101:685-696.
- White NM, Jarman AP (2000) *Drosophila* atonal controls photoreceptor R8-specific properties and modulates both receptor tyrosine kinase and Hedgehog signalling. *Development* 127:1681-1689.
- Wolff T, Ready DF (1993) Pattern formation in the *Drosophila* retina. In: Bate M., Martinez-Arias A, eds. *The Development of Drosophila melanogaster*. Cold Spring Harbor: Cold Spring Harbor Press 1363-1491.
- Xu T, Rubin GM (1993) Analysis of genetic mosaics in developing and adult *Drosophila* tissues. *Development* 117:1223-1237.
- Yamagata M, Sanes JR (2008) Dscam and Sidekick proteins direct lamina-specific synaptic connections in vertebrate retina. *Nature* 451:465-469.
- Yamagata M, Weiner JA, Sanes JR (2002) Sidekicks: synaptic adhesion molecules that promote lamina-specific connectivity in the retina. *Cell* 110:649-660.
- Yoon M (1971) Reorganization of retinotectal projection following surgical operations on the optic tectum in goldfish. *Exp Neurol* 33:395-411.
- Yoon MG (1976) Progress of topographic regulation of the visual projection in the halved optic tectum of adult goldfish. *J Physiol* 257:621-643.
- Yoshida S, Soustelle L, Giangrande A, Umetsu D, Murakami S, Yasugi T, Awasaki T, Ito K, Sato M, Tabata T (2005) DPP signaling controls development of the lamina glia required for retinal axon targeting in the visual system of *Drosophila*. *Development* 132:4587-4598.
- Zelina P, Avci HX, Thelen K, Pollerberg GE (2005) The cell adhesion molecule NrCAM is crucial for growth cone behaviour and pathfinding of retinal ganglion cell axons. *Development* 132:3609-3618.
- Zhang J (2012) Genetic redundancies and their evolutionary maintenance. *Adv Exp Med Biol* 751:279-300.
- Zuker CS, Cowman AF, Rubin GM (1985) Isolation and structure of a rhodopsin gene from *D. melanogaster*. *Cell* 40:851-858.
- Zuker CS, Montell C, Jones K, Laverty T, Rubin GM (1987) A rhodopsin gene expressed in photoreceptor cell R7 of the *Drosophila* eye: homologies with other signal-transducing molecules. *J Neurosci* 7:1550-1557.

ACKNOWLEDGEMENTS

Curriculum vitae